

# Separation of fresh and brackish water in polder water canals

MSc Thesis



Irene de Vries





# Separation of fresh and brackish water in polder water canals

by

Irene de Vries

to obtain the degree of Master of Science  
at the Delft University of Technology,  
to be defended publicly on Thursday May 25, 2023 at 04:00 PM.

Student number: 5180767  
Project duration: May 1, 2022 – May 25, 2023  
Faculty: Civil Engineering and Geosciences  
Thesis committee: Prof. dr. ir. R. Uijlenhoet TU Delft  
Dr. ir. O. A. C. Hoes TU Delft  
Prof. dr. ir. W. S. J. Uijttewaal TU Delft  
A. van der Heijden MSc Acacia Water  
Cover: Negenboerenpolder (the Netherlands) Taken by Irene de Vries (November 2, 2022)

An electronic version of this thesis is available at <http://repository.tudelft.nl/>.





## Preface

Before you lies the master thesis “Separation of fresh and brackish water in polder water canals.” With this thesis, my studies will come to an end. My studies started with the Bachelor Soil, Water, Atmosphere at Wageningen University & Research, and they have now ended with my graduation from the MSc Programme in Water Management at Delft University of Technology.

When I saw this topic in the list of M.Sc. topics, it was clear to me that this was exactly what I wanted to do for my master’s thesis. The practical applicability in the field of the topic was what attracted me. It motivates me to make a difference, to help solve a problem which people encounter in their daily life. I want to combine experiences in the field with theoretical knowledge.

I would like to express my gratitude to all of my committee members: Olivier, Anne, Remko, and Wim. In particular, I would like to thank my daily supervisors Olivier and Anne for the weekly meetings. There were some highs and lows during the period of my thesis, but they were always positive and supportive. They helped me to put everything in perspective, for which I am grateful.

During this thesis, I had the opportunity to work together with Acacia Water. The company included me in their team, showed me what working in a company is like, and there was always a nice lunch whenever I was in the office in Gouda. I would like to thank Acacia Water and its employees for their time, support, and enthusiasm for my research.

Finally, I want to thank my family and friends for being supportive and helpful. At the moments when I was down and needed cheering up, or when I was enthusiastic and needed someone to share my joy with, I could come to you. I feel really lucky to know that you are always there for me.

Irene de Vries  
Delft, May 12, 2023



---

# Contents

<b>List of Figures</b>	<b>iv</b>
<b>List of Tables</b>	<b>vii</b>
<b>List of Symbols</b>	<b>viii</b>
<b>Abstract</b>	<b>ix</b>
<b>1 Introduction</b>	<b>1</b>
1.1 Problem and relevance . . . . .	1
1.2 Research gaps . . . . .	3
1.3 Aim of this research . . . . .	3
1.4 Research questions . . . . .	4
1.5 Report outline . . . . .	4
<b>2 Background</b>	<b>5</b>
2.1 Salinization . . . . .	5
2.1.1 Mechanism . . . . .	5
2.1.2 Observation . . . . .	5
2.1.3 Salinity . . . . .	6
2.2 Hydraulics . . . . .	8
2.2.1 Laminar and turbulent flow . . . . .	8
2.2.2 Influences on water flow in a polder . . . . .	9
2.2.3 Density stratified flow . . . . .	11
2.3 The modified weir . . . . .	12
2.3.1 Development . . . . .	12
2.3.2 Current situation . . . . .	13
2.4 Negenboerenpolder . . . . .	14
2.4.1 General . . . . .	14
2.4.2 Water system . . . . .	14
2.4.3 Challenges . . . . .	17
2.4.4 Projects and motivation . . . . .	17
<b>3 Method</b>	<b>19</b>
3.1 Flume experiments . . . . .	19
3.1.1 Motivation . . . . .	19
3.1.2 Design of experiments . . . . .	19
3.1.3 Method and process . . . . .	20
3.2 Field campaign . . . . .	23
3.2.1 Depth profiles . . . . .	23
3.2.2 Transects . . . . .	23
3.2.3 Continuous data series . . . . .	26
3.3 2D simulations . . . . .	27
3.3.1 Theory . . . . .	28
3.3.2 Geometry and boundary conditions . . . . .	28
3.3.3 Mesh and time step . . . . .	30





3.3.4	Simulation set-up . . . . .	31
3.3.5	Cases . . . . .	33
<b>4</b>	<b>Results</b>	<b>35</b>
4.1	Fresh and brackish water distribution . . . . .	35
4.1.1	Distribution over the depth . . . . .	35
4.1.2	Distribution over the area . . . . .	37
4.1.3	Distribution over time . . . . .	40
4.1.4	Possible explanations . . . . .	41
4.2	Separating densities . . . . .	43
4.2.1	Flume experiments . . . . .	43
4.2.2	2D simulations . . . . .	45
<b>5</b>	<b>Implementation of a modified weir</b>	<b>47</b>
5.1	Recommendations for the location . . . . .	47
5.2	Recommendations for the design . . . . .	48
5.3	Effect on the water system . . . . .	49
5.4	Recommendations for measuring the effect . . . . .	50
<b>6</b>	<b>Discussion</b>	<b>53</b>
6.1	General . . . . .	53
6.2	Flume experiments . . . . .	54
6.3	Field campaign . . . . .	55
6.4	2D simulations . . . . .	56
<b>7</b>	<b>Conclusions and recommendations for future research</b>	<b>57</b>
7.1	Conclusions . . . . .	57
7.2	Recommendations for future research . . . . .	57
	<b>References</b>	<b>59</b>
	<b>Appendix</b>	<b>65</b>
A	Relation EC, Chloride concentration and salt tolerance of various crops . . . . .	65
B	Maps of the Negenboerenpolder . . . . .	65
C	Electrical Conductivity routing in the Negenboerenpolder in August 2021 . . . . .	66
D	Schematic drawings of the sensor depths at the three locations . . . . .	68
E	Overview of the flume experiments . . . . .	69
F	Results of the other flume experiments . . . . .	70
G	Temperature profiles over the depth . . . . .	70
H	Temperature measurements at two depths around the weir at Hornhuizerkief . . . . .	72
I	Temperature measurements at two depths along two transects in the Negenboerenpolder . . . . .	72
J	Possible explanations for the water levels and EC at the measurement locations in the Negenboerenpolder . . . . .	74
K	Classification of water canals in the Negenboerenpolder . . . . .	76
L	Overview of the four geometries for 2D CFD Model in ANSYS Fluent . . . . .	76
M	Preparation for a 3D model of a modified weir in ANSYS Fluent . . . . .	78
N	Animations of the five runs in the 2D CFD model . . . . .	78



## List of Figures

2	Salinization in a polder, because of saline seepage [Own drawing] . . . . .	1
3	Sea level rise and land subsidence in a typical polder in the Netherlands [van de Ven, 1993] . . . . .	2
4	Traditional weir [Based on Groen et al., 2017] . . . . .	3
5	Modified weir ("Zoete Stuw") [Based on Groen et al., 2017] . . . . .	3
6	Schematic drawing of seepage coming up in a polder [Kalsbeek, 2014] . . . . .	6
7	Water canal for the Reynolds Number example . . . . .	8
8	Design of a control notch [Ankum, 2002] . . . . .	10
9	Submerged flow underneath a vertical gate [Ankum, 2002] . . . . .	10
10	Concrete modified weirs of TexelBeton . . . . .	13
11	Displacement of saline water by pushing it to the sea (left) and inflow of fresh river water at the surface (Design Ir. W. Lases) [Redactie Waterforum, 2022] . . . . .	14
12	Location of the Negenboerenpolder next to the Wadden Sea [Adapted from Google Maps, n.d.] . . . . .	15
13	Elevation map of the Negenboerenpolder [PDOK, n.d.-a] . . . . .	15
14	Flow direction of surface water in the Negenboerenpolder [Based on van Meijeren et al., 2019] . . . . .	16
15	Flume used for the experiments on the campus of the TU Delft . . . . .	20
16	Wooden construction used for the flume experiments (dimensions in <i>mm</i> ) [Hoes, 2022] . . . . .	21
17	Side view with the set-up of the flume experiments [Hoes, 2022] . . . . .	21
18	Used EC meter during the flume experiments [Profishop, n.d.] . . . . .	21
19	Locations of the measured profiles over the depth . . . . .	24
20	Conductivity meter with yellow stripes used for the measurements of the depth profiles . . . . .	24
21	Locations of the measured transects in the Negenboerenpolder . . . . .	25
22	Locations of the continuous measurement locations in the Negenboerenpolder . . . . .	27
23	Geometry 2 of the 2D CFD model in ANSYS Fluent . . . . .	29
24	Legend with boundary conditions of the CFD model in ANSYS Fluent . . . . .	29
25	Overview of all locations during the field campaign in and around the Negenboerenpolder . . . . .	35
26	Conductivity profiles over the depth – July 2022 . . . . .	36
27	Conductivity profiles over the depth – November 2022 . . . . .	36
28	Conductivity measurements at two depths around weir Hornhuizerklief – July 2022 . . . . .	37
29	Conductivity measurements at two depths around weir Hornhuizerklief – November 2022 . . . . .	37
30	Conductivity measurements at two depths along the Dijkslot transect – July 2022 . . . . .	38
31	Conductivity measurements at two depths along the Waddenweg transect – July 2022 . . . . .	39
32	Conductivity measurements at two depths along the Waddenweg transect – November 2022 . . . . .	39
33	Pictures taken along the Waddenweg transect during the field campaign in the Negenboerenpolder on November 2, 2022 . . . . .	39
34	Measured chloride concentrations (2012) in the Negenboerenpolder on four locations of Waterschap Noorderzijlvest [van Meijeren et al., 2019] . . . . .	40
35	Water levels at the three measurement locations in the Negenboerenpolder . . . . .	41
36	Measured conductivity at the three locations in the Negenboerenpolder (Period 1) . . . . .	41
37	Measured conductivity at the three locations in the Negenboerenpolder (Period 2) . . . . .	41

38	Wadden Sea tides and water levels in the Negenboerenpolder at the end of July . . .	42
39	Wadden Sea tides and conductivity levels in the Negenboerenpolder at the end of July	42
40	Wadden Sea tides and conductivity levels in Negenboerenpolder in August and September . . . . .	43
41	Wadden Sea tides and conductivity levels in Negenboerenpolder in October and November . . . . .	43
42	Flume experiment 1 – April 22, 2022 . . . . .	44
43	Flume experiment 3 – May 13, 2022 . . . . .	44
44	Flume experiment 5 – June 3, 2022 . . . . .	44
45	Flume experiment 7 – July 25, 2022 . . . . .	45
46	Fresh water (red) flowing over a traditional weir, saline water (yellow) is staying behind in the water canal ( $\Delta t = 2260$ , $v = 0.01$ m/s, geometry 1) . . . . .	45
47	Saline water (yellow) is flowing through the modified weir, fresh water (red) is staying behind in the water canal ( $\Delta t = 2260$ , $v = 0.01$ m/s, geometry 2) . . . . .	45
48	Dots of fresh water (red) in the saline (yellow) layer in the CFD model of a modified weir with an inlet velocity of 0.10 m/s ( $\Delta t = 2800$ , geometry 3) . . . . .	46
49	Fresh (red) is flowing underneath the underflow gate in the CFD model of a modified weir with an inlet velocity of 0.10 m/s ( $\Delta t = 270$ , geometry 3) . . . . .	46
50	Blocked velocity vector in the CFD model of a modified weir with an inlet velocity of 0.01 m/s ( $\Delta t = 150$ , geometry 4 (0.3 m)) . . . . .	46
51	Spread out velocity vector in the CFD model of a modified weir with an inlet velocity of 0.01 m/s ( $\Delta t = 150$ , geometry 2 (2.0 m)) . . . . .	46
52	The Negenboerenpolder, with a potential location for the modified weir indicated with the red circle . . . . .	48
53	Table with the salt tolerance of various crops [Translated from de Olde, 2022] . . . . .	65
54	Soil type map of the Negenboerenpolder [Based on van Meijeren et al., 2019; Translated from PDOK, n.d.-b] . . . . .	66
55	Land use map of the Negenboerenpolder in 2020 [Based on van Meijeren et al., 2019; Translated from Wageningen Environmental Research, 2021] . . . . .	66
56	Routing of the Electrical Conductivity in the Negenboerenpolder during August 2021 [van der Heijden, 2021] . . . . .	67
57	Schematic drawing of continuous measurement locations [Own drawing, 2023] . . .	68
58	Flume experiment 2 – April 29, 2022 . . . . .	70
59	Flume experiment 4 – May 20, 2022 . . . . .	70
60	Flume experiment 6 – June 10, 2022 . . . . .	71
61	Temperature profiles over the depth – July 2022 . . . . .	71
62	Temperature profiles over the depth – November 2022 . . . . .	71
63	Temperature measurements at two depths around weir at Hornhuizerkief – July 2022	72
64	Temperature measurements at two depths around weir at Hornhuizerkief – November 2022 . . . . .	72
65	Temperature measurements at two depths along Dijkslot transect – July 2022 . . . .	73
66	Temperature measurements at two depths along Waddenweg transect – July 2022 . .	73
67	Temperature measurements at two depths along Waddenweg transect – November 2022	73
68	The Wadden Sea tides and the water levels in the Negenboerenpolder (Period 1) . . .	74
69	The Comparison of Wadden Sea tides and the water levels in the Negenboerenpolder (Period 2) . . . . .	74

---

70	Comparison of Wadden Sea tides and conductivity levels in the Negenboerenpolder (Period 1) . . . . .	75
71	Comparison of Wadden Sea tides and conductivity levels in the Negenboerenpolder (Period 2) . . . . .	75
72	Comparison of precipitation and conductivity levels in the Negenboerenpolder (Period 1) . . . . .	75
73	Comparison of precipitation and conductivity levels in the Negenboerenpolder (Period 2) . . . . .	75
74	Water flow in the Negenboerenpolder with the classification of the waterways [Translated from van Meijeren et al., 2019] . . . . .	76
75	Legend with boundary conditions of the CFD model in ANSYS Fluent . . . . .	76
76	Geometry 1 of the CFD model in ANSYS Fluent . . . . .	77
77	Geometry 2 of the CFD model in ANSYS Fluent . . . . .	77
78	Geometry 3 of the CFD model in ANSYS Fluent . . . . .	77
79	Geometry 4 of the CFD model in ANSYS Fluent . . . . .	77
80	Animation of the phases in geometry 1 . . . . .	78
81	Animation of the phases in geometry 2 . . . . .	79
82	Animation of the velocity vectors in geometry 2 . . . . .	79
83	Animation of the phases in geometry 3 . . . . .	79
84	Animation of the velocity vectors in geometry 4 . . . . .	80



---

## List of Tables

1	Classification of water based on EC and calculated corresponding Chloride concentrations [Adapted from Rhoades et al., 1992, and Vos et al., 2016] . . . . .	7
2	Soil salinity classes and crop growth [Adapted from Abrol et al., 1988, and Vos et al., 2016] . . . . .	7
3	Reynolds numbers for flow regimes [Abdurrasheed et al., 2018; Westerweel, 2020; Simscale, 2021] . . . . .	8
4	Overview of the input discharge parameters of a previous modelling study of the modified weir [Groen et al., 2017] . . . . .	12
5	Overview of the input design parameters of a previous modelling study of the modified weir [Groen et al., 2017] . . . . .	12
6	Short overview of practical input for all flume experiments . . . . .	22
7	Overview of measurement locations and measuring periods . . . . .	26
8	Overview of difference between shallow and deep sensors at the measurement locations	27
9	Input and answer for Equation 7 . . . . .	30
10	Input parameters for mesh and time . . . . .	30
11	Cases for 2D CFD model in ANSYS Fluent . . . . .	33
12	Full overview of practical input 1 . . . . .	69
13	Full overview of practical input 2 . . . . .	69





---

## List of Symbols

$2D$	Two Dimensional
$3D$	Three Dimensional
$\beta$	Thermal expansion coefficient = $1/T_0$ [ $^{\circ}C^{-1}$ ]
$\mu$	Viscosity [ $m^2/s$ ]
$\rho$	Density [ $kg/m^3$ ]
$\rho_0$	Constant density [ $kg/m^3$ ]
$A$	Crosssectional area [ $m^2$ ]
$C$	Courant Number [–]
$C_{max}$	Maximum Courant Number = 0.7 [–]
$Cl$	Chloride concentration [ $mg/l$ or $g/l$ ]
$EC$	Electrical Conductivity [ $mS/cm$ ]
$g$	Gravity constant = 9.81 [ $m^2/s$ ]
$h$	Height of the underflow gate [ $m$ ]
$l$	Length of the canal [ $m$ ]
$Q$	Discharge [ $m^3/s$ ]
$R$	Hydraulic radius [ $m$ ]
$Re$	Reynolds number [–]
$T$	Temperature [ $K$ or $^{\circ}C$ ]
$T_0$	Operating temperature [ $K$ or $^{\circ}C$ ]
$V$	Volume [ $m^3$ ]
$v$	Velocity [ $m/s$ ]
$w$	Width of the canal [ $m$ ]
$y$	Water depth [ $m$ ]



## Abstract

Polders water canals are sometimes exposed to brackish seepage from the nearby saline sea (salinization). This is a problem because the canal water is used to irrigate crops. A characteristic of water is that less dense (fresh) water floats on top of dense (saline) water. In lakes and oceans, it is common that water layers with various densities flow on top of each other (stratification). However, this has not been observed yet on a small scale, such as in polder water canals. It is assumed that, with a traditional weir, fresh water is discharged, and saline water stays behind. To encounter this, a modified weir is developed. It uses an underflow gate in front of the traditional weir to discharge the bottom water out of the canal. This research aimed to investigate if stratification happens in polder water canals and to explore how a modified weir can be implemented. The Negenboerenpolder in Groningen (the Netherlands) served as an example. Multiple methods are used because of the broad and practical nature of the problem. First, field measurements in the Negenboerenpolder demonstrated stratification in polder water canals. At multiple locations in the polder, the Electrical Conductivity (EC) is measured over the depth or continuously measured at two depths. Secondly, flume experiments gave information about the experimental procedure and implementation of a modified weir. Thirdly, 2D simulations of a modified weir are done in ANSYS Fluent, a Computation Fluid Dynamics (CFD) software. The simulations suggest that a modified weir works as expected, but the model is not completely representative. Observations are that such a weir is more effective in discharging brackish water with a low flow velocity and a larger distance between the underflow gate and the weir. Implementation advice for a modified weir is also included in this research. To conclude, this research implies that a modified weir can be used to discharge brackish water, but the design and implementation need to be done carefully. Recommendations for future research are to experiment with a modified weir in a polder and to build a 3D CFD model to investigate the flow around the underflow gate.

*Keywords:* ANSYS Fluent, CFD model, density controlled stratification, experiment, modified weir, salinization.



# 1 Introduction

Salinization is caused by saline seepage to surface water. This is a problem for farmers and nature managers, who work in areas close to the coast, like Dutch polders. Due to climate change and land subsidence, natural and human-induced, the sea level is rising, and this causes even more seepage. In addition, there is a difference in density between saline and fresh water. It is assumed that this induces the stratification of water in open canals, as is happening in lakes and oceans. However, this has never been demonstrated at a small scale, which creates a research gap. If this stratification happens in polder water canals, a traditional weir only discharges the fresh surface water. With a modified weir, the bottom (brackish) water can be discharged. The aim of this research is to investigate if such a modified weir is useful in areas with brackish seepage and how it can be implemented. The main research question is: “*Can a modified weir discharge brackish water from a stratified shallow polder water canal?*”. The used methods are field measurements, 2D simulations, and flume experiments.

## 1.1 Problem and relevance

Sufficient fresh water is crucial for life: the irrigation of crops, and the drinking water supply, among others, are dependent on freshwater [Ministerie van Infrastructuur en Waterstaat, 2020]. Coastal zones and deltas, often directly next to saline seas, have always attracted humans. The benefits of these coastal areas are largely due to fertile soils, the absence of elevation, and easily accessible for transport via water [Aerts et al., 2009]. The Netherlands is located in the deltas of the rivers Rhine and Meuse and consists, for a large part, of polders, especially along the Wadden Sea and the North Sea. Polders are (artificially) reclaimed land from a sea or lake, and are often beneath sea level [Schultz, 1996]. These lowlands are separated from the hydrological regime of the surrounding areas and need intensive (water) management to keep the land dry and useful [Segeren, 1983]. However, there is an upcoming threat for the entire North Sea Region: salinization [Gould et al., 2021].

Salinization (Dutch: “Verziltting”) is the increase of salinity in surface water, the soil, or groundwater (Figure 2) [Nederlandse Hydrologische Vereniging, 2002]. Low-lying areas can receive groundwater seepage fluxes from deep saline aquifers, which are in direct contact with the sea [Hilgersom, 2017]. This seepage leads to an increase in salt concentration of the polder surface water system [de Louw, Vandenbohede, et al., 2013]. Sometimes, seepage can also flow through boils, which are small openings in the Holocene layer which make them suitable for high-velocity groundwater flow [de Louw et al., 2010]. The standard management solution in polders in the Netherlands is often diluting the salinity concentration by frequently flushing the polder ditches [Delsman et al., 2014].

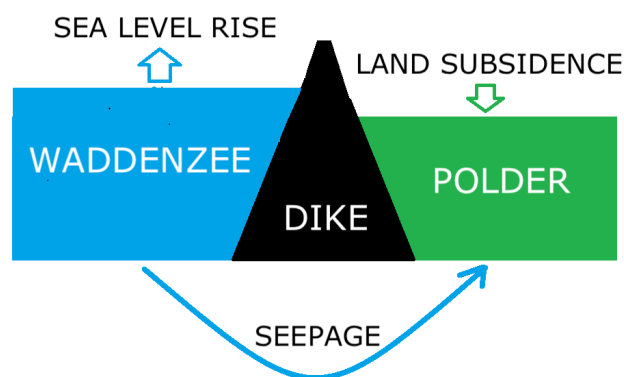


Figure 2: Salinization in a polder, because of saline seepage [Own drawing]

Land subsidence in the Dutch North Sea Region is also not beneficial for salinization, this subsidence is caused by gas extraction [Schoonbeek, 1976] and peat oxidation [Nieuwenhuis and Schokking, 1997]. When land subsides, the sea level becomes relatively high. With sea-level rise, the relative land subsidence is even more. Figure 3 shows the development in the Netherlands over time, related to land subsidence and sea-level rise. In the figure can also be seen that the mean sea level has risen over time. Recent research proved that there is regional sea-level rise acceleration for the North Sea Region [Steffelbauer et al., 2022]. The rise of sea level reinforces the saline seepage flux (Figure 2), because of the pressure difference between the polder canal and sea level [de Louw et al., 2010].

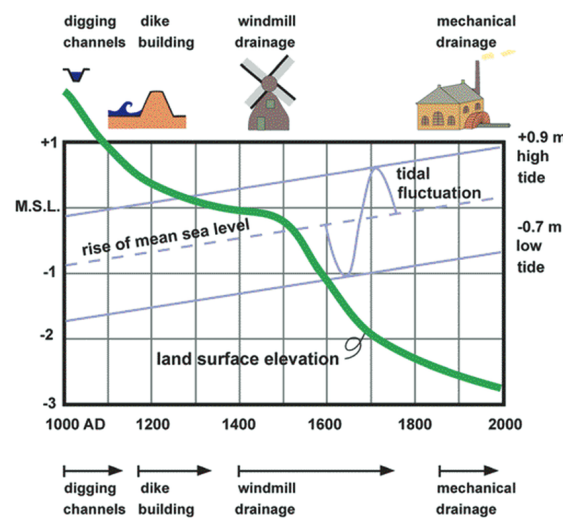


Figure 3: Sea level rise and land subsidence in a typical polder in the Netherlands [van de Ven, 1993]

The land subsidence, sea-level rise, and resulting salinization are not only happening in the Netherlands. The problem is known in various countries and coastal zones [Negacz et al., 2021], like Italy, Australia, South Africa, Pakistan, Bangladesh, Uzbekistan, the Ganges Delta, the Near East and North Africa (NENA) Region, and other parts of the North Sea Region (Germany, United Kingdom, Belgium, Sweden, Denmark).

Polders are often dominated by agricultural land use [Delsman et al., 2014], and the amount of salinization can have an effect on the yield. Farmers use the surrounding surface water to irrigate their crops and are dependent on the water quality of the surface water. Saline water is not useful for most farmers as this influences the growth of crops negatively [Yildiz et al., 2020]. The salt tolerance level of crops is dependent on the type [de Olde, 2022], see Appendix A. Flower bulbs and potatoes are extremely sensitive to the chloride concentration of water compared to grass and wheat, which can withstand a high salinity. The clay soils in the north of the Netherlands are excellent to grow potatoes, 8% of the worldwide export of potatoes is from this area [The Potato Valley, n.d.]. Next to this, damage to crops by salt stress can not be seen directly. The suffering of a crop, caused by water stress, has the same signs as a crop suffering from salt stress [Wageningen Environmental Research, 2018]. This all makes the brackish seepage a large problem for agriculture, especially along the North Sea Region of the Netherlands.

## 1.2 Research gaps

In general, dense fluids sink to the bottom and less heavy water floats on top. Brackish water has a higher density than freshwater and will thus stay at the bottom of a canal. Temperature differences have the same effect: denser cold (ground) water gathers at the bottom and warm water, also heated by the sun, stays at the surface [Schönfeld and Kranenburg, 1977]. Both cause the layering of fluids with different densities and thus stratification: this is already visible in oceans and lakes [Li et al., 2020]. However, this phenomenon on a small scale has never been described in scientific literature.

When stratification can be demonstrated, an adjusted weir can possibly be used to separate the water and discharge the saline water. Traditional weirs discharge the upper water of a ditch: water can only leave the canal by flowing over the weir (Figure 4). However, the upper water is freshwater and the bottom and brackish water stays behind in the polder canals: the same canals used for the irrigation of crops. Acacia Water, Svasek Hydraulics, and Hoogheemraadschap Noorderkwartier (Waterboard in Noord-Holland (the Netherlands)) developed the "Zoete Stuw" or "modified weir" in English (Figure 5) [Groen et al., 2017]. The two modified weir types drain the bottom (brackish) water upstream of the weir. However, no research is done on the exact working of the modified weir: for example, how it can separate water and how the weir can be implemented [Groen et al., 2017].

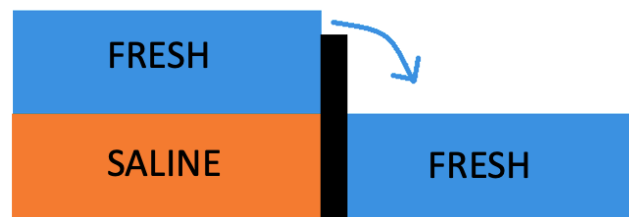


Figure 4: Traditional weir [Based on Groen et al., 2017]



Figure 5: Modified weir ("Zoete Stuw") [Based on Groen et al., 2017]

## 1.3 Aim of this research

The aim of this research is to investigate if a modified weir can be used in areas with saline seepage, this can prevent salinization problems worldwide. As saline water is denser than freshwater [Schönfeld and Kranenburg, 1977], the seepage can cause stratification of water with different densities. To reach this goal, it must be demonstrated first that stratification can be found in smaller polder canals. Thereafter, it is investigated how and if a modified weir works, and is explored under which circumstances a modified weir can be successfully implemented (based on previous results). The used methods are literature research, flume experiments, field measurements and data analysis, and 2D simulations in Computational Fluid Dynamics (CFD) software.

In this research, a combination of multiple methods is used because of the practical nature of the problem. The modified weir is specifically designed for one kind of situation in particular locations. Flume experiments give insight into how to make a modified weir in practice and which locations are useful to measure. The 2D simulations build upon the experiments, they are useful because they show what can happen in theory. However, the modelling results cannot grasp the actual situation in the field, which is measured by (continuous) field measurements. With all methods, useful locations for a modified weir are indicated, together with how such a weir should be made and put into practice. In short, this research can function possibly as the start of three different follow-up studies.

## 1.4 Research questions

The main research question is: “*Can a modified weir discharge brackish water from a stratified shallow polder water canal?*”. This question will be answered by the following sub-questions. A small explanation is given for each sub-question.

1. How is the fresh-brackish water distribution in the polder canals?

This sub-question investigates where fresh and brackish water can be found in the Negenboerenpolder. Field measurements will be done at three scales: all around the polder (spatial), over the depth (local), and over time (temporal). The measurements give indications of where stratification can be found.

2. How is the modified weir able to separate water with different densities in a polder?

This sub-question investigates how a modified weir works in practice through flume experiments and 2D simulations. The results give indications for useful dimensions and locations.

3. How can the modified weir be implemented successfully in a polder, based on previous results?

This sub-question investigates the implementation of a modified weir, based on the answers of the previous two sub-questions. Recommended locations (in the Negenboerenpolder) and information about useful dimensions for a modified weir are given here.

## 1.5 Report outline

An outline of the structure of the report is listed here. Chapter 2 gives background information about salinization itself (Chapter 2.1), the hydraulics behind turbulence and stratification (Chapter 2.2), (the development of) the modified weir (Chapter 2.3) and information about the Negenboerenpolder (Chapter 2.4). Chapter 3 describes the used method for the flume experiments (Chapter 3.1), field campaign (Chapter 3.2), and 2D simulations (Chapter 3.3). The results of the activities will be described in Chapter 4, divided over the first two sub-questions (Chapters 4.1 and 4.2). Chapter 5 will answer the third sub-question and gives recommendations for the implementation, based on this research. In Chapter 6, the research will be discussed and Chapter 7 gives the overall conclusion and recommendations for future research.



## 2 Background

This background chapter provides information about salinization in general (Chapter 2.1), the hydraulics in stratified polder canals (Chapter 2.2), the modified weir itself and its development (Chapter 2.3), and the study area which is taken as an example in this research (Chapter 2.4).

### 2.1 Salinization

In Chapter 1 the problem and relevance of salinization are discussed, and this section elaborates further on salinization itself. First, the mechanism behind salinization is described in more detail. Further, information about the observation and salinity is given. Salinity is the total salt concentration in a solution, which consists of (charged) ions [Corwin, 2003], hence this is a fast measurement method. The more ions present, the higher the salinity. With a higher salinity, more ions can conduct electricity, and the (electrical) conductivity will be larger. In this research, Electrical Conductivity (EC) is used as a measurement for salinity. An EC-value below  $2 \text{ mS/cm}$  is considered desirable (fresh enough) irrigation water. An EC-value above  $10 \text{ mS/cm}$ , water is considered saline and in between the two values, water is brackish.

#### 2.1.1 Mechanism

Salinization is the increase of salinity in surface water, the soil, or groundwater [Nederlandse Hydrologische Vereniging, 2002]. In polders in the North of The Netherlands, salinization happens when saline seepage from the Waddenzee comes underneath the dike (Figure 2). In other polders in the Netherlands, boils play a role [de Louw, Vandenbohede, et al., 2013]. Boils are preferential groundwater flow paths, caused by differences in soil characteristics [Hilgersom, 2017]. Cracks and low-resistance areas in the soil are excellent pathways for groundwater, which do not occur in the North of the Netherlands. In deep polders, boils often transport water from a deep (saline) aquifer, which is directly connected to the sea. The upward flux of saline seepage in the ditches is caused by a pressure difference in the water level (Figure 2). The boils deliver saline groundwater to canal beds in polders and sometimes even to the subsurface (Figure 6) [Hilgersom, 2017]. Boils can be detected by changes in temperature, but this is dependent on the season [Vandenbohede et al., 2014].

Other factors influencing salinization are land subsidence and incoming drains. Drains discharge in the ditches and can make the water quality even more saline. However, the salinity of these drains is heavily influenced by rainfall events [de Louw, Eeman, et al., 2013]. In case of heavy precipitation, drain water will be fresh and dilute the brackish polder canals. Further, relatively more saline seepage will come up in a polder with land subsidence [Pauw et al., 2012], as is visible in Figure 2. The water pressure from the sea is higher and the elevation is lower, so more saline seepage will be present.

#### 2.1.2 Observation

Salinity is the total salt concentration in a solution and consists of solved and dissolved salts, including (charged) ions [Corwin, 2003]. Weathering of rocks is the dominant source of these salts, other sources are human activities and atmospheric removal [Corwin and Yemoto, 2017]. Knowledge about the salinity of irrigation water is important for agriculture because it can reduce crop yield. For example, a high salinity makes it difficult for plants to extract water, the high salinity level influences the nutrients composition and soil permeability and can intoxicate the plant [Corwin, 2003]. For salinity, four main cations ( $Na^+$ ,  $K^+$ ,  $Mg^{2+}$  and  $Ca^{2+}$ ) and four main anions ( $Cl^-$ ,  $HCO_3^-$ ,  $SO_4^{2-}$

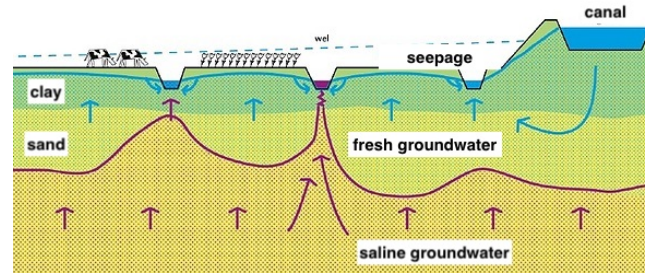


Figure 6: Schematic drawing of seepage coming up in a polder [Kalsbeek, 2014]

and  $CO_3^{2-}$ ) are important in a solution [Corwin and Yemoto, 2017]. The bicarbonate concentration ( $HCO_3^-$ ) in freshwater is usually higher than in saline seawater, while seawater usually has a higher sodium ( $Na^+$ ) and chloride ( $Cl^-$ ) concentration [Fondriest Environmental, Inc., 2014]. A detailed and direct analysis of the entire chemical composition of a solution gives a full insight but takes too much time and financial resources. In the field, the salinity is not measured directly, instead, it is derived from the Electrical Conductivity (EC) [Fondriest Environmental, Inc., 2014], this is a relatively fast method [Corwin and Yemoto, 2017]. The chemical position and total salt concentration of water, form together the EC [US Salinity Laboratory Staff, 1954].

In this research, the (electrical) conductivity of the water will be measured and used as a degree of salinity to compare water qualities. The conductivity shows how well water "conducts" electrical flow, this is directly related to the concentration of ions in the solution. Ions can pass electrical flow because they are positively or negatively charged. The ions that conduct well are chlorides, carbonate compounds, sulphides, and alkalis. Electrolytes are combined molecules that dissolve into ions, they split into cations (positively charged ions) and anions (negatively charged ions). Because the ions are charged, electrical flow can be passed easily. The conductivity of water will be higher, if there are more ions present in water. Saline water, and thus seawater, has a high conductivity [Fondriest Environmental, Inc., 2014]. The unit of conductivity is Siemens per metre, in this research, the unit milliSiemens per centimetre [ $mS/cm$ ] is used. As conductivity is heavily dependent on temperature, the Specific EC is used to compare measurements at different temperatures. The specific conductivity is the conductivity as if measured at 25 °C [Fondriest Environmental, Inc., 2014].

### 2.1.3 Salinity

There is no standard definition of fresh and saline water, it is often dependent on the use and purpose of the water. Various organisations, research institutes, and authors use different EC-values to indicate saline, brackish, and freshwater. In this research, the classifications in Tables 1 and 2 will be used, both show the general classifications for crop salt tolerance research in the Netherlands. The classifications are based on the measured electrical conductivity, these values are translated to corresponding chloride concentrations ( $mg/l$ ), as this unit is more often used in the Netherlands [de Olde, 2022]. Freshwater has an EC below 2  $mS/cm$  and saline water above 10  $mS/cm$ , brackish water has thus EC-values between 2 and 10  $mS/cm$ . From Table 1, the maximum chloride concentration of irrigation water is 2  $mS/cm$  (or 480  $mg/l$ ) [Vos et al., 2016]. Table 2 is a worldwide-used general soil salinity classification for the effect of various water qualities on crops [Vos et al., 2016].

Table 1: Classification of water based on EC and calculated corresponding Chloride concentrations [Adapted from Rhoades et al., 1992, and Vos et al., 2016]

Class	EC [ $mS/cm$ ]	Chloride [ $mg/l$ ]	Description
Non-saline	<0.7	<150	Drinking water and irrigation water
Slightly saline	0.7-2	150-480	Irrigation water
Moderately saline	2-10	480-2940	
Highly saline	10-25	2940-8250	
Very highly saline	25-45	8250-15970	
Brine	>45	>15970	Seawater=55 $mS/cm$ or 19,000 $mg/l$

Table 2: Soil salinity classes and crop growth [Adapted from Abrol et al., 1988, and Vos et al., 2016]

Soil salinity class	EC [ $mS/cm$ ]	Effect on crop plants
Non-saline	0-2	Salinity effects negligible
Slightly saline	2-4	Yields of sensitive crops may be restricted
Moderately saline	4-8	Yields of many crops are restricted
Strongly saline	8-16	Only tolerant crops yield satisfactorily
Very strongly saline	>16	Only a few very tolerant crops yield satisfactorily

Het Grondwaterzakboekje2016 [Bot, 2016] is a Dutch practical guide for geohydrologists. It describes the appearance and properties of fresh and saline groundwater and gives a couple of useful formulas for density, chloride concentration, and electrical conductivity. The relation between density [ $kg/m^3$ ] and chloride concentration [ $mg/l$ ] is shown in Equation 1. The North Sea has a chloride concentration of 32,000  $mg/l$ , which corresponds to 46  $mS/cm$ .

$$\rho \approx (1,000 + 25 \cdot \frac{[Cl^-]}{18630}) \quad (1)$$

Equation 2 applies to saline water ( $EC \geq 10 mS/cm$ ), for the relation between the chloride concentration in  $g/l$  and the Electrical Conductivity in  $mS/cm$  [Bot, 2016].

$$[Cl^-] \approx 0.37 \cdot EC \quad (2)$$

Equation 3 is another relation between the chloride concentration [ $g/L$ ] and the EC [ $mS/cm$ ], now based on groundwater samples [de Louw et al., 2011].

$$[Cl^-] = 0.36 \cdot EC - 0.45 \quad (3)$$

All water canals in the Netherlands also have to comply with ecological standards [Evers et al., 2018]. Most water canals of polders in the Dutch coastal zone are classified as 'M1b': these canals contain no fresh water, are buffered, and are often on marine clay. The standards of the water quality classification are based on the ecological potential, this has to be between the maximum and good ecological potential. The salinity, measured as the chloride concentration in  $mg/l$ , of an 'M1b' water canal has to be between 150 and 1000  $mg/l$  [Evers et al., 2018]. A chloride concentration of 150  $mg/l$  can be translated to an EC of 0.7  $mS/cm$ , and a chloride concentration of 1000  $mg/l$  is 3.5  $mS/cm$ .

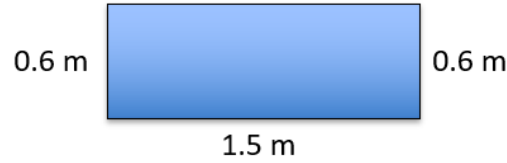


Figure 7: Water canal for the Reynolds Number example

## 2.2 Hydraulics

This background chapter will give a short introduction to the most important hydraulics basics needed for this research. For the working of the modified weir, turbulence is important, as this will possibly cause a mixing of fresh and brackish water and thus the loss of fresh water. The flow of water is influenced by various water works like culverts, weirs, and underflow gates, to control or transport the water. Further, the flow of water in a canal can be influenced by density differences over the water depth. These differences can be caused by temperature or salinity and create layers in the fluid. This is called stratification and is, for sure, found in oceans and ponds. Selective withdrawal could be used to discharge one of the layers.

### 2.2.1 Laminar and turbulent flow

For determining laminar and turbulent flow, the Reynolds number ( $Re$ ) is important, this is a dimensionless number. The Reynolds number is defined in Equation 4 [Westerweel, 2020] and is the ratio of the inertial forces to the viscous forces. In turbulent flows, inertial forces are dominant: these forces resist a change in the velocity of an object and cause movement of the fluid. In laminar flows, viscous forces play a role: they resist the flow [Simscale, 2021]. In this research the classification in Table 3 is used. Turbulent flow can cause the mixing of water, and prevent stratification. The dynamic viscosity for water is defined in Equation 5 [Viswanath et al., 1989]. In the grey text box below, the Reynolds Number for various water velocities is calculated for the water canal in Figure 7.

$$Re = \frac{\rho \cdot v \cdot R}{\mu} \quad (4)$$

$$\mu = 0.02939 \cdot e^{\frac{507.88}{(T-149.3)}} \quad (5)$$

Table 3: Reynolds numbers for flow regimes [Abdurrasheed et al., 2018; Westerweel, 2020; Simscale, 2021]

Flow type	Reynolds number $Re$
Laminar	$Re < 2300$
Transition zone	$2300 < Re < 4000$
Turbulent	$Re > 4000$

The water quality is assumed to be fresh, thus  $\rho = 1000 \text{ kg/m}^3$ , and the temperature is 293.15 K (20°C). The calculated Reynolds Numbers are translated to their flow type with Table 3.

The hydraulic radius R is calculated as follows:

$$R = \frac{\text{crosssectionalarea}}{\text{wettedperimeter}} = \frac{1.5 \cdot 0.6}{0.6 + 1.5 + 0.6} = \frac{1}{3} = 0.33$$

The dynamic viscosity  $\mu$  is calculated with Equation 5:

$$\mu = 0.02939 \cdot e^{\frac{507.88}{(293.15 - 149.3)}} = 1.0035 \cdot 10^{-3} \text{ Pa} \cdot \text{s}$$

Now, the Reynolds Number is calculated for four water velocities:

$$v = 0.001 \text{ m/s} : \text{Re} = \frac{1000 \cdot 0.001 \cdot \frac{1}{3}}{1.0035 \cdot 10^{-3}} = 332.1616 \rightarrow \text{LAMINAR}$$

$$v = 0.01 \text{ m/s} : \text{Re} = \frac{1000 \cdot 0.01 \cdot \frac{1}{3}}{1.0035 \cdot 10^{-3}} = 3321.616 \rightarrow \text{TRANSITION ZONE}$$

$$v = 0.1 \text{ m/s} : \text{Re} = \frac{1000 \cdot 0.1 \cdot \frac{1}{3}}{1.0035 \cdot 10^{-3}} = 33216.16 \rightarrow \text{TURBULENT}$$

$$v = 1 \text{ m/s} : \text{Re} = \frac{1000 \cdot 1 \cdot \frac{1}{3}}{1.0035 \cdot 10^{-3}} = 332161.6 \rightarrow \text{TURBULENT}$$

To conclude, the flow velocity of water should thus be low in order to avoid turbulent flow, and thus mixing of water.

### 2.2.2 Influences on water flow in a polder

The flow of water in a canal can be influenced by water works, and/or by external factors around and inside the channel. Examples of waterworks are weirs, culverts, and sluices. Sluices do not occur often in polders, but weirs and culverts can be found in abundance. Culverts are conveyance structures to transport water, and weirs are passive regulators, which deliver a constant water flow and work independently and without energy [Chappel, 2020]. Weirs are used to contain a certain water level in a canal, they are passive regulators with no movable parts in their structure and water flows over them. Most are built in a trapezoidal 'control notch' (Figure 8), to control the upstream water level and to ensure a constant water depth. The advantages are almost no maintenance and regulation, and that debris can pass the structure [Ankum, 2002]. However, the water in the water canal is also contracted in the horizontal direction.

In contrast, underflow gates are dependent on adjustments done by hand (manual regulators) [Ankum, 2002], and water flows underneath a vertical plate or obstruction. The opening under which the water flows can be increased or decreased by manually moving the slide gates up and down. The advantages are that the structure is simple and relatively cheap, sediment can be transported through the structure, and enough discharge can be provided downstream. Disadvantages are that measuring the discharge is difficult and that the structure does not allow the transport of waste and debris. The modified weir uses a gate under which saline water flows and this gate operate thus as an underflow gate. There are two types of underflow gates: a vertical gate for submerged underflow and a vertical gate for free underflow [Ankum, 2002]. As the water in a modified weir needs to be elevated again to pass the weir, the vertical gate is entirely submerged, and the flow will be fully-submerged underflow.

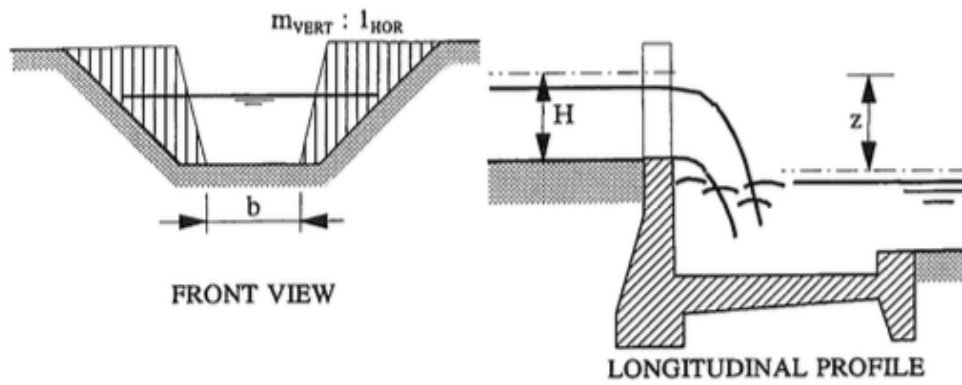


Figure 8: Design of a control notch [Ankum, 2002]

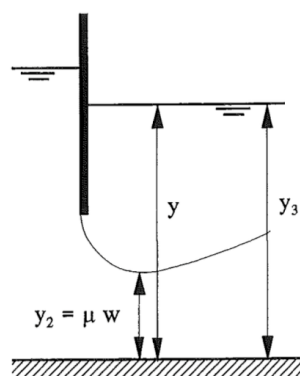


Figure 9: Submerged flow underneath a vertical gate [Ankum, 2002]

As stated before, external factors around and inside a canal can also influence the flow. The vegetation inside and around the canal can slow down or even block the water flow [Wang et al., 2015]. The amount of vegetation is partly dependent on the maintenance by the owner of the ditch. Most of the polder canals in the Netherlands are owned and thus maintained by the waterboards [Ministerie van Infrastructuur en Waterstaat, 2015]. Further, water canals in a polder are often used to store water for irrigation or to drain agricultural fields, but also to keep a high water level to suppress a seepage flux or to prevent peat oxidation. Multiple pumping stations manage the water levels in a polder, together with the previously discussed weir regulations. This causes a different water level in Summer and Winter, or a sudden inflow of (fresher) water and increasing water level.

### 2.2.3 Density stratified flow

The flow of fluids is sometimes affected by differences in density ( $\rho$ ), but this requires three conditions: the flow of the fluids is influenced by gravity, the fluid is incompressible, and the density differences are relatively small (Equation 6). These small differences in density can be caused by temperature, the number of dissolved substances (salt in water), and concentrations of suspended materials. Relative density differences caused by salinity are larger than differences caused by temperature variations [Schönfeld and Kranenburg, 1977]. In general, density stratification happens more in large rivers with a low slope, than in smaller and steeper streams [Wright and Parker, 2004].

$$\frac{\rho_{max} - \rho_{min}}{\rho} \ll 1 \quad (6)$$

If two liquids with different densities come in contact with each other without heavy mixing, the less dense (or lighter) fluid will flow on top of the heavier fluid because of gravity. As a result, stratification based on density differences appears. The change in density in the vertical direction can be gradual or with a jump. Density flow is thus the flow of two fluids with a small relative density difference (Equation 6) above each other. This stratification disappears because of mixing [Schönfeld and Kranenburg, 1977], possibly caused by turbulence. If the density decreases with the height, the density gradient is negative and will suppress possible turbulence [Schönfeld and Kranenburg, 1977] and thus stabilise the water layers.

The previously described stratification can be found in oceans, seas, and ponds [Poirrier, 1978; Yamaguchi and Suga, 2019; Li et al., 2020], these are large-scale environments with negligible changes in inflow and outflow. On a small scale, for example in polder canals, stratification is not expected because of smaller depths and continuous intensive management. Because of pumping and weir regulations, water will be in movement. As explained in Chapter 1, this research focuses on stratification by density (caused by salinity) on a small scale.

With the assumption of stratified flow and its characteristics, the modified weir is designed (Chapters 1.2 and 2.3). This weir uses selective withdrawal [Bryant and Wood, 1976], only one fluid with a specific density is drained from the canal. The upper layer (in this case, the freshwater layer) has a velocity of 0 m/s, and the maximum flow rate of the bottom one (here the brackish water layer) is what can be withdrawn without an acceleration of the upper layer [Schönfeld and Kranenburg, 1977].

## 2.3 The modified weir

This section gives a background to the modified weir, which is shortly introduced in Chapter 1.2. It can be used to store fresh water in a water canal and discharge the brackish water. The design is based on the density differences of two water qualities (Chapter 2.2). Waterboard Hoogheemraadschap Hollands Noorderkwartier implemented the first modified weirs on Texel, a Dutch island in the North Sea. Research is done to use the weir also in other areas in the Dutch North Sea region.

### 2.3.1 Development

The first 2D simulation for a modified weir was carried out by Svašek Hydraulics and Acacia Water, commissioned by Hoogheemraadschap Hollands Noorderkwartier [Groen et al., 2017]. The software used in this research was TUDflow3D, in which turbulent flow can be simulated. The modified weir is analysed with various dimensions and a constant summer and winter discharge at 20 m upstream of the weir. The exact input discharge conditions can be seen in Table 4. Fresh water is assumed to have a chloride concentration of 200 mg/l, and saline water has a chloride concentration of 10,000 mg/l. The geometric input for the design of the modified weirs is shown in Table 5.

Table 4: Overview of the input discharge parameters of a previous modelling study of the modified weir [Groen et al., 2017]

	<b>Boundary conditions</b>	<b>Initial condition</b>
<b>End of wet season (Winter)</b>	Saline water: 0.7 l/s Fresh water: 10 l/s	Sharp interface saline/fresh water Saline layer: 0.14 m
<b>Dry season (Spring)</b>	Saline water: 0.7 l/s Fresh water: 1.2 l/s	Sharp interface saline/fresh water Saline layer: 0.45 m

Table 5: Overview of the input design parameters of a previous modelling study of the modified weir [Groen et al., 2017]

	<b>Modified weir with underflow gate</b>
<b>Width canal (surface)</b>	3 m
<b>Width canal (bottom)</b>	1.5 m
<b>Water depth (middle)</b>	0.6 m
<b>Width crest normal weir</b>	1.5 m
<b>Type specific design parameters</b>	Height underflow gate: 7, 14, 28 cm Distance underflow gate and weir: 30, 100 cm

Based on this study, the most effective design is an underflow gate opening of 14 cm, and the distance between the underflow gate and the weir (30 or 100 cm) does not influence the effectiveness. The use of a modified weir will lead to a reduction of 50-85% of the salt amount in the canal. The working can possibly be influenced by branches blocking the opening. The study's results showed that the modified weir's effectiveness increased with a larger freshwater influx, until the point where the large influx will cause turbulence. At that point, the turbulence will lead to the mixing of the layered fresh and brackish water [Groen et al., 2017]. The study did not elaborate more on this.



### 2.3.2 Current situation

On the island of Texel (the Netherlands), modified weirs with the most optimal geometry based on the previously described modelling study, are implemented. The weirs can be useful on the island, as two pipes and precipitation are the only freshwater supply. Precipitation should be stored on the island to guarantee enough irrigation water [Acacia Water, 2020]. The modified weir is assumed to be the best solution for the future. TexelBeton, a company on the island, makes and sells ready-made concrete modified weirs from a mould (Figure 10) [TexelBeton, n.d.].

The concrete boxes have a circular hole in the backside, with which they can be connected to already existing drains (Figure 10b). The bottom level of the hole is the same as the bottom level of the concrete box. The size of the hole is dependent on the size of the drain to which it will be connected. However, no adjustments to the size, to fit the weir to a situation, can be made. The water levels can be manually regulated by adjusting the pieces of wood in the concrete box (Figure 10a). The geometry is based on the modelling research of Acacia Water and Svašek Hydraulics: the underflow gate opening is 14 cm and the distance between the weir plate and underflow gate is 30 cm [Groen et al., 2017; “Bezoek TexelBeton”, 2022]. Waterboard Hoogheemraadschap Hollands Noorderkwartier aimed to implement thirty concrete modified weirs from TexelBeton on Texel in 2022. Most (23) are built in polder 'Het Noorden', the remaining in polder Eijerland [de Boer, 2021; Hoogheemraadschap Hollands Noorderkwartier, 2022].



(a) Side view of the front of the concrete modified weir [TexelBeton, n.d.]



(b) Topview [Own picture, 2022]

Figure 10: Concrete modified weirs of TexelBeton

Experiments with innovations to store fresh water are done not only on Texel, similar developments are happening in the province of Zeeland (the Netherlands). The Grevelingen Lake and Oosterschelde are saline and this influences the liveability in the province. The salinization of groundwater has reached its critical point here. An earlier idea to make the lakes fresh was adapted (Figure 11). The design is similar to the modified weir but for a large-scale system. The same principle is used, denser saline water is discharged by a so-called “density-screen” [Redactie Waterforum, 2022].

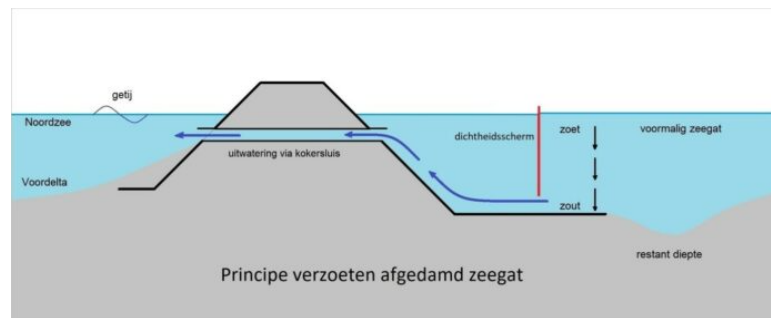


Figure 11: Displacement of saline water by pushing it to the sea (left) and inflow of fresh river water at the surface (Design Ir. W. Lases) [Redactie Waterforum, 2022]

## 2.4 Negenboerenpolder

The Negenboerenpolder is a polder in the province of Groningen in the Netherlands, it is located along the Wadden Sea coast (Figure 12). All the land in the polder is used for agriculture: potatoes, sugar beets, and wheat are most common. However, the location of the polder leads to salinization problems. Crops will be influenced by saline seepage and by irrigation from brackish ditches [de Olde, 2022]. The water system of the polder is straightforward: water flows from South to North and from East to West. The Negenboerenpolder is frequently researched by Acacia Water.

### 2.4.1 General

The Negenboerenpolder is a polder located in the north of the Netherlands, next to the Wadden Sea (Figure 12). The Lauwersmeer is situated west of the polder, and the villages Kloosterburen and Hornhuizen are south of the polder. As the polder is directly next to the Wadden Sea, it originates from a series of reclamations and was finalized in 1872. The Negenboerenpolder is part of the province of Groningen, and waterboard Noorderzijlvest manages the water system in the area [van Meijeren et al., 2019].

The history and origin of the Negenboerenpolder can be seen in the elevation map (Figure 13). The elevation range is between  $-0.968 \text{ mNAP}$  and  $9.548 \text{ mNAP}$  (at the dike) [PDOK, n.d.-a]. The layering and composition of the soil are typical for the natural sequence of reclaimed polders from the sea, the soil consists of clay and silt in various quantities. Heavier materials (heavy clay) can be found in the south of the polder, towards the north the materials become lighter (light zavel) [PDOK, n.d.-b]. This soil type is excellent for agriculture (de Bruijn, n.d.), which is the main land use in the Negenboerenpolder. Farmers live around the polder on the dikes and cultivate the fields in the polder. Nowadays, most of the crops in the area are seed potatoes, sugar beets, and wheat [van Meijeren et al., 2019]. Detailed maps of the land use and soil types can be found in Appendix B.

### 2.4.2 Water system

The flow direction of surface water in the Negenboerenpolder is shown in Figure 14. The polder water system has three inlets and two outlets. Water flows from south to north via primary water canals and goes to the outlets in the west. Secondary canals connect the primary water canals from south to



Figure 12: Location of the Negenboerenpolder next to the Wadden Sea [Adapted from Google Maps, n.d.]

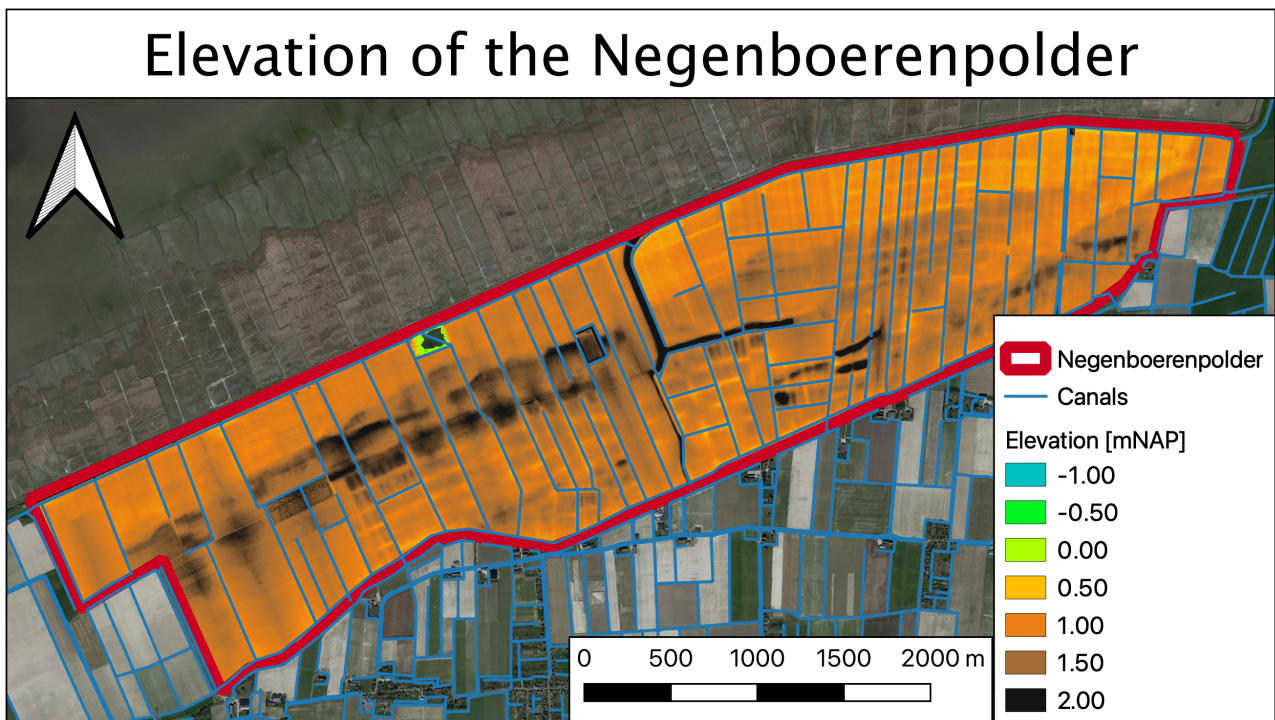


Figure 13: Elevation map of the Negenboerenpolder [PDOK, n.d.-a]

north [van Meijeren et al., 2019]. Artificial waterworks can also be found in the Negenboerenpolder. Culverts are located throughout the entire polder, and weirs at the inlet sides [van Meijeren et al., 2019]. The weirs are used by Waterboard Noorderzijlvest to keep a constant seasonal water level in the polder. In summer the water level is kept at  $-0.35$  *mNAP* as much as possible, and in the winter at  $-0.93$  *mNAP* [van Meijeren et al., 2019]. Most of the canals next to agricultural fields (tertiary canals) are dry in Summer. Their function is to discharge water from the fields, not to flush the canals.

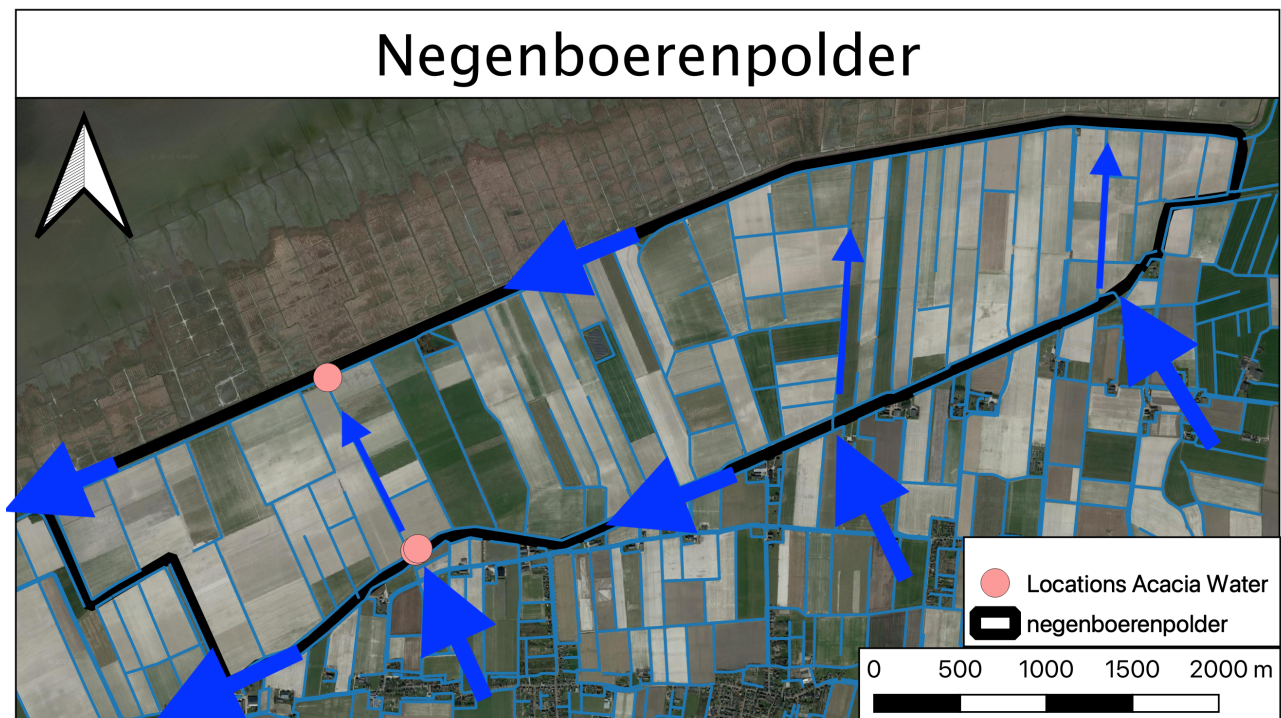


Figure 14: Flow direction of surface water in the Negenboerenpolder [Based on van Meijeren et al., 2019]

The Negenboerenpolder receives water from downstream polders, this is the water system of Pieterbuurstermaar. To ensure fresh enough irrigation water, the polder is frequently flushed by the Waterboard. By flushing, the brackish front, which has grown further inland in winter, is pushed back. In February, the waterboard starts with flushing the upstream water system. At the end of April and onward, also the Negenboerenpolder is flushed. Scenario studies with a water balance of Svašek Hydraulics and Acacia Water showed that when the flushing amount is two times smaller, the chloride concentration in the water canals of the polder will be around 30% higher [van Meijeren et al., 2019]. Flushing has thus a large positive effect on the water quality.

Inlet locations of Negenboerenpolder are at *Bokumerklief*, *Wierhuizerklief*, and *Hornhuizerklief* (Figure 14). *Bokumerklief* receives water from *Bokumertocht*, from here it flows to the east (through *Bokumertocht* and *Feddematocht*) or the west (through *Ikematocht* en *Seerattstocht*). *Wierhuizerklief* gets water from various eastern polders, which can influence the water quality negatively. From this inlet, water flows towards the north, through *Negenboerentocht*. Water then flows westwards to *Zulteriet* (or *Dijksloot*) and *Rotgansriet*, where it leaves the polder [van Meijeren et al., 2019]. *Hornhuizerklief* receives water from the polders south of the Negenboerenpolder, through *Julianatocht*.

Two major groundwater patterns can be found in the subsurface of the Negenboerenpolder. There is a (western) gradient from the Wadden Sea to the Lauwersmeer and another (southeastern) gradient towards Bedum, in the inland of Groningen. As stated multiple times, the polder is also exposed to seepage, which leads to increased chloride concentrations in groundwater. Also, the tides of the Wadden Sea are visible in the water quality of the polder water canals. This effect can especially be found in the Dijkslot along the dike, which separates the polder from the Wadden Sea [van Meijeren et al., 2019].

Agriculture also has an effect on the water quality in the Negenboerenpolder. The desirable salinity is  $3\text{ mS/cm}$ , this makes the chloride concentration about  $800\text{ mg/l}$ . Phosphate and nitrogen can be found in the surface water, because of fertilisation and atmospheric deposition. It can be noticed that the nitrogen concentrations are related to the dominant water type in the canal and to the season. Drainage water, seepage water, and inlet water all contain different nitrogen concentrations. In winter, the concentrations are much higher than in summer. On the other hand, phosphate has low concentrations in winter and high during summer [van Meijeren et al., 2019].

### 2.4.3 Challenges

The location of the Negenboerenpolder directly next to the Negenboerenpolder causes already salinization problems [Boeren Meten Water, n.d.; LTO Noord, 2021]. The entire polder consists of agricultural land, so the land is extremely valuable for the farmers who cultivate the land. Salinization is thus already a treat to the Negenboerenpolder, but this will be even larger in the future. A corresponding problem is the availability of fresh water in the polder. Needless to say, salinization reduces the quality of the surface water, which is used for the irrigation of crops. However, the polder is relatively elevated in comparison to the south of the province of Groningen. That means that water naturally drains away from the polder and needs to be pumped towards the area. Because of the large distance from the IJsselmeer, the Negenboerenpolder gets fresh water as one of the last ones and this water can already be polluted after being used by other areas. In the ideal situation, fresh (precipitation) water is stored in the Negenboerenpolder itself, to use for irrigation when needed.

### 2.4.4 Projects and motivation

The Negenboerenpolder is frequently used for research. Previous projects by Acacia Water in the polder were *Boeren Meten Water* [Acacia Institute and LTO Noord, n.d.] and *Spaarwater* [Acacia Institute, 2022]. *Boeren Meten Water* was used to gain insight into the problems of salinization and land subsidence in the areas. Two new measurement instruments (AquaPin and AquaMobile), developed by Acacia Water, were used in this project [Acacia Institute and LTO Noord, n.d.]. The purpose of the *Spaarwater* project was to research cost-effective and sustainable agricultural water usage in areas with salinization. The Negenboerenpolder was recommended by Waterboard Noorderzijlvest as it already has problems with salinization and because of the compact structure of the (water system of the) polder [Acacia Institute, 2022].

Current research in the polder is done by Tennet [Conijn and Albers-Schouten, 2020] and Acacia Water (*Zoet op Zout*, [Acacia Institute, 2021]). Tennet manages the high-voltage grid of the Netherlands and parts of Germany. A new wind farm is built in the North Sea and this field needs a connection to the power plants on the Dutch mainland next to the city of Groningen. Tennet investigates possible effects of the cable, it is possible that the cable contributes to salinization [Conijn and Albers-Schouten,

2020]. The project *Zoet op Zout* is the follow-up of the *Spaarwater* project. The aim of the project is to investigate and gain insight into what is technically and agriculturally possible to prevent damage by salinization.

In this research, the Negenboerenpolder is chosen, because of the connection with Acacia Water. The company already has contacts in the polder, measurement locations, previous data series, and background information.

## 3 Method

In this chapter, the sub-questions of Chapter 1.4 are translated to actions. The activities are divided into three categories: flume experiments (Chapter 3.1), field measurements (Chapter 3.2), and 2D simulations (Chapter 3.3). The combination of methods gives insight into the situation of the polder and the theoretical and practical knowledge about the working of the modified weir.

### 3.1 Flume experiments

This chapter describes the motivation and methodology of the flume experiments: why they are performed (Chapter 3.1.1), and the design (Chapter 3.1.2) and process of the experiments (Chapter 3.1.3). The flume experiments gave the opportunity to test the principle of a modified weir, how to build such a weir in practice, and test what does and does not work. The main purpose of the experiments was to gain insight into the set-up of a modified weir, not to create a reliable experimental dataset.

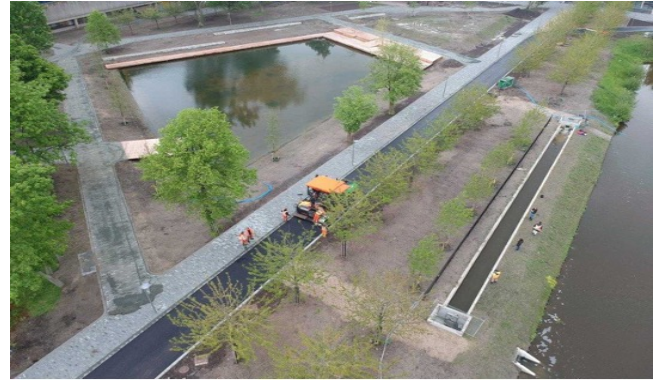
#### 3.1.1 Motivation

In this research, flume experiments with the modified weir are performed to gain insight into a real-life field setup. Earlier, a model study of the modified weir is carried out, as referred to in Chapter 2.3.1. This setup is already in use on Texel (Chapter 2.3.2). However, no experimental research is done with the modified weir and this gives a knowledge gap in the practical working of the weir. Seven flume experiments are performed between April 2022 and July 2022. The exact set-up of the flume experiments was an iterative process, it was modified every time. The starting setup was developed by Dr.ir. O.A.C. Hoes, based on an actual polder water canal and to test a larger distance between the underflow gate and weir. The wooden construction can be seen in Figure 16, with the dimensions in *mm*. In Chapter 3.1.3 the process is described. The input can also be seen in Table 6 and Appendix E contains an extended version of Table 6.

#### 3.1.2 Design of experiments

All flume experiments were carried out in the flume outside in the TU Delft campus area (Figure 15). This flume has a length of 40 *m*, a depth of 1.5 *m*, and a width of 1.5 *m* and is made of concrete (Figure 15a). The picture in Figure 15a is taken upstream of the flume. The amount of inlet water can be adjusted by opening and closing the movable weir upstream. However, it is unknown what the exact inlet discharge is. Figure 15b shows the area around the flume, water in the upper left lake is connected to the upstream part of the flume (bottom side of Figure 15a). Water flows via the flume over a movable weir towards the lake on the bottom right side of Figure 15b. This lake is part of the polder water system of Waterboard Hoogheemraadschap van Delfland. The lake on the upper left side of Figure 15b contains 700 *m*<sup>3</sup> water over a depth of 0.25 *m*.

During the experiments, the wooden construction (Figure 16) was at 20 *m* downstream from the inlet. Figure 17 shows a side view of the set-up. The opening of the underflow gate (5 *cm*) and the height of the weir (25 *cm*) were the same during all experiments. Electrical Conductivity (EC) meters (Figure 18) are used to measure the conductivity in *mS/cm*. It is unknown when was the last time the meters were calibrated, so the exact measured numbers are not reliable. The purpose of measuring during the experiment was to give insight into the change in numbers at various locations and depths in the flume.



(a) Flume, with the construction, outside on the campus of the TU Delft [Own picture, 2022]

(b) Top view of the flume area on the TU Delft campus [Hoes, 2022]

Figure 15: Flume used for the experiments on the campus of the TU Delft

Fluorescein ( $C_{20}H_{12}O_5$ ) was used during the experiments. Adding the powder to water will lead to a yellow tracer colour, which can be tracked easily. Fluorescein was added to fresh water in weeks 2 and 3, and to saline water in weeks 5, 6, and 7.

### 3.1.3 Method and process

The first experiment started with setting up the experiment as previously described. The end weir of the concrete flume was set at 0 cm and a water layer of about 15 cm was formed before the weir. Four large buckets, located inside the concrete flume upstream of the weir, were filled with water from the lake (EC around 900 mS/cm) and in total 18 kg kitchen salt (NaCl). The salt is dissolved entirely by manually mixing.

A ramp was implemented to let fresh inlet water flow gently on the brackish layer. During the first experiment, the height of the ramp is 25 cm (the same as the weir of the wooden construction) at +/- 4 m downstream from the inlet. Consequently, the buckets were knocked over to create a brackish water layer of 15 cm. Then the inlet of the flume (with fresh water) was turned on to build a fresh-water layer of 10 cm on top of the brackish water layer. However, when the water level was rising too fast during the experiment, the inlet was turned off and turned on again later. In this experiment, three EC-meters were used and located upstream, inside, and downstream of the wooden construction.

In the second experiment, two adaptations were made. The end weir of the concrete flume was set at 15 cm to create pressure on the construction from the downstream side to prevent leakage. The ramp was now located directly underneath the inlet with a height of 15 cm, but now fresh water was flowing directly into the saline layer. During the third experiment, the height of the ramp was variable, and it was located 5 m from the inlet. The ramp was raised together with the water level in the flume.



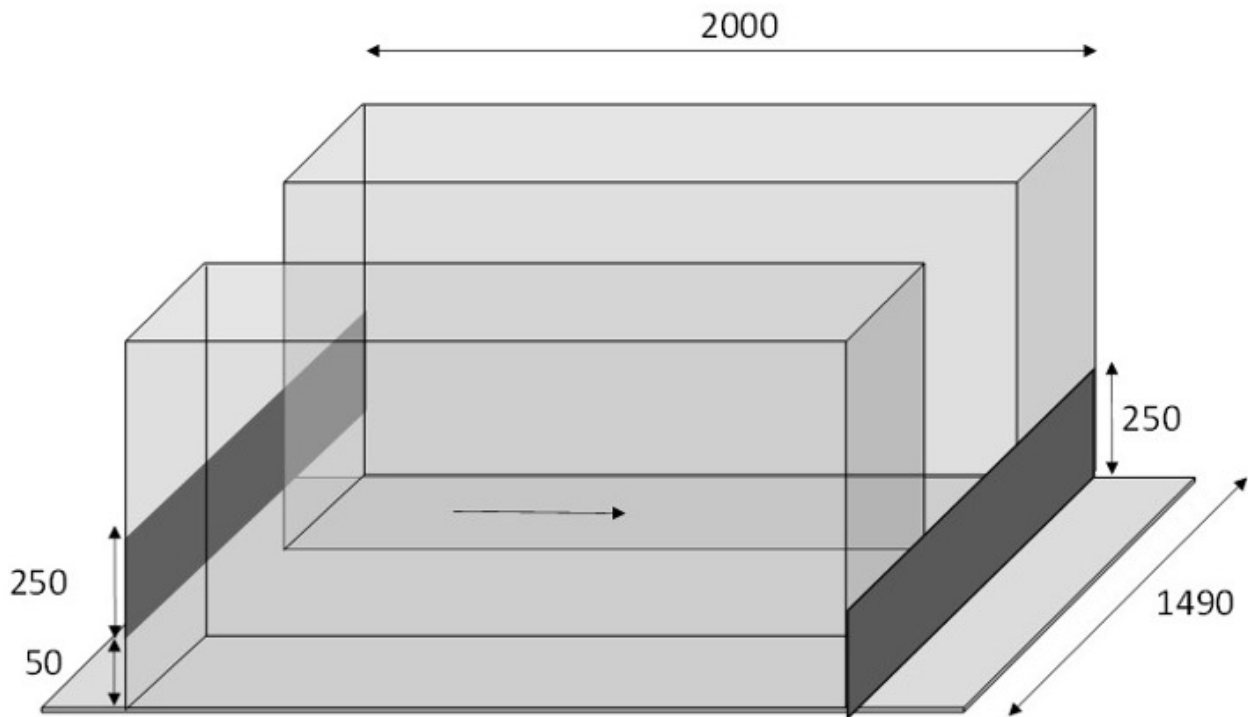


Figure 16: Wooden construction used for the flume experiments (dimensions in *mm*) [Hoes, 2022]

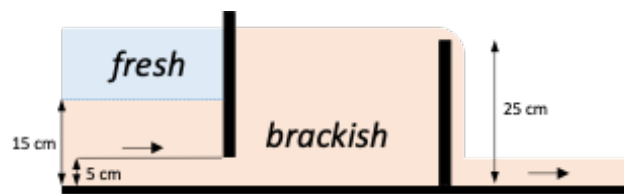


Figure 17: Side view with the set-up of the flume experiments [Hoes, 2022]



Figure 18: Used EC meter during the flume experiments [Profishop, n.d.]

Further, a waterfall was created directly underneath the inlet to make sure that inlet water was flowing slowly and steadily into the concrete flume. However, this was a lot of work and not a handy, reliable setup. An important observation was that the EC value was extremely high exactly in front of the ground plate of 1 *cm*, so the most saline water is probably 'stuck' behind the ground plate. During the fourth experiment, it was raining, so the input, set-up, and observations were not written down. This explains the question marks in Tables 6, 12, and 13 (Appendix F).

Table 6: Short overview of practical input for all flume experiments

	Date	Ground plate	Method	Inlet	Ramp	EC meters
1	April 22, 2022	Yes	Buckets	High, but on/off	Yes	3
2	April 29, 2022	Yes	Buckets	Slow and constant	Yes	3
3	May 13, 2022	Yes	Buckets	Slow and constant, buckets underneath inlet to create waterfall	Yes	5
4	May 20, 2022	No	Buckets	?	?	3
5	June 3, 2022	No	Tubes	Slow and constant	No	3
6	June 10, 2022	No	Tubes	Variable: high, slow and on/off	No	3
7	July 25, 2022	No	Tubes	Slow, but on/off	No	3

During experiments 5, 6, and 7, the salt addition method described in the previous section was changed. With this method, saline water was put underneath freshwater. The benefit of this method is that there is now a constant brackish water inflow, together with the constant freshwater inflow from the inlet. The experiment starts the same, but the four buckets now stay at the sides. The tracer Fluorescein is put into the buckets together with an amount of salt and fresh water from the close by lake. Transparent tubes with a diameter of 1 *cm* are used, and one end is put in the bucket. The other end is put underneath a stone at the bottom of the concrete flume. By suction on this end of the tube, holding this end closed and putting it on the bottom, a saline water flow is created from the bucket to the bottom of the flume. A height difference of around 2.5 *m* is bridged this way. During experiment 5, the tubes were located 5 *m* upstream of the wooden construction in the concrete flume. In experiment 6, they were located further upstream (at 10 *m*). And during experiment 7, the tubes were at 8 *m* upstream of the wooden construction.

In the first four experiments, the measuring of the Electrical Conductivity started when the freshwater inlet was turned on. From experiment 5 onward (when the salt addition method changed), the measuring started when fluorescent saline water was flowing into the concrete flume. The measuring time was different in every experiment. The longest measuring time was 53 *minutes* (experiment 6) and the shortest was 13.5 *minutes* (experiment 4, because of the weather), with an average of 27 *minutes*. Every 30 *seconds*, the EC value on all EC meters was written down.

## 3.2 Field campaign

For sub-question 1, field measurements are done in and around the Negenboerenpolder, this chapter describes the methods used during the field campaign. The objective was to investigate the current situation of fresh and brackish water in the polder, on the local (Chapter 3.2.1), spatial (Chapters 3.2.2), and temporal (Chapter 3.2.3) scale. Combining the measurements gave insight into the fresh and brackish water distribution of the Negenboerenpolder, but can also be used as a demonstration that the EC can differ over the depth in a polder canal, which can indicate stratification.

### 3.2.1 Depth profiles

This method is used to investigate if the electrical conductivity varies over the depth in and around the Negenboerenpolder. It gives insight into the fresh and brackish water distribution at the local scale and indicates if stratification of different water qualities is present at the locations. For this method, the conductivity at various depths in a water column is measured to create a depth profile. At four locations in and around the Negenboerenpolder (Figure 19) these profiles are made. The locations have different water levels and elevations, so the depth profiles are local and relative to the local water depth. The purple dot in the figure is named 'Around weir', here two measurements are carried out: one directly upstream and one downstream of the weir. 'Waddenweg South' is done in the south part of a vertical water canal, close to a road called Waddenweg. 'Eendenkooi culvert' is a measurement location outside the Negenboerenpolder close to the duck cage 'Nieuw Onrust', the depth profile is made next to the inlet of a culvert. The location is directly next to the dike with the Wadden Sea and one of the outlets of one part of a water system, managed by Waterschap Noorderzijlvest.

For the measurements, an EC meter from Acacia Water (Figure 20) was used: the 'WTW Cond 3110' [WTW, 2022], this meter was recently calibrated. Along the cord of the conductivity meter, yellow tapes indicate five *cm* (Figure 20a) to measure the conductivity every five *cm* along the water depth (Figure 20b). The EC values are written down in *mS/cm*, together with the temperature in °C. The results of the temperature measurements will be included in Appendix G, as they are less important than the EC values, which can be found in Chapter 4.1.1.

### 3.2.2 Transects

At two depths along a water canal the EC (and temperature, Appendix I) is measured to investigate the variation. If there is a difference between the two measurements, it can be an indication of stratification. The measurements give insight into the fresh and brackish water distribution and possible stratification on the spatial scale, the results can be found in Chapter 4.1.2. To prevent that the same water depth is measured twice, shallow measurements are done just below the water surface, and deep measurements are done at the bottom of the canal. The bottom measurement was sometimes difficult because of duckweed. Further, it is important to carry out first the surface measurements and then the bottom measurements, to prevent mixing and the loss of possible stratification.

The measurements are executed with an AquaMobile Handheld developed by Acacia Water [Fixeau, n.d.-a], the numbers can be seen directly in the field with the Fixeau app on a mobile phone and will be uploaded to the Fixeau dashboard [Fixeau, n.d.-b]. The locations of the transects can be seen in Figure 21, these locations are based on an earlier EC-routing in August 2021 (Appendix C). The two chosen water canals for the measurements are a dead end of the canal along the Wadden Sea dike (Dijksloot) and a vertical water canal, directly next to a road called Waddenweg.

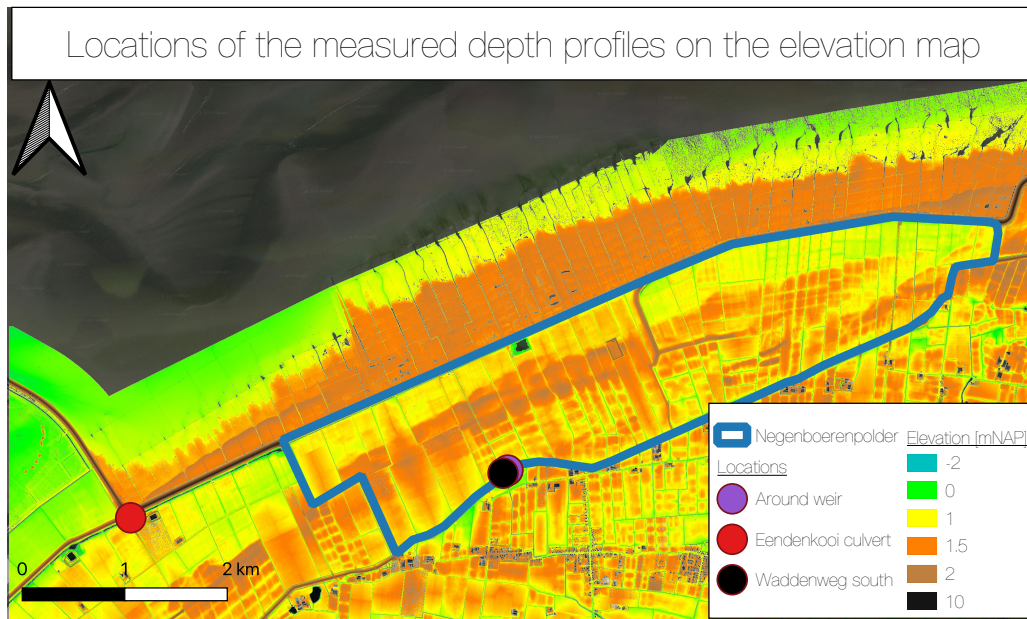


Figure 19: Locations of the measured profiles over the depth



(a) Attaching the yellow tape to the cord [Own picture, 2022] (b) Measuring the conductivity over the depth using the yellow stripes [Own picture, 2022]

Figure 20: Conductivity meter with yellow stripes used for the measurements of the depth profiles

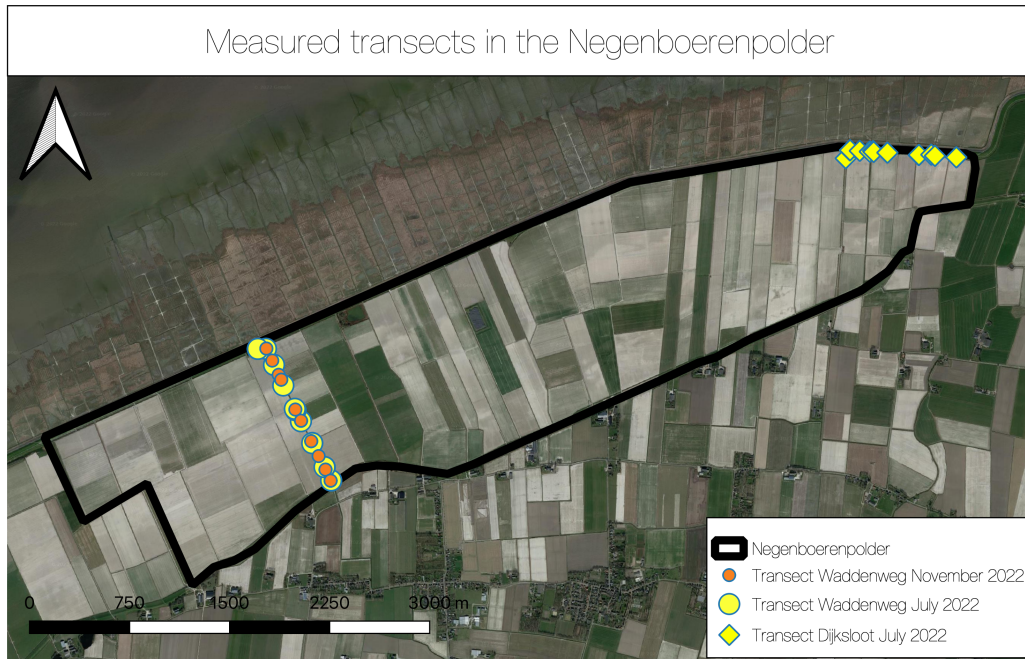


Figure 21: Locations of the measured transects in the Negenboerenpolder

The transect 'Dijkslot' is indicated with yellow diamonds in Figure 21, these measurements are performed on July 13th, 2022. This part of the polder is a dead end and not flushed by Waterboard Noorderzijlvest, this means that the water canal is exposed to brackish seepage from the Wadden Sea. In earlier research [van Meijeren et al., 2019], it is stated that the water quality in this part is quite brackish, which makes it an interesting transect to measure. However, this part of the Dijkslot is interrupted by three culverts. The culverts are at a distance of 180 m, 500 m, and 700 m. The start of the transect is at a Waterboard maintenance shed.

The transect 'Waddenweg' is indicated with yellow and orange dots in Figure 21. The yellow dots are measurements performed on July 14th, 2022, the orange dots are measurements of November 2nd, 2022. This canal is used as a flushing canal by Waterboard Noorderzijlvest and has a north-south orientation. The transect is interesting because the canal is in the middle of two agricultural fields. The start of this transect is the southern side of the canal, close to inlet Hornhuizerklief, which is also used for a depth profiles measurement (Chapter 3.2.1). The canal discharges in the Dijkslot at the North, which is the end of the transect.

When looking at the elevation map (Figure 13) an elevated area in the middle of the polder can be noticed, the Waddenweg transect cuts through this area. This elevated area is an old dike and can possibly influence the groundwater flow and water quality. The elevated area is between 300 and 800 m from the starting location, with the highest elevation around 600 m. However, in Autumn 2022 this elevated area is removed from the landscape by Waterboard Noorderzijlvest.

### 3.2.3 Continuous data series

For the temporal scale, results of continuous measurements are used. Figure 22 shows three measurement locations in the Negenboerenpolder, they are measuring every 15 *minutes*. Here two sensors are installed to measure the conductivity at two depths in the water column. One sensor measures the conductivity at the surface and the other measures the conductivity at the bottom. One measurement location is called 'Lutjewat' and is located in the Dijkstoot, on the north side of the polder. The other two measurement locations are on the south side of the polder. They are located around the weir, one downstream ('Downstream') and one upstream of the weir ('Upstream'). One sensor at Lutjewat and one sensor downstream of the weir are installed for the *Spaarwater* project by Acacia Water [Acacia Institute, 2022]. For the project *Zoet op Zout* [Acacia Institute, 2021] and this research, a third location ('Upstream') with two sensors is added, together with extra sensors at the other two locations. At the beginning of December, the weir is relocated by Waterboard Noorderzijlvest.

An overview of the measuring periods at the three locations can be found in Table 7. The periods are not consecutive, because of empty batteries and malfunctioning of the equipment. At the start of Period 1 (Table 7), two extra sensors are installed at the locations 'Lutjewat' and 'Downstream', and both sensors are installed at 'Upstream'. The end was chosen, because the water levels changed, and the sensors became above the water surface. At the beginning of November 2022, the sensors were relocated (Period 2). The sensor 'Downstream' did not start measuring and sending data, the equipment is probably broken. The weir in the Negenboerenpolder was relocated at the beginning of December 2022 and the sensor 'Upstream' was attached to it, so the end date of this period is December 1, 2022. During the time periods in Table 7, the EC is measured at two depths at all three locations. The water temperature and the water pressure above the sensor are measured here too. With the water pressure and the dimensions of the set-up, the water level and thus the depth of the sensors can be obtained. The water depths are translated to *mNAP*, to be able to compare them to each other.

Table 7: Overview of measurement locations and measuring periods

Location	Start Period 1	End Period 1	Start Period 2	End Period 2
Lutjewat	August 24, 2022	September 17, 2022	November 3, 2022	December 1, 2022
Upstream	July 14, 2022	September 17, 2022	November 3, 2022	December 1, 2022
Downstream	July 13, 2022	September 17, 2022		

Table 8 shows the difference between the surface and bottom sensors in meters. Period 2 started after a field visit to change the depths. The water levels in the polder were set to the lower winter levels, so the upper sensor was not measuring water any more. The measurement location 'Lutjewat' did not have a change in sensor depths, as the water level was low, and the sensors were already quite close to each other. Appendix D shows schematic drawings of the sensor depths at the three locations.

The continuous data series are analysed and indications of stratification are described, but this is not always visible (Chapter 2.2.2). A comparison is made of the water levels with factors possibly influencing the variations in conductivity. The pumping data could not be taken into account, due to too late delivery of the data. The patterns of the tides in the North Sea and precipitation are also possible factors. These last two will be compared to the continuous conductivity measurements in the Negenboerenpolder. It will be investigated if a similar pattern can be observed in the data series.

Table 8: Overview of difference between shallow and deep sensors at the measurement locations

Location	Period 1	Period 2
Lutjewat	0.28 m	0.28 m
Upstream	0.60 m	0.25 m
Downstream	0.36 m	0.21 m

For the tides, the Rijkswaterstaat measurement location at Lauwersoog is used, this is around 10 km West of the Negenboerenpolder [Rijkswaterstaat, n.d.]. The tides are measured every ten *minutes* in *mNAP*. With high tides, more seepage can occur, which can cause higher water levels or increased conductivity levels in the polder. For the precipitation, the data from the KNMI weather station at Lauwersoog is used. Both the hourly [KNMI, n.d.-b] and daily precipitation data [KNMI, n.d.-a] are used for the analysis. The comparison with precipitation is useful to investigate if the conductivity levels decrease during or after periods with high precipitation, because of the flushing of the canals.

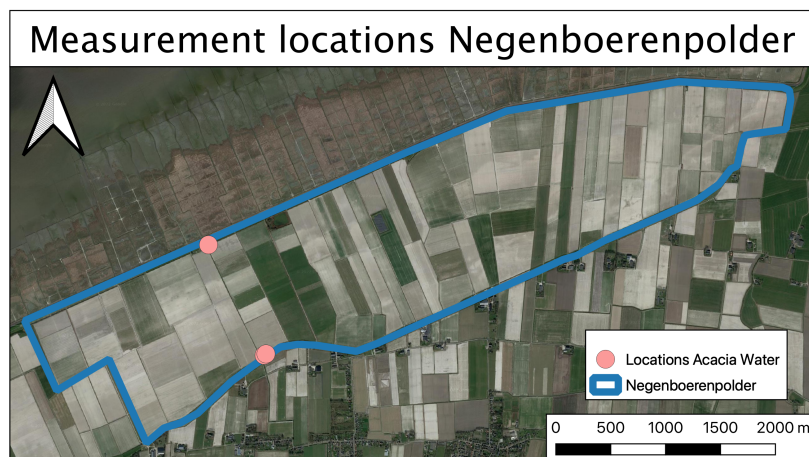


Figure 22: Locations of the continuous measurement locations in the Negenboerenpolder

### 3.3 2D simulations

In this research, 2D simulations are used to study the functioning of a modified weir, and the CFD software ANSYS Fluent is used [ANSYS Inc., 2023]. This chapter contains an overview of the input and settings of the software. The goal is a 2D ANSYS Fluent model of a modified weir to analyse three cases. For the first case, the functioning of a traditional weir and a modified weir in a real situation are analysed. The second case compares two velocities, and the third case compares two geometries. The results of the CFD modelling will be considered as indications, and not as hard results about the working of a modified weir. One reason is that the theory is never predicting practice completely because of the many variables. The second reason is that there was limited time and knowledge of ANSYS Fluent and Computational Fluid Dynamics (CFD).

### 3.3.1 Theory

To investigate the working of a modified weir, Computational Fluid Dynamics (CFD) modelling is used. CFD uses numerical analysis to simulate and predict the behaviour of fluids, it can thus analyse and solve fluid problems [ScienceDirect, 2023]. However, the use of CFD in the modelling of hydraulic structures with a free surface is relatively new. Sixteen years ago, the software was not good enough to model these flows [Hargreaves et al., 2007]. In recent years, numerical modelling has imitated experiments with open channel flow, this demonstrates that CFD can be used to model the flow over a weir [Naik et al., 2017]. CFD can also help the analysis of fluid flow because the software can deal with aspects of fluid flow which are difficult to observe during experiments [Naik et al., 2017].

Computational Fluid Dynamics uses applied mathematics, physics, and computational software to visualize how fluids flow, and how they flow past an object. The flow is approximated with numerical modelling, for this a discretization method is needed. This method approximates the differential equations by a system of algebraic equations, which can be solved by a computer. The approximations are done to small lengths or time steps. The accuracy of the discretization, and thus the CFD model, is dependent on the quality of the used discretization [Ferziger and Peric, 2002].

In this research the CFD software ANSYS Fluent is used [ANSYS Inc., 2023], this was available through TU Delft. The software is used in Mechanical Engineering at TU Delft to investigate the use of a bubble screen to counter the salt tongue in sluices [Feng, 2019], another CFD model (STAR-CCM+) is used to analyse selective withdrawal of saline water at a sluice at TU Eindhoven [Maijvis, 2022]. The CFD software ANSYS Fluent is used, to investigate if it can be used for such problems. Modelling with ANSYS Fluent consists of three stages: pre-processing, solving, and post-processing [Versteeg and Malalasekera, 2007; Naik et al., 2017]. The components of pre-processing are geometry, mesh, and boundary conditions. In the second stage, a simulation set-up is made, and results are visualized and analysed during the last stage [Naik et al., 2017].

### 3.3.2 Geometry and boundary conditions

2D designs with and without a modified weir for the cases are made in the DesignModeller of ANSYS Fluent. Figure 23 shows one of the designs (geometry 2). Fresh water flows into the design by a pressure inlet, such an inlet is used for buoyancy-driven flows [ANSYS Inc., 2009d]. As the open channel setting is turned on, a free surface level, bottom level, and velocity need to be chosen. In this research, the free surface level is  $0.35\text{ m}$  and the bottom water level is  $0\text{ m}$ . An inlet velocity of  $0.01\text{ m/s}$  is used for freshwater, and the inlet velocity of saline water is  $0\text{ m/s}$ . This freshwater velocity is fast enough to make the flow visible and should prevent turbulent flow (see example in Chapter 2.2.1). However, a velocity of  $0.01\text{ m/s}$  is not realistic for a polder water canal. A maximum flow velocity is  $0.1\text{-}0.2\text{ m/s}$  is more common [Hoes and vd Giesen, 2015], but this will probably lead to turbulent flow.

The outlet boundary condition is a pressure outlet, and for open channel flow again a free surface level and bottom level need to be chosen. At the outlet, the free surface level is  $0.2\text{ m}$  and the bottom water level is  $0\text{ m}$ . The part of the design which is in contact with air (blue area) is given a pressure outlet, it is given the default value of  $0\text{ Pa}$ . In this design, the height of the underflow gate is  $0.10\text{ m}$  and the distance between the underflow gate and the weir is  $2\text{ m}$ . This distance is based on the experimental setup. The chosen water levels are realistic for polder water canals, the height of the underflow gate is a guess based on the water level. Figure 23 shows geometry 2, mentioned in the overview of the cases (Table 11). Figure 24 contains an explanatory legend of the geometry and boundary conditions.





Figure 23: Geometry 2 of the 2D CFD model in ANSYS Fluent

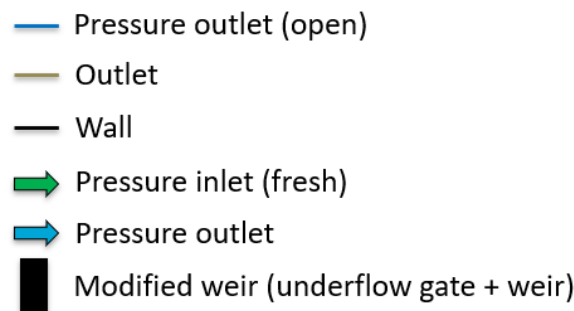


Figure 24: Legend with boundary conditions of the CFD model in ANSYS Fluent

The geometry in Figure 23 is based on a winter situation in the polder. The water depth (0.35 m) is shallow to ensure the discharge of stormwater. As there is no flushing in winter, saline seepage is present and the saline layer is thick. The distance of 20 m is chosen to investigate the stratification upstream of the modified weir. The opening of the underflow gate in this design is 0.1 m to make the flow around it visible in the results, an opening of 0.05 m (flume experiments) would be too small.

For the modelling of a modified weir, two water qualities are needed: fresh and brackish/saline water. Both are the same liquid and in the same state ('liquid water'), but they have different densities. However, a variation in density cannot be implemented in ANSYS directly, this density difference needs to be translated to a temperature difference, based on the Boussinesq approximation [ANSYS Inc., 2009a]. The Boussinesq approximation in formula form can be seen in Equation 7, Table 9 shows the parameter values for this equation. The value for  $T$  in the blue square in Table 9, can be calculated with the other values in said table.  $T_0$  in the equation is a guessed temperature for fresh water, which is needed to calculate the temperature of saline water ( $T$ ). The density given to saline water is  $1025 \text{ kg/m}^3$ , which is the density of seawater and too dense for brackish water. However, a large difference between fresh and saline is needed to make them visible in the model.

Three fluids are indicated in the Materials section of ANSYS Fluent: air, freshwater, and saline water. The standard set-up for air is used, but for both fresh and saline water some adaptations to the standard set-up of water, are made. Separate densities  $\rho$ , temperatures  $T$ , and thermal expansion coefficients  $\beta$  are filled in, to distinguish fresh and saline water in ANSYS Fluent. As fresh and saline water are two different fluids, mixing the two cannot happen in the model and this is unrealistic.

$$(\rho - \rho_0) \approx -\rho_0 \cdot \beta \cdot (T - T_0) \cdot g \quad (7)$$

Table 9: Input and answer for Equation 7

Parameter	Value
$\rho$	1025 kg/m <sup>3</sup>
$\rho_0$	1000 kg/m <sup>3</sup>
$\beta=1/T_0$	3.41 · 10 <sup>-3</sup>
$T$	285.68 K
$T_0$	293.15 K

### 3.3.3 Mesh and time step

The geometry in Figure 23 is divided into cells and nodes, this is called discretization. The fluid flow equations for momentum and continuity are solved based on the discretization, and variables are calculated numerically for each cell. ANSYS Fluent saves the variables on the nodes [Naik et al., 2017]. To check the mesh quality, the Courant number  $C$  can be used. This number is a measure of how fast quick data travels across the grid [Maijvis, 2022]. The Courant number is calculated with Equation 8 [Courant et al., 1928], the maximum Courant number  $C_{max}$  is 0.70.

$$C = \frac{v \cdot \Delta t}{\Delta x} \leq C_{max} \quad (8)$$

Table 10 contains the used values for the mesh creation and the calculation of the Courant number. A mesh was made in ANSYS Fluent with the following settings. The element size is set at  $\Delta x = 0.01$  m with a high smoothing. Capture curvature and capture proximity were turned on, with a minimum of  $1 \cdot 10^{-4}$  m. Now, a grid with 121,440 nodes and 119,300 elements is created for geometry 2. The average surface area of this geometry is 11.93 m<sup>2</sup>. Specific areas of the mesh are selected with Named Selection, and given a name to recognise the areas. The mesh is divided into the following areas: outlet, ambient, inlet-fresh, and wall. The default Courant number in ANSYS Fluent is 0.25, so with this and the chosen velocity and grid size, the needed time step size  $\Delta t$  can be calculated.

Table 10: Input parameters for mesh and time

Parameter	Value
Grid size $\Delta x$	0.01 m
Time step size $\Delta t$	0.01 s
Number of time steps $\Sigma t$	5000
Max Iterations/Time step	20
$C$	0.25
Full simulation time	50 s
Reporting Interval	1
Profile Update Interval	1

### 3.3.4 Simulation set-up

This section contains the simulation set-up in the shape of multiple lists. It can be read as a manual about how to reproduce the simulations done for this research and why some settings are chosen. First, some general settings:

- The pressure-based solver is chosen instead of the density-based solver. The reason for this is that the used solver is for incompressible flow, where the density is assumed to be constant [Quora, 2023]. The fluids in the CFD model have a constant density of either entirely fresh or entirely saline.
- Transient flow was chosen, because the flow parameters are varying in time [Naik et al., 2017].
- Gravity is turned on and a value of -9.81 is entered for the Z-axis. The z-direction is used because gravity operates in this direction. However, it moves downwards, so a minus is put in front of the value [Naik et al., 2017].
- Operating Conditions: Operating Pressure = 101325 Pa, Reference Pressure Location Y = 0.6 m
- Boussinesq Parameters: Operating Temperature = 288.16 K (default)
- Variable-Density Parameters: Specified Operating Density = on, Operating Density = 1.225 kg/m<sup>3</sup>
- Surface Tension Fore Modelling = On, Surface Tension Coefficient air and fresh = 0.072 n/m, Surface Tension Coefficient air and saline = 0.072 n/m, Surface Tension Coefficient saline and fresh = none

Set up: dimension = 2D, double precision, parallel (Local Machine) Solver with processes = 4, GPG-PUs per machine = 0

- Multiphase model: Volume Of Fluid, Number of Eulerian phases = 3, VOF Sub-Models: Open Channel Flow, Formulation: Implicit, Body Force Formulation: Implicit Body Force, Interface Modelling Type: Dispersed
  - The multiphase model is used, because it can simulate flushing. The model can handle a high density difference between two fluids and a free water surface. The setting solves the continuity and momentum equations for each involved phase (air, fresh and saline water) [Zhang et al., 2008].
  - The Volume Of Fluid (VOF) method of Hirt and Nicholas [Hirt and Nichols, 1981] is used to indicate the intersection between air and water and can calculate solutions dependent on time [Naik et al., 2017]. This method solves a transport equation for the volume fraction at each time step, and the free surface is calculated by the division of the volume fractions over the design [Naik et al., 2017].
  - Open Channel Flow in ANSYS Fluent is turned on in the Multiphase model because it is open channel flow [ANSYS Inc., 2009b; ANSYS Inc., 2009c].
- Energy: Energy Equation = On

- Viscous model: k-epsilon (2 eqn), Realizable k-epsilon model, Near-Wall Treatment = Enhanced Wall Treatment
  - The k-epsilon turbulence model is used for modelling in the free surface flow region far from a wall, the realizable variant can capture the mean flow around complex structures correctly [Seyyedvalilu, 2018].
  - Enhanced Wall Treatment is turned on to improve the calculations near the wall. The walls are stationary walls and contain a no-slip condition [Naik et al., 2017].
- Cell Zone Conditions: Fluid: surface-body (fluid, id=2)
  - Multiphase: Numerical Beach Treatment: Numerical Beach = On, Beach Group ID = 1, Damping Type = Two Dimensional, Computer from Inlet Boundary = Inlet-fresh
  - Level Inputs: Free Surface Level = 0.35 m, Bottom Level = 0 m
  - Uni-Directional Beach Inputs:” X-Direction = 1, Y-Direction = 0, End Point = 20 m, Start Point = 17.2 m (for geometries 1, 2, and 3) or 15.5 m (for geometry 4)
  - Resistance Inputs: Relative Velocity Resistance Formulation = On, Linear Damping Resistance =  $10 \text{ s}^{-1}$  (Default), Quadratic Damping Resistance =  $10 \text{ m}^{-1}$  (Default)

## Methods

- Pressure-Velocity coupling: Scheme = SIMPLE
- Spatial Discretization: Gradient = Least Squares Cell Based, Pressure = Body Force Weighted, Momentum = Second Order Upwind, Volume Fraction = Compressive, Turbulent Kinetic Energy = Second Order Upwind, Turbulent Dissipation Rate = Second Order Upwind, Energy = Second Order Upwind
  - Second Order discretization schemes are chosen, because of the use of momentum, turbulence kinetic energy, and dissipation equations [Hargreaves et al., 2007].
- Transient Formulation: First Order Implicit
- Initialization: Standard Initialization
  - Compute from: Inlet-fresh, Reference Frame: Relative to Cell Zone, Open canal Initialization Method: Flat
  - Initial Values: Gauge Pressure = 0 Pascal, X velocity = 0.01 m/s (or 0.1 m/s, dependent on geometry/case), Y velocity = 0 m/s, Turbulent Kinetic Energy =  $3.75\text{e-}07 \text{ m}^2/\text{s}^2$  (default), Turbulent Dissipation Rate =  $1.261839\text{e-}09 \text{ m}^2/\text{s}^3$  (default), Temperature = 293.15 K, Saline volume fraction = 0, Fresh volume fraction = 1.
- Patch: Volume fraction fresh = 1 for fresh areas and 0 for other areas, Volume fraction salt = 1 for salt areas and 0 for other areas, Volume fraction = 1 for open-air areas and 0 for other areas (Figures 23 and 24).
  - The saline water area is patched with an initial concentration of 1, and the same is done for the freshwater areas with the patching of fresh water and for air. The same method is used in another research [Feng, 2019].

- The patching gives the following legend in the results: PhaseId = 0 and the colour blue indicates air, PhaseId = 2 and the colour yellow indicates saline water, and PhaseId = 3 and the colour red indicates fresh water.
- An extra fluid was still in the settings in ANSYS Fluent (PhaseId=1, default water), this was to make the three fluids better visible with the three primary colours. This fluid is patched with a volume fraction of 0 for all areas.

Solution animations: Animations of the solutions are made to understand what happens in the design over time

- Record after every 1 time-step, Storage type = HSF file, Contour plot = PhaseID, Vectors = Velocity, write MPEG file

### 3.3.5 Cases

This chapter contains an explanation of three cases (four runs) done in ANSYS Fluent, the overview can be found in Table 11. The simulation setup for all runs is, in general, the same as described in the previous chapters. The specific details for all cases are reported in the upcoming three sections. In Appendix L the geometries are visualised in the same way as in Figure 23.

Table 11: Cases for 2D CFD model in ANSYS Fluent

	Cases	Geometry	Information
A	Functioning of traditional and modified weir	Geometry 1	Traditional weir
		Geometry 2	Modified weir in real situation
B	Comparison of two velocities	Geometry 2	Freshwater velocity = 0.01 <i>m/s</i>
		Geometry 3	Freshwater velocity = 0.10 <i>m/s</i>
C	Comparison of two distances	Geometry 2	Distance between underflow gate and weir = 2.0 <i>m</i>
		Geometry 4	Distance between underflow gate and weir = 0.3 <i>m</i>

**Functioning of a traditional and modified weir** For this case, two animations are compared to analyse the functioning of a traditional and modified weir. The results of this case should give insight into why a modified weir is useful in contrast with a traditional weir. When modelling a realistic polder water canal, the geometry is elongated: the water depths are small, but the lengths of the water canals are long. In the first run, a geometry is made with a traditional weir without the underflow gate (Figure 76). The second run contains a geometry with a modified weir, this is a representation of how a modified weir is functioning in an actual polder water canal (Figure 77).

**Comparison of two velocities** In this case, one geometry with two different velocities is compared to each other. As mentioned in Chapter 2.2.1, the water velocity should not be too high in order to have a low Reynolds Number. When the Reynolds Number is small, the water flow is laminar or in a transition zone to turbulent, and thus turbulent mixing of fresh and saline water is prevented. In the first run, a velocity of 0.01 *m/s* is used, this geometry and design are the same as the last run from the previous case (Figure 77). In the second run, a velocity of 0.10 *m/s* is used, and the geometry is the same, only the velocity is ten times higher (Figure 78). The velocity of 0.10 *m/s* is more realistic

for a polder water canal [Hoes and vd Giesen, 2015]. Because freshwater and saline water are two different fluids in the model, mixing the two cannot happen, which is not realistic.

**Comparison of two distances** This last case compares two geometries with a different distance between the underflow gate and the weir. A distance of 2.0 *m* (based on the experiment, Figure 77), and a distance of 0.3 *m* (based on the TexelBeton design, Figure 79) are both analysed in ANSYS Fluent. The distance between the two plates is, in contrast to the size of the opening of the underflow gate, not directly dependent on the water level in the polder canal. However, the distance is important to investigate if there is turbulent flow in the area between the plates and if the flow over the weir is influenced by the flow of water underneath the underflow gate. As mentioned multiple times before, turbulence can cause mixing of fresh and saline water and the effectiveness of a modified weir weakens.

## 4 Results

In this chapter, the methods in Chapter 3 are combined to answer the first two sub-questions (Chapter 1.4). The results of the field measurements will answer the first sub-question about the fresh and saline water distribution in the polder on different scales and if this indicates stratification (Chapter 4.1). The results of the simulations and flume experiments are used to answer the second sub-question about how stratified fresh and brackish water can be separated by a modified weir (Chapter 4.2).

### 4.1 Fresh and brackish water distribution

The results in this chapter are point and continuous field measurements in and around the Negenboerenpolder, and it is indicated where stratification can be found. Figure 25 gives an overview of the locations of the measurements during the field campaign. In short, the stratification of water can be found at all measurement scales in the Negenboerenpolder. The best examples can be found in the transects of both the Waddenweg and Dijkslot and around the weir at Hornhuizerklief.

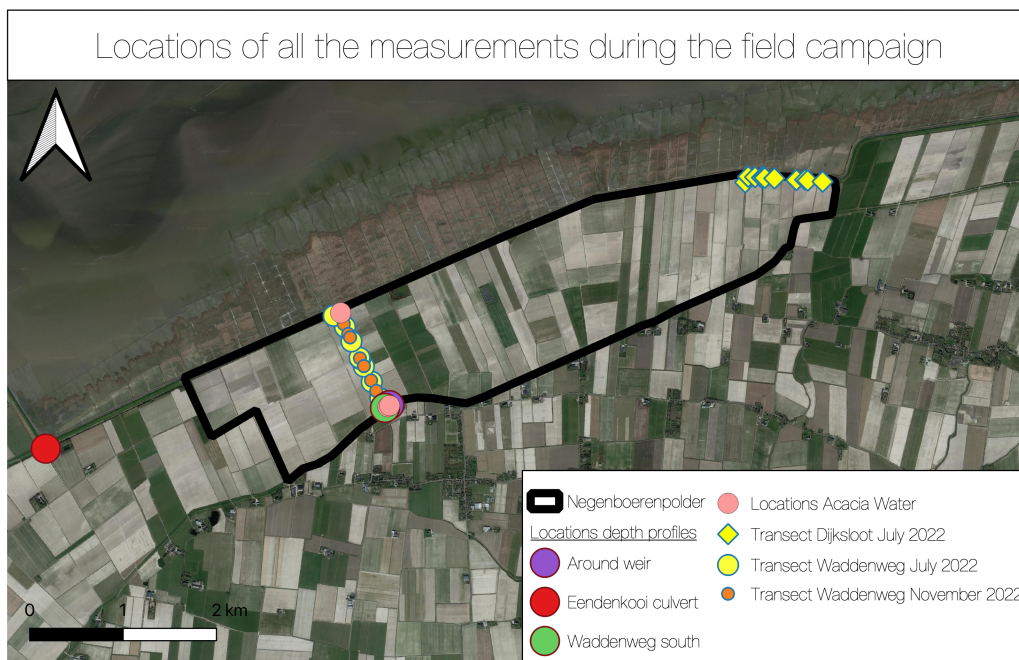


Figure 25: Overview of all locations during the field campaign in and around the Negenboerenpolder

#### 4.1.1 Distribution over the depth

Figures 26 and 27 show the results of conductivity measurements over the depth at four locations. The measurement locations are described in Chapter 3.2.1 and presented in Figure 19. The corresponding temperature measurements over the depth at the same locations can be found in Appendix G.

In July 2022, the conductivity at both sides of the weir does not change over the depth, the values are around  $1.8 \text{ mS/cm}$ . This observation means that there is no stratification directly up and downstream of the weir, and this water column is entirely fresh.

At the location of the weir complex towards the north, 'Waddenweg South', the conductivity differs slightly over the depth. In July 2022 (Figure 26) the conductivity starts at 1.3 and rises to 3.2  $mS/cm$ , especially beyond a depth of  $-0.40\ m$  the EC values are rising. This means that there is a gradient in conductivity here from fresh to brackish water, and thus slight stratification of water based on density differences. In November 2022 (Figure 27) the EC values are much higher than in July, but stratification cannot be seen. The water depth in November is also much lower than in July 2022.

The depth profiles in front of the culvert at the Eendenkooi, outside the Negenboerenpolder, are shown in Figures 26 and 27. These depth profiles are entirely different in comparison to the previous locations. Yet, the EC values measured in November 2022 are again much higher than in July 2022. In July 2022 (Figure 26), the conductivity stays constant (around 8.2  $mS/cm$  and brackish) towards a depth of  $-0.60\ m$ . In the next  $0.1\ m$ , the EC rises quickly to around 18  $mS/cm$ . Beyond a depth of  $-0.70\ m$ , the conductivity remains around 18  $mS/cm$ , which is saline. This observation shows a sharp interface between the brackish and saline layers. In November 2022, the same pattern is visible. In Figure 27, the jump in EC is now at a depth of  $-0.70\ m$ . Towards this depth, the conductivity stays around 21.8  $mS/cm$ , but after the values rise quickly to around 29  $mS/cm$ . The entire water column is saline now, and the water level is higher than in July, but the sudden rise in conductivity is around the same depth.

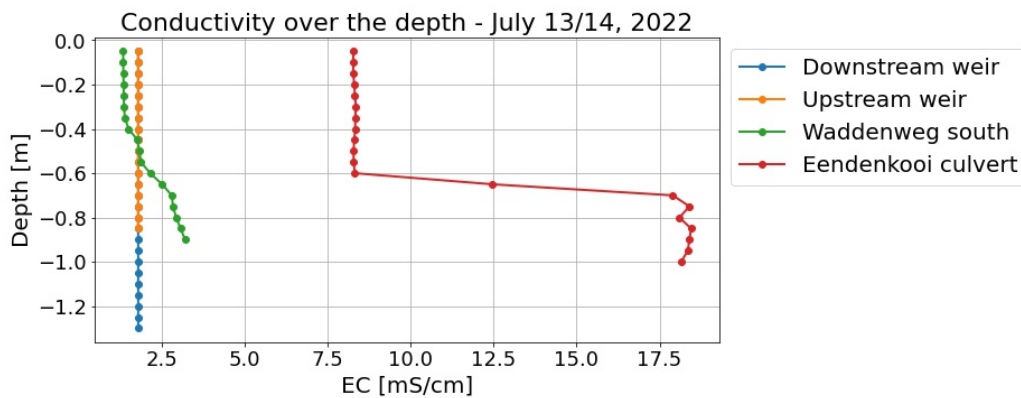


Figure 26: Conductivity profiles over the depth – July 2022

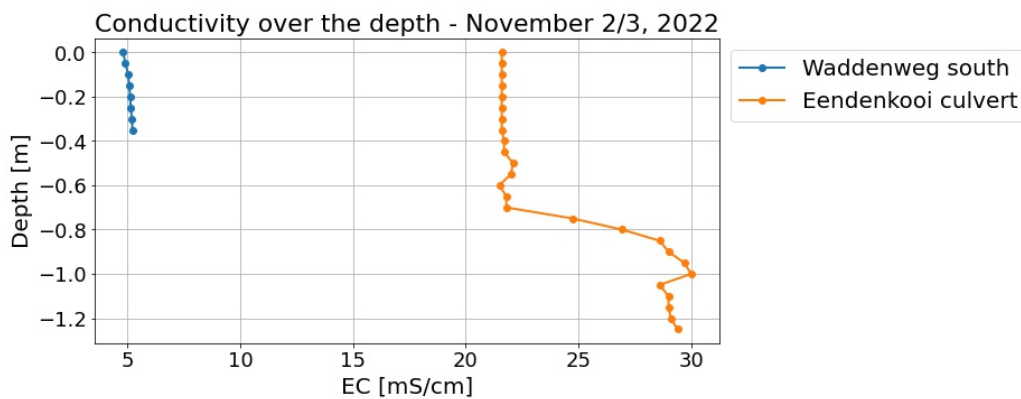


Figure 27: Conductivity profiles over the depth – November 2022



### 4.1.2 Distribution over the area

**Around weir** At three locations around the weir at Hornhuizerklief conductivity and temperature measurements at two depths are performed, the temperature results can be found in Appendix H. The conductivity measurements in July 2022 (Figure 28) and November 2022 (Figure 29) are compared. The range in conductivity values in July 2022 is wider than in November 2022. The largest difference between the surface and bottom measurements is at 4 m upstream of the weir in July, in November the differences are negligible.

All measurements in November are considered as brackish, just like the bottom measurements upstream of the weir in July 2022. The surface measurement and the measurements downstream of the weir in July 2022 are considered fresh because they are below  $2 \text{ mS/cm}$ . This means that there is a stratification of water in the canals during Summer, but it is gone in Winter. The figures show the influence of a weir on stratification. At 1 m upstream of the weir there is a difference in conductivity between the surface (fresh) and bottom (brackish) water layer of at least  $1 \text{ mS/cm}$ . However, 1 m downstream of the weir, this difference is gone. On this side of the weir, the surface and bottom measurements are both fresh. This shows that the theoretical situation in Figure 4 indeed happens in the field, and that stratification happens in this polder water canal.

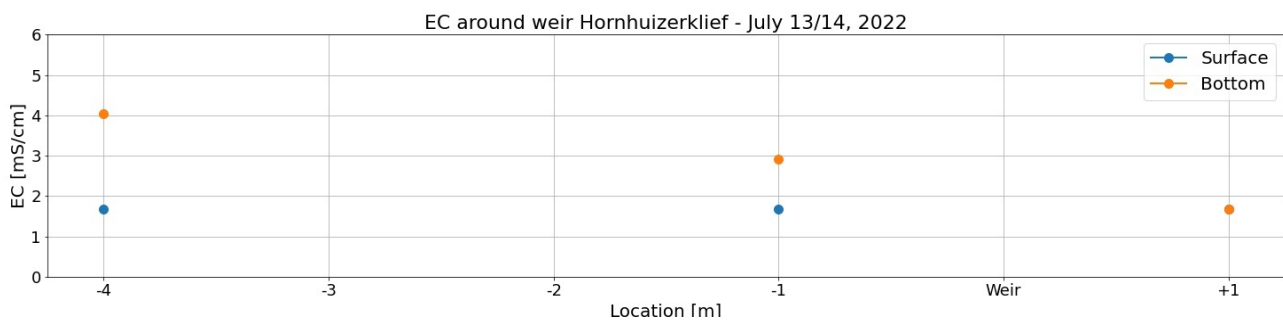


Figure 28: Conductivity measurements at two depths around weir Hornhuizerklief – July 2022

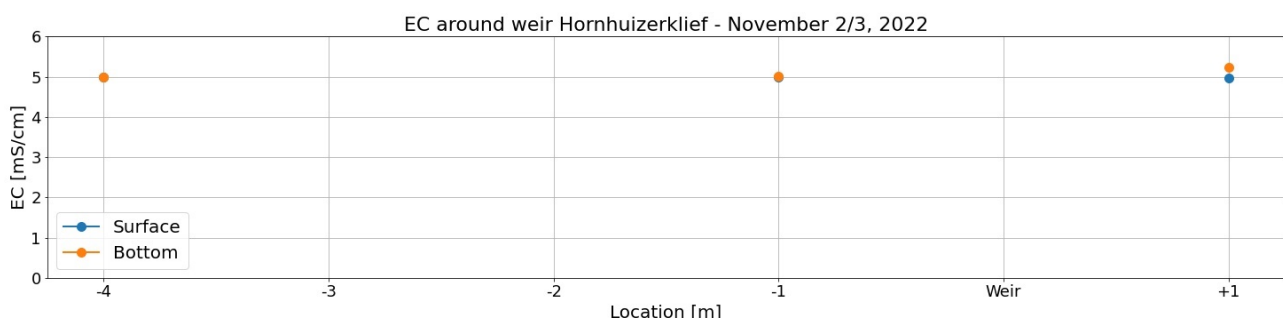


Figure 29: Conductivity measurements at two depths around weir Hornhuizerklief – November 2022

**Transects** Measurements along two transects are performed during Summer (July 2022) and Winter (November 2022), a map of the transects is given in Chapter 3.2.2. Figures 31 and 32 show the results from the same transect (Waddenweg) from the south to the north. Figure 30 shows the results of measurements along a dead end of the Dijkslot from the West to the East. The corresponding temperature measurements can be found in Appendix I.

The results of the conductivity measurements in the Dijkslot in July 2022 (Figure 30) show an increasing conductivity towards the dead end. At 150 m the measured EC-value makes a large jump from brackish to saline, a smaller jump can be seen around 500 m. These jumps match the locations of the culverts in the canal. When comparing the conductivity of the bottom and surface, a trend can be seen. Mixing by culverts or flushing can cause the surface and bottom measurements to be around the same value, which happens at the start of the transect. However, the difference rises to 5 mS/cm, which indicates possible stratification in this part of the Dijkslot. Because this transect is a dead end and not flushed with fresh water, saline seepage can come up and stay in the ditch.

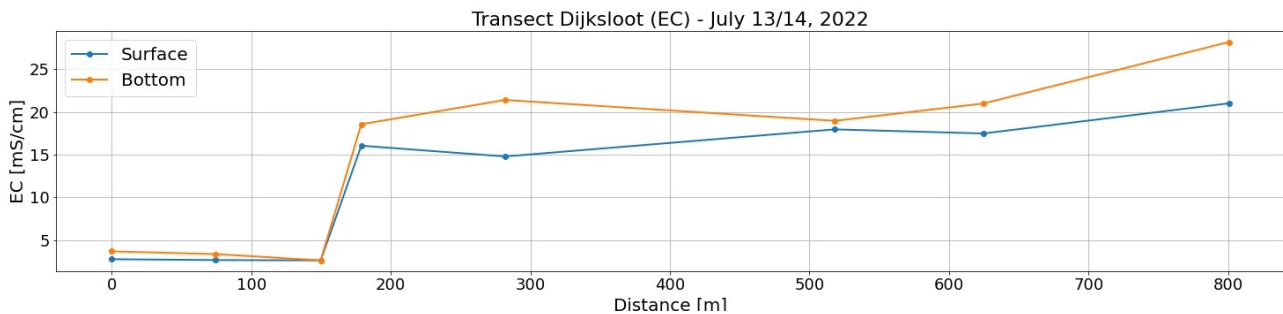


Figure 30: Conductivity measurements at two depths along the Dijkslot transect – July 2022

Figures 31 and 32 are both results of conductivity measurements along the Waddenweg transect. The measurements in July 2022 (Figure 31) show a gradually increasing conductivity from south to north, the measured EC values start as fresh and rise to brackish. However, the measurements in November 2022 (Figure 32) do not show this pattern and vary between brackish and saline. At the start of the Waddenweg transect during the measurements in July 2022, there is a difference in conductivity of almost 2 mS/cm between the surface and bottom water layers. This difference is gone beyond 300 m, the measured EC values are the same between 300 and 800 m and rise again at the end of the transect.

During the measurements in November 2022, the differences between the surface and bottom are larger in certain parts of the canal. At some locations, the bottom water layer is highly saline, and some interesting observations were done in the field (Figure 33). Figure 33a shows a seepage film on water, which indicates seepage [Dijkema, 2017]. Figure 33b shows a white film on the bottom of the water canal, which possibly indicates the precipitation of salt. When comparing differences in conductivity of the surface and bottom water in July 2022 with the elevation differences in the polder, a similar pattern can be noticed. At the old dike, between 300 and 800 m of the transect, the measured surface and bottom conductivity are around the same values. This can indicate a possible natural buffer against saline seepage from the Wadden Sea.

**Summary** The conductivity of water in the Negenboerenpolder is higher when measuring close to the dike with the North Sea. A high conductivity means a high salinity in the polder water canals. At some locations, there is a significant difference between the surface and bottom measurements, which can indicate stratification. The elevated area in the middle of the Negenboerenpolder, an old dike, had influenced the water quality significantly, and could especially be seen in the north-south orientated water canals. The ditch along the Wadden Sea dike (Dijkslot) is heavily saline and the water canals at the south of the polder (Bokumertocht, Ikematocht, and Seeratstocht) are kept as fresh as possible. Further, the inlet water quality of the Negenboerenpolder at the three inlet locations is dependent on the water quality upstream of the polder.

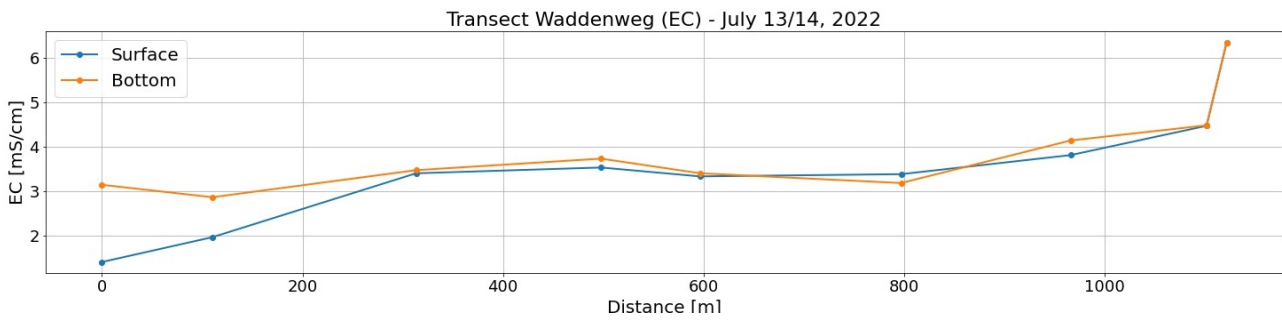


Figure 31: Conductivity measurements at two depths along the Waddenweg transect – July 2022

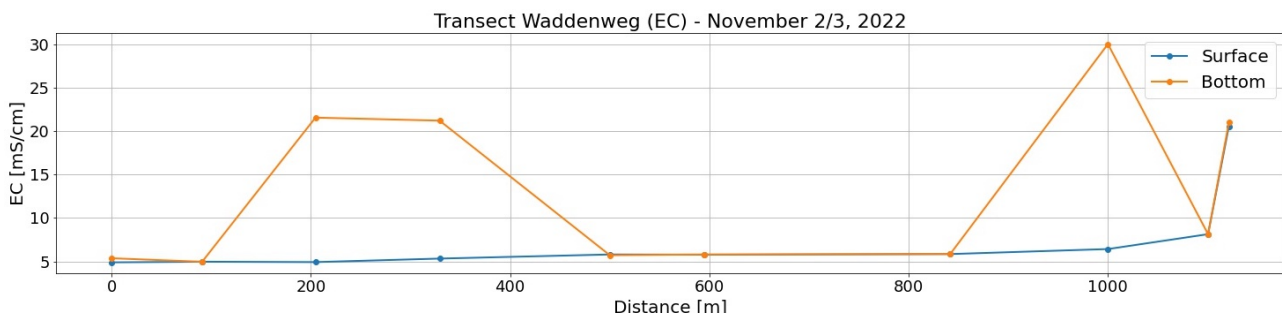


Figure 32: Conductivity measurements at two depths along the Waddenweg transect – November 2022



(a) Seepage film on the water surface [Own picture, November 2, 2022], (b) Possible precipitation of salt [Own picture, November 2, 2022]

Figure 33: Pictures taken along the Waddenweg transect during the field campaign in the Negenboerenpolder on November 2, 2022

### 4.1.3 Distribution over time

This chapter contains results of conductivity measurements in the Negenboerenpolder through time, both on the short and long scales. The long scale is classified in years and discusses the distribution during one year on one water depth. The short scale discusses continuous measurements at two water depths during a shorter time period. In the Negenboerenpolder continuous measurements of the EC, temperature, and water level are done. However, due to malfunctioning equipment and varying set-ups, there are gaps in the data series.

**Long time** During one year, the chloride concentrations vary depending on the amount of precipitation and inlet water. The amount of precipitation is high during winter, and there is discharge from the farmlands, the chloride concentrations are around 1000-3000  $mg/l$  (3.5-9  $mS/cm$ ). During spring, the concentrations will be even higher due to an increasing seepage pressure. However, from April onward the Waterboard starts flushing, fresher water enters the polder and the chloride concentrations decrease. This only lasts until July, then the inlet water becomes brackish and the chloride concentrations in the polder canals increase again. In the late Summer, the conductivity can increase towards 25  $mS/cm$  (8250  $mg/l$ ). The previously described variation can be seen in Figure 34, Zulteriet is the Dijkvloot in the Negenboerenpolder [van Meijeren et al., 2019]. As the measurements are done on one depth, stratification cannot be seen.

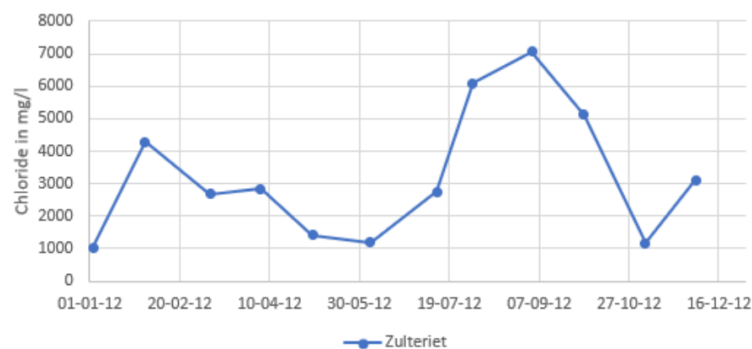


Figure 34: Measured chloride concentrations (2012) in the Negenboerenpolder on four locations of Waterschap Noorderzijlvest [van Meijeren et al., 2019]

**Short time** At three locations in the Negenboerenpolder two conductivity meters are installed to measure the conductivity at two depths in the water column (Figure 22). The sensors are also measuring the water pressure, which can be translated to the water levels in the water canal. The water depths at the measurement locations during the discussed time periods (Table 7) are shown in Figure 35. The water levels at Lutjewat are higher than around the weir because this area has a higher elevation. The levels around the weir in the first period show the same pattern, but the upstream water level is more constant, which can be caused by the weir. It can also be noticed that the water levels in Period 2 are in general lower than in Period 1, this is the difference between the Summer and Winter water levels of Waterboard Noorderzijlvest.

Figures 36 and 37 contain the conductivity values during both measuring periods. The measured conductivity in Period 1 is between 1 and 9  $mS/cm$ , and the values at 'Lutjewat' are in general higher than around the weir. At the locations 'Lutjewat' and 'Downstream', the difference between shallow and

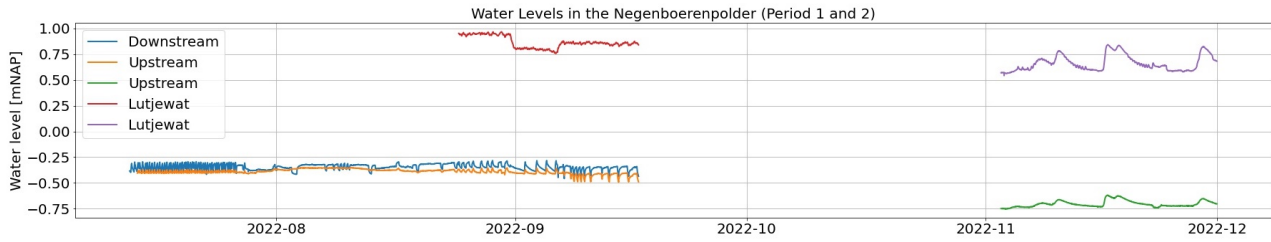


Figure 35: Water levels at the three measurement locations in the Negenboerenpolder

deep is negligible, so stratification is not found. At the location upstream of the weir, 'Upstream', a difference of  $2\text{ mS/cm}$  can be found between the shallow and deep measurements. These observations are in line with the theoretical drawing of stratification around a weir (Figure 4). Further, measurement location 'Lutjewat' is located in the Dijksloot close to the Wadden Sea, thus more brackish seepage is present here.

When comparing the range in measured EC values during both periods, it can be seen that the EC is much higher during Period 2 than during Period 1. The EC values are between  $5$  and  $25\text{ mS/cm}$  in Period 2. Additionally, there is a difference between the surface and bottom measurements, which increases to around  $20\text{ mS/cm}$ . Again, the water upstream of the weir has high conductivity values, but this cannot be compared to the downstream data as this is missing. With the measurements upstream of the weir, it is demonstrated that Figure 4 happens in the Negenboerenpolder. In the measured conductivity at 'Lutjewat' no trend can be found.

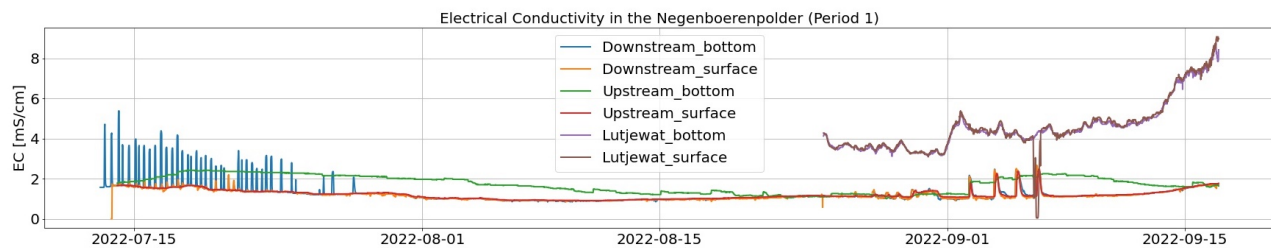


Figure 36: Measured conductivity at the three locations in the Negenboerenpolder (Period 1)

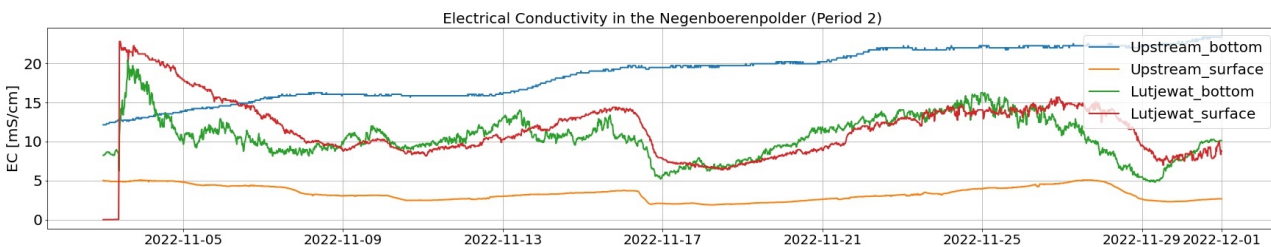


Figure 37: Measured conductivity at the three locations in the Negenboerenpolder (Period 2)

#### 4.1.4 Possible explanations

Previous results demonstrated that stratification can be found in continuous field measurements, but this is not always visible. In this section, the continuous data series are compared with a few factors

that can influence salinity. The used factors are the North Sea tides at Lauwersoog and the precipitation at KNMI weather station in Lauwersoog. The most interesting periods are shown here, Appendix J contains the entire measuring period.

Figure 38 shows fluctuating water levels around the weir in the Negenboerenpolder. These fluctuations seem to follow the tide oscillations. However, the water levels are stable at the end of July. The tides and conductivity in the Negenboerenpolder for the same period, are compared in Figure 39. The first half of the figure shows high peaks in conductivity of the measurements downstream of the weir at the bottom. These peaks sometimes correspond with the high tides in the Wadden Sea. Yet, also two peaks during one high tide can be seen and these conductivity oscillations are absent in the last part of the measurements. So, it is difficult to say if there is a similar pattern between the North Sea tides, water levels and conductivity in the Negenboerenpolder.

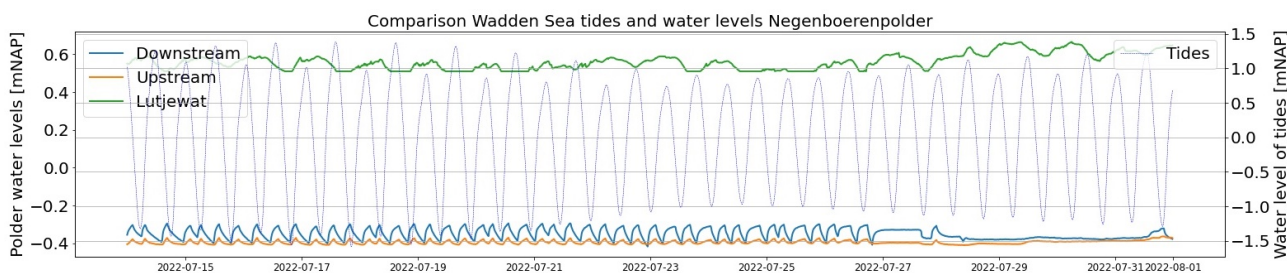


Figure 38: Wadden Sea tides and water levels in the Negenboerenpolder at the end of July

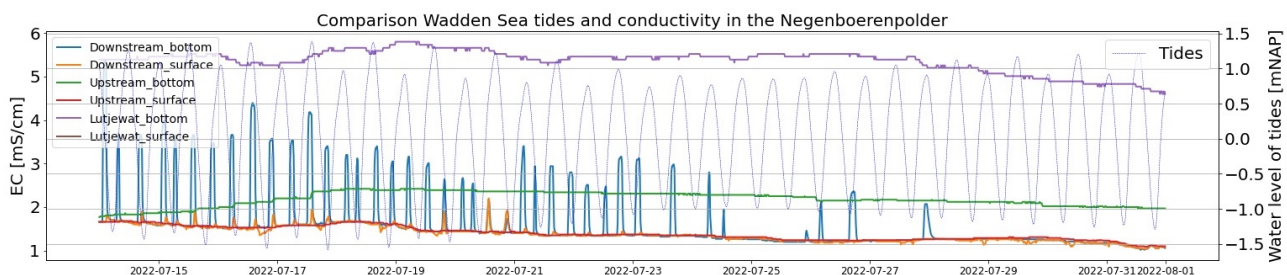


Figure 39: Wadden Sea tides and conductivity levels in the Negenboerenpolder at the end of July

A comparison of the tides with the conductivity for the period between the end of August and the beginning of September can be seen in Figure 40. This figure shows four peaks in conductivity around the weir at the beginning of September, but the tides are not at the same moments as these peaks. An interesting fact is that the peaks are not visible upstream of the weir at the bottom, where the EC is constantly high. This implies an accumulation of brackish water before the weir (Figure 4). Fresh water is flowing over the weir, which causes lower EC levels there.

Figure 41 presents also the tides and conductivity in the Negenboerenpolder, but now during the Winter season (end of October and November). During this season, the EC has a higher value than during Summer. The conductivity upstream of the weir is not fluctuating. The conductivity measurements at Lutjewat are fluctuating, but not in a similar pattern as the Wadden Sea tides. However, the surface and bottom sensors seem to switch places, it is possible that the sensors were loose and not measuring at their fixed depth.

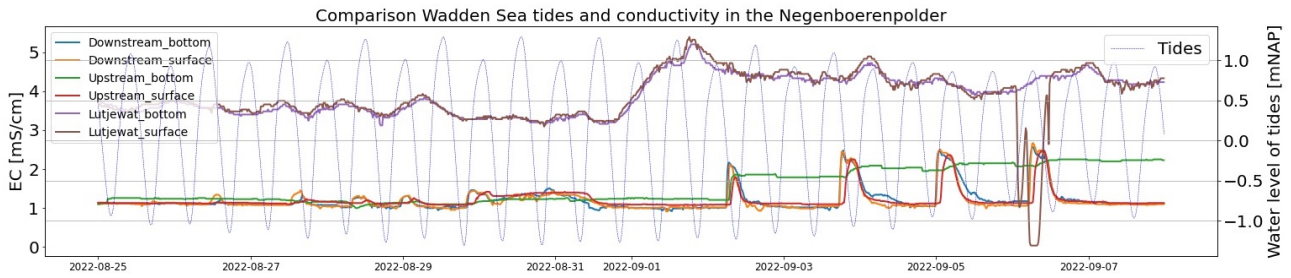


Figure 40: Wadden Sea tides and conductivity levels in Negenboerenpolder in August and September

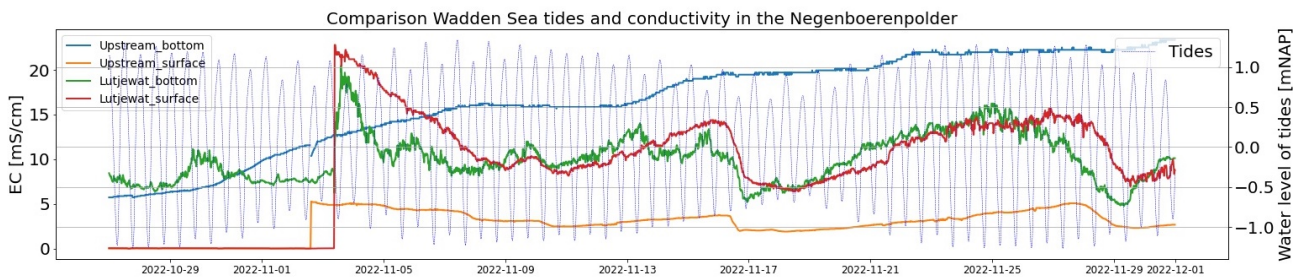


Figure 41: Wadden Sea tides and conductivity levels in Negenboerenpolder in October and November

## 4.2 Separating densities

This chapter aims to solve the second sub-question stated in Chapter 1.4, with the use of a practical experiment (Chapter 4.2.1) and 2D simulations in a theoretical CFD model (Chapter 4.2.2). It will be investigated how a modified weir can be used to separate densities, and thus how to discharge brackish water. First, observations are done during flume experiments. Later, 2D simulations in CFD software are done to analyse how water flows around and over the weir.

### 4.2.1 Flume experiments

This section describes the results of the flume experiments. Only the graphs from experiments 1, 3, 5, and 7 are shown here as these results are the most reliable, the other graphs can be found in Appendix F. These experiments are not representative, because of a changed set-up (experiments 2 and 6), or missing inlet, set-up, and measuring information (experiment 4).

Figure 42 of experiment 1 showed that the conductivity decreases upstream and increases downstream of the structure, this implies that a brackish water wave goes through the structure. In contrast, the results from experiment 3 (Figure 43) were important for the process and set-up of the flume experiment. It showed that strongly saline water stays at the bottom upstream of the ground plate, it does not move. Further, in Figure 44 (experiment 5) it can be seen that the conductivity measurements downstream of the structure can be delayed measurements from inside the structure. Also, freshwater ( $EC < 1 \text{ mS/cm}$ ) stays at the surface upstream of the structure. This implies again that a brackish water wave is flowing underneath the underflow gate. Experiment 7 (Figure 45) showed that the conductivity upstream of the structure (underneath the underflow gate) increases. After some time, the conductivity inside the structure also increases, and the conductivity downstream of the structure increases slowly. However, the differences in conductivity in this figure are smaller, because less salt

was used to create brackish water. In general, the inlet has a big influence, as it creates high peaks in conductivity. This implies that when the inlet is turned on heavily, brackish water is pushed through the flume towards the structure.

It is difficult to compare the graphs to each other because the setup and input changed. Only supposed patterns in the figures can be found. Experiments 1 and 7 (Figures 42 and 45) seem to have a similar pattern: they suggest that a wave of brackish water flows from the inlet through the structure to the end weir. The figures from the flume experiments need to be used carefully. The results are considered in the form of indications of how to build a modified weir. One of them is that the experimental set-up of a modified weir should not have a ground plate, or, more generally, a threshold on the ground before the underflow gate. Also, possible stratification before a modified weir is gone entirely downstream of the weir. The water flow over the weir can lead to the mixing of the fresh and brackish water, which causes that supposed stratification is gone downstream of the weir.

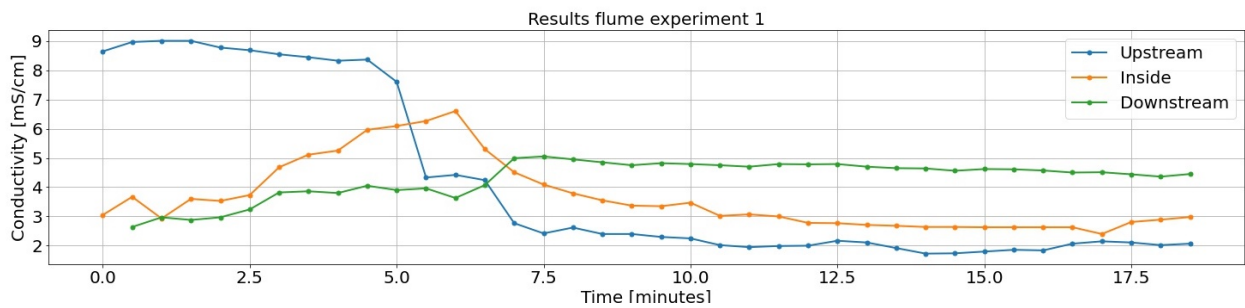


Figure 42: Flume experiment 1 – April 22, 2022

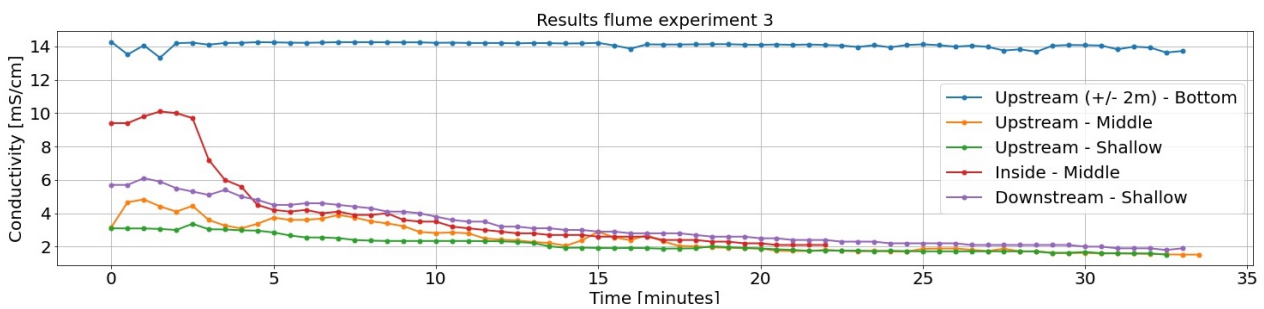


Figure 43: Flume experiment 3 – May 13, 2022

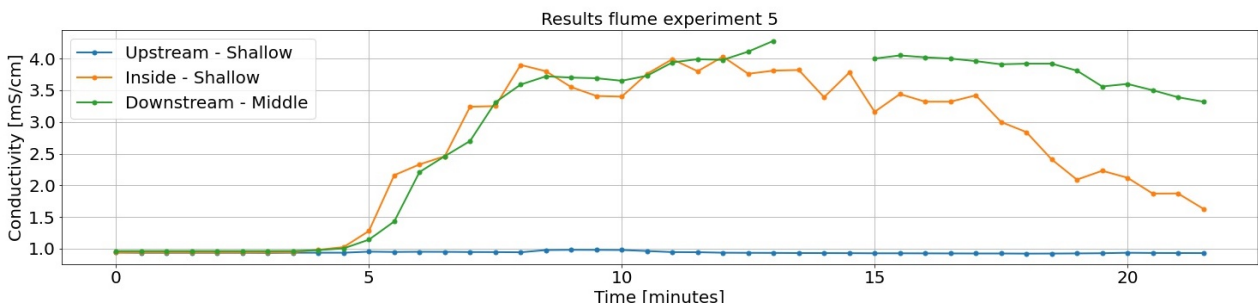


Figure 44: Flume experiment 5 – June 3, 2022



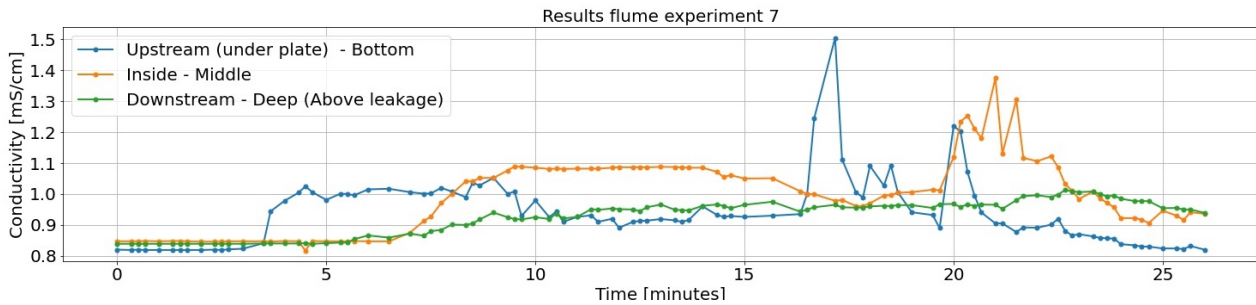


Figure 45: Flume experiment 7 – July 25, 2022

#### 4.2.2 2D simulations

This chapter contains the results of 2D simulations in the CFD software ANSYS Fluent, three cases are worked out with the model. First, it is used to investigate the benefit of a modified weir in comparison to a traditional weir. Next, two water flow velocities and two distances between the underflow gate and weir are compared to each other to analyse how a modified weir works optimally. Animations of the simulations can be found in Appendix N.

**Functioning of a traditional and modified weir** To investigate the effect of a modified weir in comparison to a traditional weir, two geometries are made. A realistic water canal with a traditional weir and incoming fresh water is modelled (geometry 1, Figure 46), this showed that fresh water is flowing over the weir and saline water remains upstream of the weir. This represents the theoretical situation in Figure 4. In geometry 2, the traditional weir is replaced by a modified weir. The results of geometry 2 (Figure 47) show that a modified weir is discharging saline water (yellow). The thickness of the freshwater layer (red) is increasing, and saline water is flowing through the underflow gate and over the weir. In Figure 47, stratification is completely gone downstream of the modified weir, which complies with the results of the flume experiments (Chapter 4.2.1).

Figure 46: Fresh water (red) flowing over a traditional weir, saline water (yellow) is staying behind in the water canal ( $\Delta t = 2260$ ,  $v = 0.01$  m/s, geometry 1)Figure 47: Saline water (yellow) is flowing through the modified weir, fresh water (red) is staying behind in the water canal ( $\Delta t = 2260$ ,  $v = 0.01$  m/s, geometry 2)

**Comparison of two velocities** The comparison of a freshwater flow velocity of  $0.10$  m/s (geometry 3) to a velocity of  $0.01$  m/s (geometry 2), was based on the Reynolds Number (Chapter 2.2.1). A velocity of  $0.01$  m/s avoids transitional flow. However, a velocity of  $0.10$  m/s is a realistic flow velocity [Hoes and vd Giesen, 2015] but is supposed to cause turbulent flow. In the results with a flow velocity of  $0.10$  m/s, 'dots' of fresh water (red) can be seen in the saline (yellow) fluid (Figure 48). Fresh water is creeping underneath the underflow gate (Figure 49), probably because of the higher

inlet velocity. The higher velocity of the freshwater inflow causes swirls and a tumultuous flow, which can cause the mixing of fresh and saline water. However, the mixing is impossible in the CFD model, because of the settings. As the objective was to investigate if a modified weir discharges brackish water, a modified weir with the realistic flow velocity ( $0.10 \text{ m/s}$ ) is working. Then the conditions are less optimal, hence less brackish water will be discharged. On the other hand, if the higher velocity causes turbulence and the fresh layer disappears, a modified weir is not useful.



Figure 48: Dots of fresh water (red) in the saline (yellow) layer in the CFD model of a modified weir with an inlet velocity of  $0.10 \text{ m/s}$  ( $\Delta t = 2800$ , geometry 3)



Figure 49: Fresh (red) is flowing underneath the underflow gate in the CFD model of a modified weir with an inlet velocity of  $0.10 \text{ m/s}$  ( $\Delta t = 270$ , geometry 3)

**Comparison of two distances** This case investigated two distances between the underflow gate and the weir, the sizes of the distances are  $0.3 \text{ m}$  and  $2.0 \text{ m}$ . The most important motivation is that the weir itself does not have an influence on the water flow underneath the underflow gate. When comparing the results of geometries 2 ( $2.0 \text{ m}$ ) and 4 ( $0.3 \text{ m}$ ), it seems that the flow underneath the underflow gate is restricted by the weir plate. Velocity vectors in Figure 50 (geometry 4,  $0.3 \text{ m}$ ) are indicating that water convergences and that it flows back to the underflow gate. This can cause turbulent flow, which should be prevented for the optimal functioning of a modified weir. In contrast, the velocity vectors of geometry 2 ( $2.0 \text{ m}$ ) in Figure 51 show the results when the water has more space between the weir and underflow gate. So, based on these simulations a larger distance between the underflow gate and the weir is better. The velocity underneath the underflow gate is around  $0.20 \text{ m/s}$  (in contrast to the inlet velocity of  $0.01 \text{ m/s}$ ) in both figures.



Figure 50: Blocked velocity vector in the CFD model of a modified weir with an inlet velocity of  $0.01 \text{ m/s}$  ( $\Delta t = 150$ , geometry 4 ( $0.3 \text{ m}$ ))



Figure 51: Spread out velocity vector in the CFD model of a modified weir with an inlet velocity of  $0.01 \text{ m/s}$  ( $\Delta t = 150$ , geometry 2 ( $2.0 \text{ m}$ ))

To conclude, the results of the 2D simulations suggest that the modified weir does what it is designed for. However, the model settings are not entirely representative of the real situation. The results gave indications about the design of a modified weir, but hard conclusions are difficult to make. The main observations in the 2D simulations of this research were that a modified weir works better with a lower flow velocity and a larger distance between the underflow gate and the weir.

## 5 Implementation of a modified weir

This chapter discusses the implementation of a modified weir (sub-question 3), based on the results of all methods used in this research. It can serve as advice to water managers, who want to try a modified weir in their area to decrease salinization. General recommendations for possible locations for a modified weir are given, and with this, a potential location in the Negenboerenpolder is indicated. This chapter also contains some recommendations on the design of a modified weir, an analysis of the system effect of such a weir, and recommendations for how to measure the effect of the weir.

### 5.1 Recommendations for the location

Based on this research, the following recommendations are important for the location of a modified weir.

- Water needs to flow through the canal in order for the modified weir to work. As a modified weir is used for the discharge of (brackish) water, such a weir should be implemented in water canals that can be flushed, not in a dead end.
- A modified weir should not be installed in a primary water canal, to avoid flooding. Primary polder water canals are often used for the discharge of water. The modified weir can be an obstacle during heavy precipitation events and can cause an accumulation of water upstream of the weir.
- Negative effects on downstream agriculture and nature should be diminished. When implementing a modified weir, it should be taken in mind that the downstream part of the weir will receive more brackish water. It should be investigated if that is possible.
- Modified weirs should not be implemented directly back-to-back. It was seen in the field that the stratification builds up in a few days. However, saline water flows over the weir, and this causes mixing as the water comes on top and cannot flow directly to the bottom again. The exact time and distance to build up stratification are unknown and should be investigated.
- The location where a modified weir is implemented should have a significant water depth. When the water depth is small, the underflow gate needs to be even smaller, until the point it is too small to let water flow through it. If the depth is small and the underflow gate is too large, all water in the canal will flow through it.

In the Negenboerenpolder a modified weir could be implemented in the SE-NW oriented (secondary) waterways, because flushing happens from the northeast to the southwest (along the primary water canals). The described weir in this research, the weir at Hornhuizerkief, is a traditional weir, but it is located in a primary water canal (Appendix K). An adaption of this weir is not ideal. Stratification is found in the Waddenweg transect, which is supposed to be a secondary water canal, discharging in the brackish Dijkslot. So, it would be interesting to implement a modified weir in the water canal along the Waddenweg. The exact location could be in the second half of the water canal, as this will result in freshwater storage in the entire canal upstream of the weir. The red circle in Figure 52 indicates the best location for a modified weir, based on this research. Downstream of this location, there is no freshwater demand by farmers.

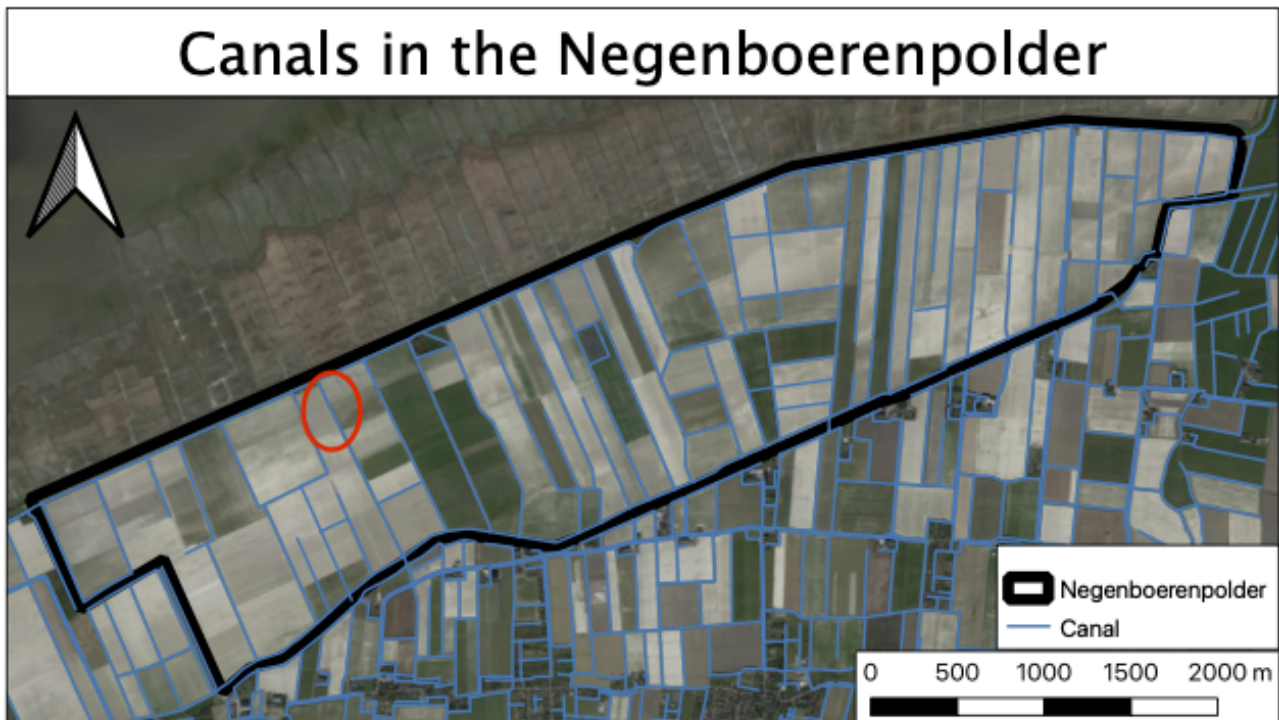


Figure 52: The Negenboerenpolder, with a potential location for the modified weir indicated with the red circle

## 5.2 Recommendations for the design

The following recommendations are important for the dimensions of a modified weir, based on the flume experiments and 2D simulations in this research.

- An adjustable modified weir is recommended. For example, with loose planks that can be piled up. If the planks are removed manually before an extreme rainfall event, the accumulation of precipitation upstream of the weir can be prevented, and the weir can be adjusted to summer and winter polder water levels. For example, the TexelBeton design (Figure 10) consists of removable planks.
- The underflow gate opening of the modified weir should not be too small. This is dependent on the water depth, but it will be difficult to discharge water. Further, a too small gate opening gets clogged more easily, which makes discharging even more difficult. When the weir is adjustable and can be removed, the cleaning of the opening can be done better, to prevent clogging.
- A relatively low velocity in the water canal is needed to avoid turbulence and mixing, the Reynolds Number could be an indication for this (Equation 4). However, a higher and more realistic velocity also works, but it will be less effective in discharging brackish water. With the higher velocity, fresh water is dragged along underneath the underflow gate, which will dilute the brackish water and the total discharged salt load will be smaller.
- The distance between the underflow gate and the weir is important, as it influences the flow underneath the underflow gate and the convergence of streamlines behind it. The simulations with a 2.0 m distance in this research gave a better result than the 0.3 m (from the TexelBeton design in Figure 10).

### 5.3 Effect on the water system

Implementing a modified weir definitely has an effect on the water system of a polder. Canals can be turned fresher with a modified weir, but this effect will be reduced if brackish water is discharged towards the same canal. Therefore, it would be smart to modify the entire water system. Based on field measurements in the polder and the water demands, it can be decided to make certain canals fresh and other canals brackish. For example, one (or more) inlet canals can be chosen, which are as fresh as possible, but they are dependent on the available water upstream of the polder. The water in this inlet canal can be used for irrigation of the agricultural fields. Then, there is also one (or more) outlet canals, which discharge the most brackish seepage water and the used irrigation water. It would be best to implement a modified weir in the fresh canals. However, one modified weir in a polder will not solve the salinization problem in the entire polder.

As a modified weir requires stratification, flushing of the water system just upstream of a modified weir is not recommended. This is done to meet the irrigation water demand from the farmers. Flushing also causes the dilution of saline water, the water in the canals will be fresher, but the required stratification disappears. So, the waterboard can flush the system with a lower volume or lower velocity to enhance stratification and optimize the positive effects of a modified weir.

For the implementation, it is important to know how much saline water or chloride can be discharged with a modified weir. To explore this, rough example calculations are made in the grey text boxes below. The calculations are based on geometry 3 of the 2D simulations (Chapter 3.3), which is a winter situation without flushing with a realistic water velocity. The numbers in the calculations are based on the proposed location in the canal along the Waddenweg in the Negenboerenpolder.

#### Example 1:

In this example, the dimensions of a canal are as follows: width ( $w$ ) = 1.50 m, and total water depth ( $y$ ) = 0.35 m. The flow velocity ( $v$ ) is 0.10 m/s (Chapter 3.3.5). In this canal, a modified weir is implemented, and the height of the underflow gate ( $h$ ) is 0.10 m. It is assumed that there is stratification and the saline layer at the bottom has an EC of 10 mS/cm.

The cross-sectional area of the underflow gate:

$$A = w \cdot h = 1.50 \cdot 0.10 = 0.15 \text{ m}^2$$

Discharge through underflow gate:

$$Q = A \cdot v = 0.15 \cdot 0.10 = 15.0 \cdot 10^{-3} \text{ m}^3/\text{s} = 15.0 \text{ dm}^3/\text{s} = 15.0 \text{ l/s}$$

With an EC of 10 mS/cm, the chloride concentration (Cl) is 3000 mg/l = 3.00 g/l (Table 1).

Now, the discharged chloride concentration can be calculated:

$$\text{Discharged chloride concentration} = Q \cdot \text{Cl} = 15.0 \text{ l/s} \cdot 3.00 \text{ g/l} = 45.0 \text{ g/s}$$

So, in this canal and with this underflow gate size, 45 grams of chloride can be discharged per second through the underflow gate of a modified weir.

**Example 2:**

In this example, a modified weir is implemented in the canal along the Waddenweg at a distance of 1000 *m* (l) downstream of Hornhuizerklief. The same dimensions and numbers as in the previous example are applicable. The saline layer in the canal does have an assumed depth ( $y_{saline}$ ) of 0.30 *m*, this is the same as in the 2D simulations (Chapter 3.3).

The volume of the saline layer in the canal is:

$$V = l \cdot w \cdot y_{saline} = 1000 \cdot 1.50 \cdot 0.30 = 0.45 \cdot 10^3 m^3 = 450 m^3$$

The time it takes for this volume to flow through the underflow gate is:

$$t = \frac{V}{Q} = \frac{450m^3}{0.015m^3/s} = 30000 \text{ seconds} = 8 \text{ hours and } 20 \text{ minutes}$$

So, it takes 8 *hours* and 20 *minutes* to discharge the saline layer by the modified weir.

The effects of an operating modified weir are not directly visible in the polder. The weir can be used to discharge brackish water and store fresh water, but this will not happen instantly after the implementation. It takes time and patience to let the modified weir do its work. However, if a farmer wants to irrigate his crops, the water canal needs to be fresh. When a farmer puts his pump in the canal to irrigate, the water will be taken out with such a force that the carefully build up stratification will disappear directly and a large amount of water is taken out of the canal. For the implementation, it is essential to bear in mind that, if a farmer needs to irrigate immediately and the entire water system is not changed to fresh and brackish canals, it can already be enough to let fresh water into the polder at the moment of irrigation and all the inlet water will directly be used for irrigation.

## 5.4 Recommendations for measuring the effect

Here one recommendation is given on how the effect of the just discussed implementation of a modified weir can be measured. The measuring method is based on the proposed location, and with unlimited financial resources. The water canal along the Waddenweg is around 1100 *m*, a modified weir can be implemented at for example 1000 *m* downstream of Hornhuizerklief, so 100 *m* upstream of the Dijkslot. The 1000 *m* can thus be used to measure the conductivity in the canal upstream of the modified weir. At 1000, 500, 100, 50, 10 and 5 *m* upstream of the modified weir the Electric Conductivity is measured at certain depths, to investigate if, where, and when stratification can be found. The number of vertical measurement points is dependent on the water level, the EC should be measured every 0.15/0.20 *m*. It is not necessary to do continuous measurements at these locations. The measurements can be done manually and should be repeated frequently. It could be an idea to measure the conductivity two or three times a day to keep track of the situation upstream of the weir.

Further, the conductivity depth profiles should be made directly around the modified weir to investigate the salinity around it in more detail. The measurements should be done at 1 *m* upstream and 1 *m* downstream of the modified weir. With a distance of 2 *m* between the underflow gate and the weir plate, the measurements should also be done 1 *m* downstream of the underflow gate (exactly in the middle of the plates). The method of the depth profiles should be the same as in this research, the conductivity has to be measured every 0.05 *m*. The most ideal would be to measure these three locations continuously. If this is not possible, the depth profiles can also be made manually by measuring the conductivity every 1 *hour*.

These previously described recommendations are quite labour-intensive. To prioritize, the measurements directly around the modified weir are to most critical to measure the effect and should certainly be measured. So, another suggestion would be to measure the conductivity continuously at two depths at the three locations. The conductivity should be measured continuously at the water surface and at the bottom. The three locations around the modified weir are 1 *m* upstream, in the middle between the underflow gate and weir plate (1 *m* downstream of the underflow gate), and 1 *m* downstream of the weir.

When a modified weir is functioning properly in the canal next to the Waddenweg, it can be seen in the EC measurements at the discussed locations. In the beginning, brackish water (higher EC) should be found at the bottom over the entire length of the canal and freshwater (lower EC) at the surface of the canal. Over time, the brackish layer should become thinner and there should be more freshwater. That means that the measured EC values should go down upstream of a modified weir. Inside and downstream of a modified weir, a high EC is expected as a modified weir discharges the brackish water out of the canal.





## 6 Discussion

This chapter discusses the topic and methods of this research. First, general topics such as the salinity and the modified weir are discussed (Chapter 6.1). Next the flume experiments (Chapter 6.2), the field campaign (Chapter 6.3), and the 2D simulations (Chapter 6.4) are reviewed.

### 6.1 General

In Chapter 2.1.3 the definitions of fresh, brackish, and saline water for this research are given. However, the exact definitions of 'brackish' and 'saline' are variable and dependent on the water user or researcher. Each research, company, water board, instance, etc has often its own classification system. Some people consider water with an EC of  $3\text{ mS/cm}$  already brackish, but other people consider  $5\text{ mS/cm}$  still fresh enough, this can be influenced by the salt tolerance of their crops. Further, Chapter 2.1.2 states that salt can consist of multiple ions. The most common assumption is that the ions are Sodium (Na) and Chloride (Cl), which makes sodium chloride (NaCl). During the flume experiments, both sodium chloride and potassium chloride (KCl) are used to create the brackish water layer.

Additionally, Electrical Conductivity is heavily dependent on temperature. All measurements should be corrected to the standard temperature, which is done by the used equipment, but they were not always reliable. So, the conductivity measurements can slightly be influenced by the (water) temperature, which is again dependent on the weather and season. Temperature can also cause stratification based on density differences.

When implementing a modified weir, an extensive maintenance plan should be made. The innovation has some features, which require special attention. For example, the opening of the underflow gate has to be clean to enable the flow of the brackish water. This demands frequent monitoring of the situation and acting directly if something is wrong. In addition, the vegetation at the watersides of the polder canals is mowed during Spring and in August with tractors. Another potential problem is that the product of the mowed canals can also block the weir. The modified weir is also attached to the water sides, so it can get broken by the large equipment if the location is unknown. The location of the modified weir should be marked with a flag or pole. A brush cutter can then be used to mow the plants around the modified weir. However, this is only the case if a modified weir is implemented in a water canal managed by the water board. If the weir is implemented in a smaller canal of an agricultural field, the maintenance needs to be done by the farmer, who owns the canal.

As discussed in Chapter 5, the implementation of a modified weir is up for debate. Implementing one modified weir is not going to solve the salinization problem, the entire water system should be adapted as well. A modified weir is vulnerable, because of the maintenance and because the design comes precise.

## 6.2 Flume experiments

As mentioned before, the results from the flume experiment need to be taken with some hesitancy. There are discussion points about the varying factors, set-up, and translation into reality.

**Varying factors** There were quite some varying (external) factors during the outside experiments, for example, the weather, wind, added amount of salt, degree of mixing, inlet, and location and depth of the EC-meters. During most of the experiments, the weather was sunny and warm, only once it rained the entire time. However, the exact weather conditions and (water) temperature were not written down. These conditions can have influenced the experiment, for example, the temperature can also cause stratification of water or because of evaporation of fresh water.

The exact salt concentrations during the experiments were unknown because the amount of salt added varied, the mixing was done manually and the amount of water varied. In the experiments, in which a brackish water layer was created, the concentration was supposed to be  $4000 \text{ mg/l}$ . However, the implementation of a ramp was not considered, this shortened the length of the brackish water layer and increased the concentration. Yet, the addition of the buckets with brackish water decreased probably the concentration. Also, the inlet of fresh water to the concrete flume changed every experiment and even during the experiment itself. In Figures 42, 43, 44, 45, it can be seen that when the inlet was constant and high, brackish water was pushed towards and through the structure, though the exact inlet discharges are unknown. The variable inflows influenced the data series of the experiments, random high peaks are visible in the graphs.

**Design of experiments** The set-up of the experiments also changed. Sometimes based on the experiences of previous experiments, or on what was available, and sometimes unknowingly. The degree of mixing, the amount of water wherein the salt dissolved, the exact amount of inlet water, and the exact locations and depths of the EC-meters during the experiments are conditions that cannot be repeated. This causes that, even though the method was the same, the exact setup was unknown. So, the influence of one changed factor cannot be described for sure.

The set-up of the flume experiment, outside with a wooden structure in a concrete flume, was also not ideal. The fresh and brackish water flows were visualized with fluorescein. However, the exact depths and layering were not visible, as the concrete flume could only be observed from the side. Also, the concrete flume has small holes at the bottom, two were exactly downstream of the wooden construction of the modified weir. Water could flow from inside the structure through the holes and leave the structure here instead of over the weir, which causes a constant flow of brackish water underneath the weir. This leakage influences the measurements downstream of the structure, as not all water there has flown over the weir. It was visible, especially during experiment 7.

**Translation into reality** In reality, the brackish water layer is created by saline seepage. Creating this layer and simulating seepage in an experiment is difficult. In this research, the salt addition method with tubes worked better than creating the layer manually. Bringing brackish water underneath a freshwater layer with tubes works the same way as saline seepage. So, it is better to bring brackish water underneath fresh water rather than letting freshwater flow on top of brackish water. Further, these flume experiments were performed in a squared block of concrete. Water flow in a canal can be influenced by plants and varying beds, which were not present in the experiments. This raises the question of how representative the flume experiments were.

### 6.3 Field campaign

One discussion point for the field campaign is the spatial distribution of the measurements over the Negenboerenpolder. When looking at Figure 25, the measurements are not equally divided over the polder. There are a lot of measurements around the weir on the south side, and there is a measurement location for the depth profile outside the polder, but there is no continuous EC-routing like the one in August 2021 (Appendix C). Also, most measurements are local point measurements, which only represent the situation at that exact moment. The used locations were chosen, because of accessibility and a time limit. The EC routing was not possible due to a lack of time and incomplete equipment. So, because of the limited selected locations, a representative and total fresh-brackish water distribution of the Negenboerenpolder could thus not be made in this research.

To get insight into the full fresh-brackish water distribution in the Negenboerenpolder, it would be interesting to do a seasonal EC-routing. One routing during Summer and one during Winter would help to observe the distribution during one year. Further, continuous conductivity measurements at two depths in the primary (and main secondary) water canals every 500 *m* are also an option to investigate the salinity in the polder and possibly the stratification. With these measurements, knowledge is gained about the locations where saline seepage is more present and locations where stratification occurs. Based on this, a new water system can be designed for the Negenboerenpolder, with selected fresh and brackish water canals.

For the analysis of the local fresh and brackish water distribution, only four depth profiles are made, and one of them was outside the Negenboerenpolder. This makes the results not representative of the entire polder. Further, these conductivity measurements are done manually. As the water was moving, the rope of the sensor was not always vertically in the water. There was no weight used at the end of the EC sensor to create a straight line over the water depth, so the exact depths of the measurements are unknown. This makes the measurements at the indications less reliable.

The analysis of the continuous measurements gave also some discussion points. The most important one is the empty battery and malfunctioning of the equipment, both let to gaps in the data series. The results of the measurement location downstream of the weir were especially important for the indication of stratification (Figure 4) in the Negenboerenpolder. Moreover, only two possible explanations for the conductivity and water level results are analysed during this research, but there are much more influencing factors. For example, the vegetation and seepage flux are not taken into account.

For the comparison of the continuous measurements with the precipitation and tides, the measurements at Lauwersoog are used, this is around 10 *km* West of the Negenboerenpolder. The KNMI has a weather station in this village, Rijkswaterstaat measures the tides at the Wadden Sea side at Lauwersoog. It is questionable how accurate this weather data is for the Negenboerenpolder, because of its local variability. Lastly, it was the goal to compare the results to the pumping data of Waterboard Noorderzijlvest, but this was not made available on time. The data could have been helpful to explain and justify the sudden water level variations that are visible in the results. The abstractions for irrigation by the farmers would also be useful data for this assessment, but this is not registered.

## 6.4 2D simulations

This section contains discussion points for the 2D simulations in the CFD software. In general, there was limited time and knowledge to learn how to work with ANSYS Fluent, and there were computational constraints. It is not simple to model a modified weir with open channel flow and fresh and brackish water in ANSYS Fluent, it takes some time to master the software. Also, during this research no calculation software or cloud is used, only two standard PCs. Further, the CFD model is not compared to the same experimental situation to check the CFD model results. This makes it difficult to check if the modelling results were sufficient.

Regarding the input and settings of ANSYS Fluent, there are some points of discussion. For example, the fluids used in the CFD model are perfect fluids, they are either fully fresh ( $1000 \text{ kg/m}^3$ ) or a full saline solution ( $1025 \text{ kg/m}^3$ ). Secondly, there is no mixing of fresh and saline water, they are two entirely different fluids. The CFD model consists thus of two perfect layers, but there is a salt gradient and mixing in practice. A modified weir can never discharge the saline water layer, there is a salt gradient, and thus only the most saline water at the bottom is discharged. This means that the 2D simulations with two layers gave an incorrect image of the discharge of saline water. Another shortcoming is that the saline water inlet velocity was set at  $0 \text{ m/s}$ , in comparison to a freshwater inlet velocity of  $0.01 \text{ m/s}$  or  $0.10 \text{ m/s}$ . However, it is not sure that the saline water layer is fixed. This set-up could only be the case downstream of a traditional weir, which discharges fresh water into an already saline water canal towards a modified weir. Also, the saline water volume is relatively large in comparison to the freshwater volume, this can only be the case during winter when there is limited flushing.

Further, to simulate open water flow, the open canal flow settings are used, which causes again some discussion points. First, waves are not included in the CFD model, but they will be there in nature. Additionally, the design in ANSYS Fluent does not contain vegetation and debris, this perfect flume is not representative of a field situation. The setting 'enhanced wall roughness' is used, but this can never be enough to model the actual circumstances. Besides, during the field campaign, a preferential flow path in the water canals could be observed caused by vegetation in the canal. Water was not flowing over the entire width of the water canal, which is not taken into account during the CFD modelling, but also difficult to model as it is constantly changing. Lastly, a modified weir can cause an accumulation of mud at the upstream side of the weir and removal of soil downstream of the weir, which should be investigated.

During this research, a 2D model of the modified weir is made and analysed. A 2D model has a grid with sufficient precision in the horizontal and vertical direction [Hargreaves et al., 2007]. So, it is better to use 2D instead of 3D, which supports this research. However, when using 3D, the entire design of a modified weir (also with a 'control notch') can be investigated. This is explained further in Appendix M.

## 7 Conclusions and recommendations for future research

This chapter contains the answer to the main research question given in Chapter 1.4. The performed research implies that a modified weir can discharge brackish water in a shallow polder water canal, whenever the weir is designed and implemented carefully. This chapter also contains a list of recommendations for future research, like implementing a modified weir (in the Negenboerenpolder) and investigating the flow around an underflow gate with a 3D CFD model.

### 7.1 Conclusions

This research investigated if a modified weir is useful in areas with brackish seepage and how such a weir can be implemented. The main research question was: “*Can a modified weir discharge brackish water from a stratified shallow polder water canal?*”. With a combination of fieldwork, flume experiments, and 2D simulations, an answer to the main research question is found.

The presented results showed that a modified weir can be used to discharge brackish water from a stratified water canal. However, the modified weir needs to be designed precisely for the correct functioning of the weir. As is demonstrated in this research (for the Negenboerenpolder), stratification of fresh and brackish water occurs in shallow polder water canals. The flume experiments gave information about the procedure of conducting experiments with a modified weir and about the implementation of the weir. For example, tracers are useful to distinguish fresh and brackish water and stratification is entirely gone downstream of the weir, so multiple modified weirs cannot be implemented in a sequence. The 2D simulations suggest that a modified weir operates as predicted, but the settings were not entirely representative. Observations in this research were that a modified weir works better with a lower flow velocity and a larger distance between the underflow gate and the weir.

Furthermore, implementation advice for the modified weir is given in this research. It stated that a modified weir should be installed in canals that can be flushed, and upstream of locations that can handle a higher water salinity. It is also important that such a weir could be adjusted to avoid obstruction of the water flow. However, it is expected that only the implementation of one modified weir in a polder is not enough to prevent salinization problems, the entire water system should be reconsidered. A point of discussion is that this research assumed two perfect layers, fresh and saline water, in contrast to a salt gradient in an actual canal. To conclude, the flume experiments and 2D simulations in this research showed that a modified weir can be used in areas with salinization problems, but the design and implementation should be done carefully.

### 7.2 Recommendations for future research

This section contains an overview of recommendations for future research, based on this research, for the three methods: experiments, fieldwork, and modelling.

Recommendations for flume experiments:

- Test the modified weir in a transparent flume, to visibly investigate the water flow. It is important to bring brackish water underneath fresh water and to use a tracer for visible separation.
- Test the modified weir with a narrow underflow gate and an underflow gate over the entire width of the flume to compare the influence of horizontal contraction on the flow.

Recommendations with field data and/or in the field:

- Compare the continuously measured data with the pumping data of Waterschap Noorderzijlvest, as it could not be done during this research.
- Implement a modified weir in the field (possibly in the Negenboerenpolder) and measure how it works. Important is to measure EC at various depths at multiple locations around the weir.
- Make a standard method for farmers and field workers to measure Electrical Conductivity at the surface and bottom of water canals, to be able to compare various measurements.
- Investigate if density-controlled stratification, based on salinity, also happens in other polders in the Netherlands, or even the world, to check if the Negenboerenpolder was not the exception.

Recommendations for (CFD) modelling:

- Use another CFD modelling software, OpenFoam, instead of ANSYS Fluent. OpenFoam can do exactly the same, but the software is open and accessible, no (university) licence is needed.
- Model the modified weir in a CFD model with a salt gradient instead of the two separate fluids, fresh and saline water, because that represents an actual water canal better.
- Vary the dimensions of the 2D design of a modified weir in a CFD model, especially the size of the underflow gate with various water depths.
- Investigate with a CFD model when stratified water mixes in shallow water canals, this can be done by varying velocities, and with various vegetation types.
- Use calculation software or a cloud for longer and heavier ANSYS Fluent or CFD modelling calculations, to be able to run larger and more detailed simulations.
- Model a modified weir in 3D to investigate the design in a modelled canal. A start with this was already made in this research (Appendix M).

## References

- Abdurrasheed, A., Wan Yusof, K., Takaijudin, H., & Ab Ghani, A. (2018). Effects of backwater on hydraulic performance evaluation of rainsmart modules in sustainable drainage systems. Retrieved December 5, 2022, from [https://www.researchgate.net/publication/329306031\\_EFFECTS\\_OF\\_BACKWATER\\_ON\\_HYDRAULIC\\_PERFORMANCE\\_EVALUATION\\_OF\\_RAINDRIFT\\_MODULES\\_IN\\_SUSTAINABLE\\_DRAINAGE\\_SYSTEMS](https://www.researchgate.net/publication/329306031_EFFECTS_OF_BACKWATER_ON_HYDRAULIC_PERFORMANCE_EVALUATION_OF_RAINDRIFT_MODULES_IN_SUSTAINABLE_DRAINAGE_SYSTEMS)
- Abrol, I. P., Yadav, J. S. P., & Massoud, F. I. (1988). *Salt-affected soils and their management*. Food & Agriculture Org. Retrieved August 23, 2022, from [https://books.google.nl/books?hl=nl&lr=&id=II1HAY-DSGsC&oi=fnd&pg=PR3&ots=8NgD3yvcic&sig=8ccAIQ6IIYe6dz2njfHNkPduk10&redir\\_esc=y#v=onepage&q&f=false](https://books.google.nl/books?hl=nl&lr=&id=II1HAY-DSGsC&oi=fnd&pg=PR3&ots=8NgD3yvcic&sig=8ccAIQ6IIYe6dz2njfHNkPduk10&redir_esc=y#v=onepage&q&f=false)
- Acacia Institute. (2021). *Zoet op Zout* [Over Zoet op Zout]. Retrieved July 26, 2022, from <https://zoetopzout.nl/>
- Acacia Institute. (2022). *Spaarwater* [Spaarwater]. Retrieved July 26, 2022, from <https://www.spaarwater.com/pg-27227-7-101924/pagina/spaarwater.html>
- Acacia Institute & LTO Noord. (n.d.). *Boeren Meten Water* [Boeren Meten Water]. Retrieved August 23, 2022, from <https://boerenmetenwater.nl/>
- Acacia Water. (2020, June 7). *Boeren van Texel gaan van start met zoetwater opslag in strijd tegen droogte*. Retrieved August 2, 2022, from [https://www.acaciawater.com/nw-28008-7-3796332/nieuws/boeren\\_van\\_texel\\_gaan\\_van\\_start\\_met\\_zoetwater\\_opslag\\_in\\_strijd\\_tegen\\_droogte.html](https://www.acaciawater.com/nw-28008-7-3796332/nieuws/boeren_van_texel_gaan_van_start_met_zoetwater_opslag_in_strijd_tegen_droogte.html)
- Aerts, J., Major, D. C., Bowman, M. J., Dircke, P., & Aris Marfai, M. (2009). *Connecting delta cities: Coastal cities, flood risk management and adaptation to climate change*. Retrieved July 26, 2022, from <https://www.vliz.be/en/imis?refid=199783>
- Ankum, P. (2002). *Design of open-channels and hydraulic structures*. TU Delft, Faculteit Civiele Techniek en Geowetenschappen.
- ANSYS Inc. (2009a, January 29). *13.2.4 natural convection and buoyancy-driven flows* [ANSYS FLUENT 12.0 user's guide]. Retrieved January 24, 2023, from <https://www.afs.enea.it/project/neptunius/docs/fluent/html/ug/node470.htm>
- ANSYS Inc. (2009b, January 23). *16.3.9 open channel flow* [ANSYS FLUENT 12.0 theory guide]. Retrieved January 25, 2023, from <https://www.afs.enea.it/project/neptunius/docs/fluent/html/th/node306.htm>
- ANSYS Inc. (2009c, January 29). *24.3.1 modeling open channel flows* [ANSYS FLUENT 12.0 user's guide]. Retrieved January 25, 2023, from <https://www.afs.enea.it/project/neptunius/docs/fluent/html/ug/node731.htm>
- ANSYS Inc. (2009d, January 29). *7.3.3 pressure inlet boundary conditions* [ANSYS FLUENT 12.0 user's guide]. Retrieved March 3, 2023, from <https://www.afs.enea.it/project/neptunius/docs/fluent/html/ug/node239.htm>
- ANSYS Inc. (2023). *Ansys fluent — fluid simulation software*. Retrieved January 25, 2023, from <https://www.ansys.com/products/fluids/ansys-fluent>
- Bezoek TexelBeton. (2022, August 3).
- Boeren Meten Water. (n.d.). *Acht pilotgebieden* [Boeren Meten Water]. Retrieved August 16, 2022, from <https://boerenmetenwater.nl/acht-pilotgebieden-2/>
- Bot, B. (2016). *Grondwaterzakboekje2016*. Bot Raadgevend Ingenieur. Retrieved November 8, 2022, from <http://www.grondwaterzakboekje.nl/>
- Bryant, P. J., & Wood, I. R. (1976). Selective withdrawal from a layered fluid. *Journal of Fluid Mechanics*, 77(3), 581–591. <https://doi.org/10.1017/S0022112076002267>

- Chappel, E. (2020). A review of passive constant flow regulators for microfluidic applications [Number: 24 Publisher: Multidisciplinary Digital Publishing Institute]. *Applied Sciences*, *10*(24), 8858. <https://doi.org/10.3390/app10248858>
- Conijn, A., & Albers-Schouten, H. (2020, July 4). *Integrale Effecten Analyse: Net op zee Ten noorden van de Waddeneilanden* (Integrale effectenanalyse No. 114227-6). Witteveen+Bos Raadgevende ingenieurs B.V. Devenber. Retrieved August 16, 2022, from <https://gemeenteraad.groningen.nl/Documenten/Collegedebrieven/Bijlage-2-Integrale-Effecten-Analyse-Net-op-zee-Ten-noorden-van-de-Waddeneilanden.pdf>
- Corwin, D. (2003, January 1). Soil salinity measurement. In *Encyclopedia of water science* (pp. 852–857). Marcel Dekker.
- Corwin, D., & Yemoto, K. (2017, February 15). Salinity: Electrical conductivity and total dissolved solids [Journal Abbreviation: Methods of Soil Analysis]. In *Methods of soil analysis*. <https://doi.org/10.2136/msa2015.0039>
- Courant, R., Friedrichs, K., & Lewy, H. (1928). Über die partiellen Differenzgleichungen der mathematischen Physik. *Mathematische Annalen*, *100*(1), 32–74. <https://doi.org/10.1007/BF01448839>
- de Boer, K. (2021, August 10). *Projectplan Uitvoeringsfase 1, Werkzaamheden Eijerland* (Projectplan No. 21.0760093). Hoogheemraadschap Hollands Noorderkwartier. Retrieved August 16, 2022, from [https://www.hhnk.nl/\\_flysystem/media/20210812-21.0760093-projectplan-eijerland-uitvoeringsfase-1-texel.pdf](https://www.hhnk.nl/_flysystem/media/20210812-21.0760093-projectplan-eijerland-uitvoeringsfase-1-texel.pdf)
- de Bruijn, N. (n.d.). *Noordelijke kleischil* [Regiodeal natuurinclusieve landbouw]. Retrieved August 24, 2022, from <https://www.regiodealnatuurinclusievelandbouw.nl/gebieden/noordelijke-kleischil>
- de Louw, P., Eeman, S., Oude Essink, G., Vermue, E., & Post, V. (2013). Rainwater lens dynamics and mixing between infiltrating rainwater and upward saline groundwater seepage beneath a tile-drained agricultural field. *Journal of Hydrology*, *501*, 133–145. <https://doi.org/10.1016/j.jhydrol.2013.07.026>
- de Louw, P., Eeman, S., Siemon, B., Voortman, B., Gunnink, J., van Baaren, E., & Oude Essink, G. (2011). Shallow rainwater lenses in deltaic areas with saline seepage [Publisher: Copernicus GmbH]. *Hydrology and Earth System Sciences*, *15*(12), 3659–3678. <https://doi.org/10.5194/hess-15-3659-2011>
- de Louw, P., Oude Essink, G., Stuyfzand, P., & van der Zee, S. (2010). Upward groundwater flow in boils as the dominant mechanism of salinization in deep polders, the netherlands. *Journal of Hydrology*, *394*(3), 494–506. <https://doi.org/10.1016/j.jhydrol.2010.10.009>
- de Louw, P., Vandenbohede, A., Werner, A., & Oude Essink, G. (2013). Natural saltwater upconing by preferential groundwater discharge through boils. *Journal of Hydrology*, *490*, 74–87. <https://doi.org/10.1016/j.jhydrol.2013.03.025>
- Delsman, J. R., Waterloo, M. J., Groen, M. M. A., Groen, J., & Stuyfzand, P. J. (2014). Investigating summer flow paths in a dutch agricultural field using high frequency direct measurements. *Journal of Hydrology*, *519*, 3069–3085. <https://doi.org/10.1016/j.jhydrol.2014.10.058>
- de Olde, F. (2022, March 8). *EC-tabel schetst zouttolerantie* [Boeren Meten Water]. Retrieved July 4, 2022, from <https://boerenmetenwater.nl/ec-tabel-schetst-zouttolerantie/>
- Dijkema, J. (2017, February 19). *Kwel* [Het Reestdal]. Retrieved November 24, 2022, from <https://hetreestdal.nl/?p=6348>
- Evers, C., van den Broek, A., Buskens, R., van Leerdam, A., Knobben, R., van Herpen, F., & Pot, R. (2018). *Omschrijving MEP en maatregelen voor sloten en kanalen voor de Kaderrichtlijn Water 2021-2027* (No. 2018-50). STOWA. Amersfoort. Retrieved October 5, 2022, from <https://www.stowa.nl/publicaties/omschrijving-mep-en-maatregelen-voor-sloten-en-kanalen-voor-de-kaderrichtlijn-water-2021-2027>



- [//www.stowa.nl/publicaties/omschrijving-mep-en-maatlatten-voor-sloten-en-kanalen-voor-de-kaderrichtlijn-water-2021](https://www.stowa.nl/publicaties/omschrijving-mep-en-maatlatten-voor-sloten-en-kanalen-voor-de-kaderrichtlijn-water-2021)
- Feng, K. (2019). *Numerical simulation of bubble screens for mitigating salt intrusion through sea locks* (Master thesis). Delft University of Technology. Delft. Retrieved September 7, 2022, from <https://repository.tudelft.nl/islandora/object/uuid%3A258e23af-51eb-491e-8886-f029c4dc32b5>
- Ferziger, J., & Peric, M. (2002). *Computational methods for fluid dynamics* (3rd, rev. ed.). Springer. Retrieved October 6, 2022, from [https://docs.google.com/file/d/0B7WvmGcRs5CzanBEeDlDaEk3dEU/edit?usp=embed\\_facebook](https://docs.google.com/file/d/0B7WvmGcRs5CzanBEeDlDaEk3dEU/edit?usp=embed_facebook)
- Fixeau. (n.d.-a). *Fixeau*. Retrieved August 23, 2022, from <https://fixeau.com/>
- Fixeau. (n.d.-b). *Fixeau dashboard*. Retrieved August 22, 2022, from <https://dashboard.fixeau.com/map>
- Fondriest Environmental, Inc. (2014, March 3). *Conductivity, salinity & total dissolved solids* [Fundamentals of environmental measurements.]. Retrieved August 17, 2022, from <https://www.fondriest.com/environmental-measurements/parameters/water-quality/conductivity-salinity-tds/>
- Google Maps. (n.d.). *Google Maps* [Google Maps]. Retrieved May 7, 2023, from <https://www.google.com/maps/@53.4001845,6.3828097,5503m/data=!3m1!1e3>
- Gould, I., De Waegemaeker, J., Tzemi, D., Wright, I., Pearson, S., Ruto, E., Karrasch, L., Christensen, L. S., Aronsson, H., & Eich-Greatorex, S. (2021). Salinization threats to agriculture across the north sea region [Publisher: CRC Press]. *Future of Sustainable Agriculture in Saline Environments*, 71–92.
- Groen, K., de Wit, L., & Velstra, J. (2017, January 20). *De zoete stuw: Ontwerpen en computersimulaties van zoete stuwen met als doel de zoetwaterberging in watergangen van zoute polders te bevorderen* (Eindrapport No. 706). Acacia Water. Gouda. Retrieved July 26, 2022, from [https://www.texelwater.nl/application/files/7414/9147/3367/De\\_zoete\\_stuw\\_1.pdf](https://www.texelwater.nl/application/files/7414/9147/3367/De_zoete_stuw_1.pdf)
- Hargreaves, D. M., Morvan, H. P., & Wright, N. G. (2007). Validation of the volume of fluid method for free surface calculation: The broad-crested weir [Publisher: Taylor & Francis eprint: <https://doi.org/10.1080/19942060.2007.11015188>]. *Engineering Applications of Computational Fluid Mechanics*, 1(2), 136–146. <https://doi.org/10.1080/19942060.2007.11015188>
- Hilgersom, K. P. (2017). *Measuring and modelling salt and heat transport in low-land drainage canals: Flow and stratification effects of saline seepage* (Doctoral dissertation). Delft University of Technology. Delft. Retrieved July 4, 2022, from <https://repository.tudelft.nl/islandora/object/uuid%3A3519c954-ab49-45a9-b4c7-41867e2f38cb>
- Hirt, C. W., & Nichols, B. D. (1981). Volume of fluid (VOF) method for the dynamics of free boundaries. *Journal of Computational Physics*, 39(1), 201–225. [https://doi.org/10.1016/0021-9991\(81\)90145-5](https://doi.org/10.1016/0021-9991(81)90145-5)
- Hoes, O. (2022, April 13). Separating fresh and brackish water in the flume.
- Hoes, O., & vd Giesen, N. (2015, April). *CT4460: Polders*. TU Delft.
- Hoogheemraadschap Hollands Noorderkwartier. (2022, February 24). *Projectplan Polder Het Noorden op Texel* [Waterwet] [Journal Abbreviation: Projectplan Polder Het Noorden op Texel Publisher: Hoogheemraadschap Hollands Noorderkwartier]. Retrieved August 16, 2022, from <https://zoek.officielebekendmakingen.nl/wsb-2022-2196.html>
- Kalsbeek, G. (2014, November 24). *Zoute kwel bedreigt Droogmakerijen — De Geobronnen*. Retrieved August 17, 2022, from <https://www.geobronnen.com/zoute-kwel-bedreigt-droogmakerijen.html>

- KNMI. (n.d.-a). *Daggegevens van het weer in Nederland* [Klimatologie]. Retrieved January 9, 2023, from <https://www.knmi.nl/nederland-nu/klimatologie/daggegevens>
- KNMI. (n.d.-b). *Uurgegegevens van het weer in Nederland* [Klimatologie]. Retrieved January 9, 2023, from <https://www.knmi.nl/nederland-nu/klimatologie/uurgegegevens>
- Li, G., Cheng, L., Zhu, J., Trenberth, K. E., Mann, M. E., & Abraham, J. P. (2020). Increasing ocean stratification over the past half-century [Number: 12 Publisher: Nature Publishing Group]. *Nature Climate Change*, *10*(12), 1116–1123. <https://doi.org/10.1038/s41558-020-00918-2>
- LTO Noord. (2021, May 25). *Boeren Meten Water officieel van start in Negenboerenpolder*. Retrieved August 16, 2022, from <https://www.ltonoord.nl/regios-en-provincies/regio-noord/groningen/actueel/boeren-meten-water-officieel-van-start-in-negenboerenpolder>
- Maijvis, S. D. (2022, July). *Numerical modelling of selective withdrawal for the mitigation of salt intrusion* (Master thesis). Eindhoven University of Technology. Delft. Retrieved October 12, 2022, from [https://pure.tue.nl/ws/portalfiles/portal/217980908/0907131\\_Maijvis\\_S.D.\\_MSc\\_thesis\\_Thesis\\_MAP.pdf](https://pure.tue.nl/ws/portalfiles/portal/217980908/0907131_Maijvis_S.D._MSc_thesis_Thesis_MAP.pdf)
- Ministerie van Infrastructuur en Waterstaat. (2015, September 16). *Waterbeheer in Nederland - Water - Rijksoverheid.nl* [Last Modified: 2022-05-11T14:18 Publisher: Ministerie van Algemene Zaken]. Retrieved December 8, 2022, from <https://www.rijksoverheid.nl/onderwerpen/water/waterbeheer-in-nederland>
- Ministerie van Infrastructuur en Waterstaat. (2020, September 1). *Zoetwater - Drie thema's - Deltaprogramma* [Last Modified: 2021-08-19T10:51 Publisher: Ministerie van Infrastructuur en Waterstaat]. Retrieved July 5, 2022, from <https://www.deltaprogramma.nl/themas/zoetwater>
- Naik, B., Khatua, K., Wright, N., Sleigh, A., & Singh, P. (2017). Numerical modeling of converging compound channel flow numerical modeling of converging compound channel flow. *ISH Journal of Hydraulic Engineering*. <https://doi.org/10.1080/09715010.2017.1369180>
- Nederlandse Hydrologische Vereniging. (2002). *Hydrologische Woordenlijst*. [https://www.nhv.nl/wp-content/uploads/2021/06/NHVspecial\\_5\\_hydrologische\\_woordenlijst.pdf](https://www.nhv.nl/wp-content/uploads/2021/06/NHVspecial_5_hydrologische_woordenlijst.pdf)
- Negacz, K., Vellinga, P., Barrett-Lennard, E., Choukr-Allah, R., & Elzenga, T. (2021, June 25). *Future of sustainable agriculture in saline environments*. CRC Press. <https://doi.org/10.1201/9781003112327>
- Nieuwenhuis, H. S., & Schokking, F. (1997). Land subsidence in drained peat areas of the province of friesland, the netherlands [Publisher: Geological Society of London Section: Article]. *Quarterly Journal of Engineering Geology and Hydrogeology*, *30*(1), 37–48. <https://doi.org/10.1144/GSL.QJEGH.1997.030.P1.04>
- Pauw, P., de Louw, P., & Oude Essink, G. (2012). Groundwater salinisation in the wadden sea area of the netherlands: Quantifying the effects of climate change, sea-level rise and anthropogenic interferences. *Netherlands Journal of Geosciences - Geologie en Mijnbouw*, *91*(3), 373–383. <https://doi.org/10.1017/S0016774600000500>
- PDOK. (n.d.-a). *AHN3 downloads*. Retrieved August 25, 2022, from <https://app.pdok.nl/ahn3-downloadpage/>
- PDOK. (n.d.-b). *BRO bodemkaart - bodemvlakken, basisregistratie ondergrond (BRO)*. Retrieved August 24, 2022, from <https://app.pdok.nl/viewer/>
- Poirrier, M. (1978). Studies of salinity stratification in southern lake pontchartrain near the inner harbor navigation canal. *The Proceedings of the Louisiana Academy of Sciences*, *41*, 26–35.
- Profishop. (n.d.). *Greisinger GMH 3431 geleidbaarheidsmeetapparaat inclusief 2-polige meetcel 601917* [PROFISHOP]. Retrieved September 20, 2022, from <https://www.profishop.com/nl/greisinger-gmh-3431-geleidbaarheidsmeetapparaat-inclusief-2-polige-meetcel-601917>

- Quora. (2023). *What is the difference between pressure based solver and density based solver in ansys fluent? what is the criteria while selecting one o...* [Quora]. Retrieved January 30, 2023, from <https://www.quora.com/What-is-the-difference-between-pressure-based-solver-and-density-based-solver-in-Ansys-Fluent-What-is-the-criteria-while-selecting-one-of-them>
- Redactie Waterforum. (2022, August 11). “*Er is genoeg zoet water voor Zeeland*” [Waterforum]. Retrieved August 17, 2022, from <https://www.waterforum.net/er-is-genog-zoet-water-voor-zeeland/>
- Rhoades, J. D., Kandiah, A., & Mashali, A. M. (1992). *The use of saline waters for crop production*. Food; Agriculture Organization of the United Nations.
- Rijkswaterstaat. (n.d.). *Lauwersoog - rijkswaterstaat waterinfo*. Retrieved January 9, 2023, from [https://waterinfo.rws.nl/#!/details/publiek/astronomische-getij/Lauwersoog\(LAUWOG\)/Waterhoogte\\_\\_\\_20berekend\\_\\_\\_20Oppervlaktewater\\_\\_\\_20t.o.v.\\_\\_\\_\\_20Normaal\\_\\_\\_20Amsterdams\\_\\_\\_20Peil\\_\\_\\_20in\\_\\_\\_20cm](https://waterinfo.rws.nl/#!/details/publiek/astronomische-getij/Lauwersoog(LAUWOG)/Waterhoogte___20berekend___20Oppervlaktewater___20t.o.v.____20Normaal___20Amsterdams___20Peil___20in___20cm)
- Schönfeld, J. C., & Kranenburg, C. (1977). *Dichtheidsstromen en interne golven: Collegehandleiding*. TU Delft, Department of Hydraulic Engineering. Retrieved June 21, 2022, from <https://repository.tudelft.nl/islandora/object/uuid%3A55eb3a2f-8ddd-4edc-a35e-d88d78558eb0>
- Schoonbeek, J. B. (1976). Land subsidence as a result of natural gas extraction in the province of groningen. <https://doi.org/10.2118/5751-MS>
- Schultz, B. (1996). De waterbeheersing van droogmakerijen. *Rijkswaterstaat-serie (55)*, 130. <https://library.wur.nl/WebQuery/hydrotheek/942001>
- ScienceDirect. (2023, January 26). *Computational fluid dynamics - an overview — ScienceDirect topics*. Retrieved January 26, 2023, from <https://www.sciencedirect.com/topics/materials-science/computational-fluid-dynamics>
- Segeren, W. A. (1983). Introduction to polders of the world. *Water International*, 8(2), 51–54. <https://doi.org/10.1080/02508068308686006>
- Seyyedvalilu, H. (2018, October 25). *Difference between standard and realizable k-epsilon model?* [ResearchGate]. Retrieved January 30, 2023, from <https://www.researchgate.net/post/Difference-between-standard-and-realizable-k-epsilon-model>
- Simscale. (2021, September 3). *What is reynolds number? — SimWiki* [SimScale]. Retrieved December 5, 2022, from <https://www.simscale.com/docs/simwiki/numerics-background/what-is-the-reynolds-number/>
- Steffelbauer, D. B., Riva, R. E. M., Timmermans, J. S., Kwakkel, J. H., & Bakker, M. (2022). Evidence of regional sea-level rise acceleration for the north sea. *Environmental Research Letters*, 17(7), 074002. <https://doi.org/10.1088/1748-9326/ac753a>
- TexelBeton. (n.d.). *Zoete Stuw* [De Zoete Stuw]. Retrieved July 29, 2022, from <https://www.zoetestuwnl/>
- The Potato Valley. (n.d.). *The Potato Valley: kleigebieden Groningen en Fryslân topproducent* [The Potato Valley]. Retrieved July 27, 2022, from <https://www.thepotatovalley.nl/over-the-potato-valley-4/wereldwijde-topproducent-poot aardappelen>
- US Salinity Laboratory Staff. (1954, February). *Diagnoses and improvement of saline and alkali soils*. United States Department of Agriculture. Retrieved August 22, 2022, from [https://www.ars.usda.gov/ARSUserFiles/20360500/hb60\\_pdf/hb60complete.pdf](https://www.ars.usda.gov/ARSUserFiles/20360500/hb60_pdf/hb60complete.pdf)
- van de Ven, G. (1993). *Man-made lowlands: History of water management and land reclamation in the netherlands* [tex.lccn: lc93248051]. Uitgeverij Matrijs. <https://books.google.nl/books?id=sLshAQAAIAAJ>

- Vandenbohede, A., de Louw, P., & Doornenbal, P. (2014). Characterizing preferential groundwater discharge through boils using temperature. *Journal of Hydrology*, 510, 372–384. <https://doi.org/10.1016/j.jhydrol.2014.01.006>
- van Meijeren, S., van der Heijden, A., Gevaert, A., Velstra, J., & Landheer, J. (2019, January 17). *Spaarwater in de polder: Effecten op polderniveau* (Technische rapportage No. 681). Acacia Water. Gouda. Retrieved August 23, 2022, from [https://www.spaarwater.com/content/27227/download/clnt/87223\\_SW2-03-19\\_-\\_technische\\_rapportage\\_SW\\_in\\_de\\_polder\\_08-03-2019.pdf](https://www.spaarwater.com/content/27227/download/clnt/87223_SW2-03-19_-_technische_rapportage_SW_in_de_polder_08-03-2019.pdf)
- Versteeg, H. K., & Malalasekera, W. (2007). *An introduction to computational fluid dynamics: The finite volume method* (2nd ed) [OCLC: ocm76821177]. Pearson Education Ltd.
- Viswanath, D., Ghosh, T., Prasad, H., Dutt, N., & Rani, K. (1989). *Data book on the viscosity of liquids*. Hemisphere Publishing Corporation. <https://doi.org/10.1007/978-1-4020-5482-2>
- Vos, A. d., Bruning, B., Straten, G. v., Oosterbaan, R., Rozema, J., & Bodegom, P. v. (2016). *Crop salt tolerance under controlled field conditions in the netherlands, based on trials conducted at salt farm texel* [Publisher: Salt Farm Texel]. Salt Farm Texel. Retrieved August 23, 2022, from <https://research.wur.nl/en/publications/crop-salt-tolerance-under-controlled-field-conditions-in-the-neth>
- Wageningen Environmental Research. (2018, January). *Zouttolerantie van teelten* [Deltafacts: altijd de nieuwste feiten over klimaat, waterbeheer en waterkwaliteit]. Retrieved July 27, 2022, from <https://www.stowa.nl/deltafacts/zoetwatervoorziening/verzilting/zouttolerantie-van-teelten>
- Wageningen Environmental Research. (2021). *ArcGIS - LGN2020*. Retrieved August 24, 2022, from <https://www.arcgis.com/home/webmap/viewer.html?layers=2cbb27078b3a40a8a1bcc2080837e49e>
- Wang, C., Zheng, S.-s., Wang, P.-f., & Hou, J. (2015). Interactions between vegetation, water flow and sediment transport: A review. *Journal of Hydrodynamics*, 27(1), 24–37. [https://doi.org/10.1016/S1001-6058\(15\)60453-X](https://doi.org/10.1016/S1001-6058(15)60453-X)
- Westerweel, J. (2020, March 3). *Stromingsleer* [TU delft OCW]. Retrieved December 5, 2022, from <https://ocw.tudelft.nl/courses/stromingsleer/>
- Wright, S., & Parker, G. (2004). Density stratification effects in sand-bed rivers. *Journal of Hydraulic Engineering*, 130(8), 783–795. [https://doi.org/10.1061/\(ASCE\)0733-9429\(2004\)130:8\(783\)](https://doi.org/10.1061/(ASCE)0733-9429(2004)130:8(783))
- WTW. (2022). *Geleidbaarheidsmeters, draagbaar, Cond 3110 / 3310* [VWR]. Retrieved November 25, 2022, from <https://nl.vwr.com/store/product/824946/geleidbaarheidsmeters-draagbaar-cond-3110-3310>
- Yamaguchi, R., & Suga, T. (2019). Trend and variability in global upper-ocean stratification since the 1960s [eprint: <https://onlinelibrary.wiley.com/doi/pdf/10.1029/2019JC015439>]. *Journal of Geophysical Research: Oceans*, 124(12), 8933–8948. <https://doi.org/10.1029/2019JC015439>
- Yildiz, M., Poyraz, İ., Çavdar, A., Özgen, Y., & Beyaz, R. (2020, December 17). *Plant responses to salt stress* [Publication Title: Plant Breeding - Current and Future Views]. IntechOpen. <https://doi.org/10.5772/intechopen.93920>
- Zhang, J., Guo, Y., Shen, Y., & Zhang, L. (2008). Numerical simulation of flushing of trapped salt water from a bar-blocked estuary. *Journal of Hydraulic Engineering*, 134(11), 1671–1676. [https://doi.org/10.1061/\(ASCE\)0733-9429\(2008\)134:11\(1671\)](https://doi.org/10.1061/(ASCE)0733-9429(2008)134:11(1671))

## Appendix

### A Relation EC, Chloride concentration and salt tolerance of various crops

In this appendix, an overview of the salt tolerance of onions, potatoes, flower bulbs, sugar beets, wheat, and grass is shown. The salt tolerance is expressed in threshold values of the electrical conductivity and the chloride concentration. The classification is used for the *Boeren Meten Water* project by Acacia Institute [Acacia Institute and LTO Noord, n.d.; de Olde, 2022].

EC $\mu\text{S/cm}$	EC $\text{mS/cm}$	Chloride $\text{mg/l}$		Threshold values for damage	
				Irrigation	Groundwater
500	0.5	<500	Drinking water	Onion	
1000	1.0	<500		Potato	
1200	1.2	<500		Flower bulbs	Flower bulbs
1500	1.5	<500			
2000	2.0	<500			
2500	2.5	650			Onion
3000	3.0	850			
3500	3.5	1000		Grass	
4000	4.0	1200		Wheat	Potato
4500	4.5	1375		Sugar beet	
5000	5.0	1550			
5500	5.5	1750			
6000	6.0	1900			
6500	6.5	2100			Sugar beet
7000	7.0	2275			
7500	7.5	2450			
8000	8.0	2650			
8500	8.5	2800			
9000	9.0	3000			
9500	9.5	3175			
10000	10.0	2250			
11000	11.0	3725			
12000	12.0	4000			
13000	13.0	4500			
14000	14.0	4800			Grass
15000	15.0	5150			Wheat
20000	20.0	7000			
25000	25.0	8775			
30000	30.0	10600			
35000	35.0	12400			
40000	40.0	14200			
45000	45.0	16000	Sea water		

Figure 53: Table with the salt tolerance of various crops [Translated from de Olde, 2022]

### B Maps of the Negenboerenpolder

In this appendix, the soil and land use map of the Negenboerenpolder can be found. Figure 54 shows the distribution of soil types over the polder, it can be seen that heavy and light materials alternate.

Figure 55 is the land use map of the Negenboerenpolder, the whole area is occupied by agriculture. The most cultivated crops are wheat, sugar beets, and potatoes, but there is also a significant amount of agricultural grass [van Meijeren et al., 2019].

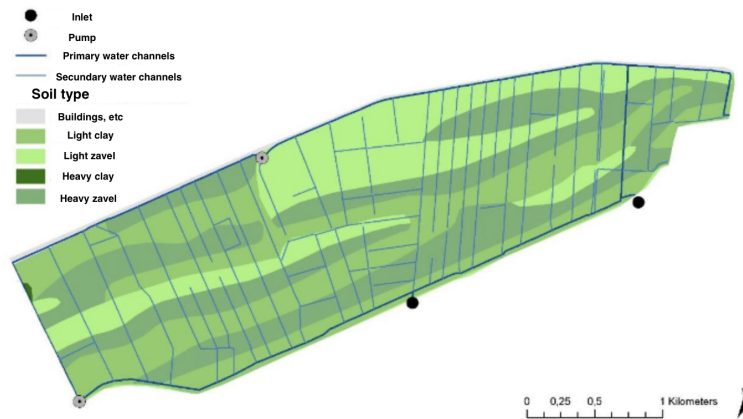


Figure 54: Soil type map of the Negenboerenpolder [Based on van Meijeren et al., 2019; Translated from PDOK, n.d.-b]



Figure 55: Land use map of the Negenboerenpolder in 2020 [Based on van Meijeren et al., 2019; Translated from Wageningen Environmental Research, 2021]

### C Electrical Conductivity routing in the Negenboerenpolder in August 2021

Figure 56 in this appendix shows the results of an Electrical Conductivity routing done by Acacia Water during the Summer of 2021. It can be seen that the Dijksloot next to the Wadden Sea dike has a higher conductivity than the southern water canal.



Figure 56: Routing of the Electrical Conductivity in the Negenboerenpolder during August 2021 [van der Heijden, 2021]

### D Schematic drawings of the sensor depths at the three locations

This appendix contains Figure 57, with schematic drawings of the dimensions and set-up of both the measurement locations and the sensor depths.

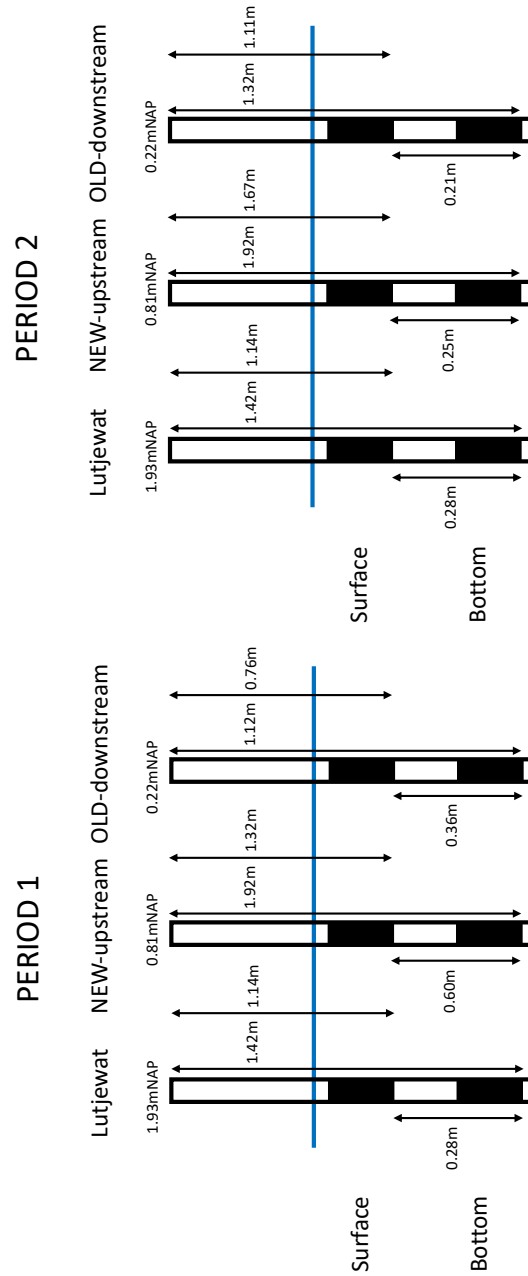


Figure 57: Schematic drawing of continuous measurement locations [Own drawing, 2023]



## E Overview of the flume experiments

This appendix shows an extended version of Table 6 in Chapter 3.1.

Table 12: Full overview of practical input 1

Week	Date	Ground plate?	Salt addition method	Salt amount
1	April 22, 2022	Yes	Buckets, creating saline water layer of 15cm underneath 10cm fresh	18kg in 0.15×1.5×20=4.5m <sup>3</sup>
2	April 29, 2022	Yes	Buckets, creating saline water layer of 15cm underneath 10cm fresh	18kg in 0.15×1.5×20=4.5m <sup>3</sup>
3	May 13, 2022	Yes	Buckets, creating saline water layer of 15cm underneath 10cm fresh	18kg in 0.15×1.5×20=4.5m <sup>3</sup>
4	May 20, 2022	No	Buckets, creating saline water layer of 15cm underneath 10cm fresh	18kg in 0.15×1.5×20=4.5m <sup>3</sup>
5	June 3, 2022	No	Tubes, creating saline layer underneath 15cm freshwater layer	22 kg in 4 buckets
6	June 10, 2022	No	Tubes, creating saline layer underneath 15cm freshwater layer	18 kg in 4 buckets
7	July 25, 2022	No	Tubes, creating saline layer underneath 15cm freshwater layer	9.5 kg in 4 buckets

Table 13: Full overview of practical input 2

Week	Concentration	Inlet	Ramp	Measurement locations
1	4000 mg/l	High, but on/off	Height of 25 cm at 4 m from inlet	3: before, in, after. Not over depth
2	4000 mg/l	Slow and constant	Height of 15 cm underneath inlet	3: same, distances larger
3	4000 mg/l	Buckets underneath inlet to create waterfall	Variable height at 5 m from inlet	5: same + two depths before/after
4	4000 mg/l	?	?	3: before at two depths, after one
5	?	Slow and constant	Not needed	3: before, in, after. Not over depth
6	?	Variable: high, slow and on/off	Not needed	3: variable, before, in, after
7	?	Slow, but on/off	Not needed	3: before, in, after. Not over depth

### F Results of the other flume experiments

This appendix contains the results of the three unreliable flume experiments: experiments 2, 4 and 6. In Figure 58 it can be seen that the conductivity downstream of the structure is quite high directly after the start, higher than the conductivity upstream of the structure. That means that the supposed freshwater layer, downstream of the structure, was already brackish. Also, after 13 minutes, the set-up of the experiment was changed, which makes the experiment not representative.

Figure 59 shows the result of an experiment in the rain. The exact setup and process were not written down because of the weather. For sure, the ground plate was not used and the water downstream of the structure was already brackish. So, this experiment was also not reliable. During the experiment in Figure 60 the set-up of the EC meters was changing. The bottom conductivity upstream of the structure is unusually high, with values around 30 mS/cm. This saline layer is probably heavy and difficult to move. Towards the end, the bottom water inside the structure is getting saline, but the conductivity of the bottom water upstream of the structure declines. This implies that the saline layer is slowly moving in the end. The measuring time should probably have been longer.

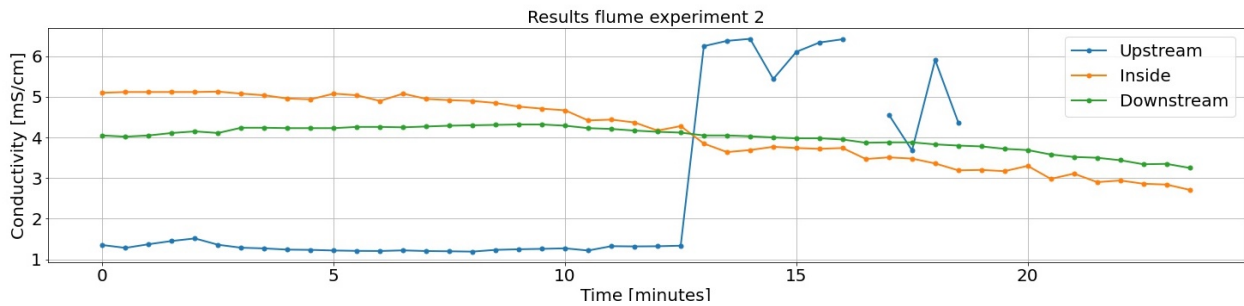


Figure 58: Flume experiment 2 – April 29, 2022

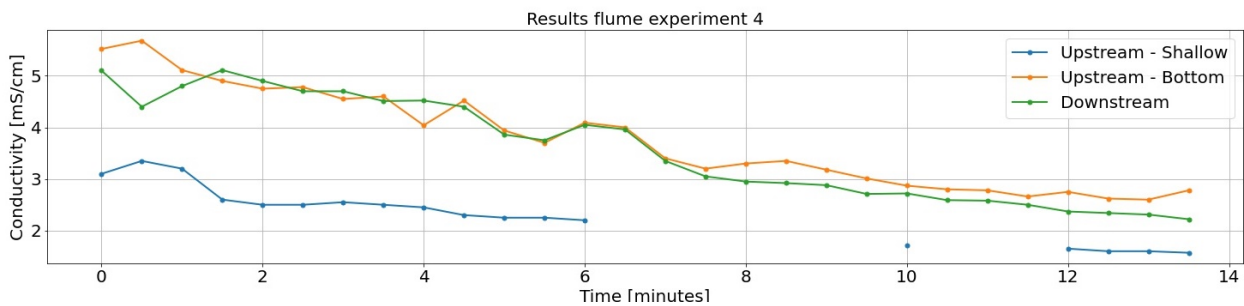


Figure 59: Flume experiment 4 – May 20, 2022

### G Temperature profiles over the depth

This appendix contains measured temperature profiles, the corresponding conductivity profiles can be found in Chapter 4.1.1. In Figure 61 it can be seen that the temperature around the weir stays constant over the depth in July 2022. However, at the location of Eendenkooi, the temperature decreases towards the bottom, beyond -0.70 m the temperature stays constant. In the depth profile at 'Waddenweg South', the water temperature decreases at first, but it is warmer at the bottom than at the surface.

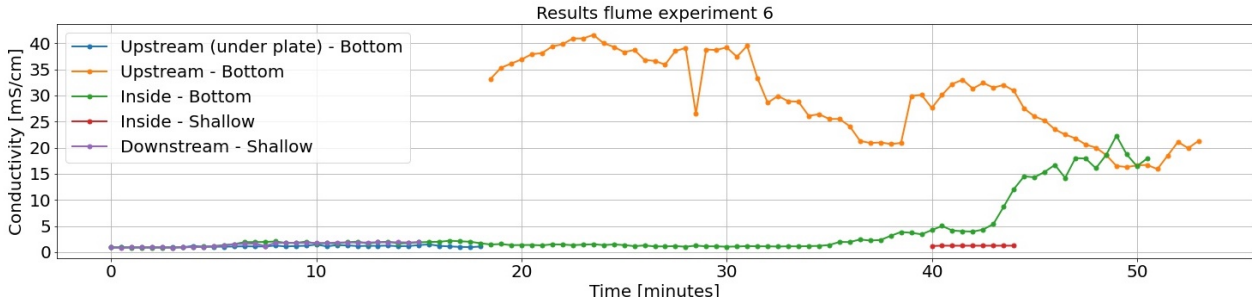


Figure 60: Flume experiment 6 – June 10, 2022

Figure 62 shows the temperature profiles of measurements at Waddenweg and Eendenkooi in November 2022. Now, Waddenweg shows another pattern, the bottom water is 0.1°C colder than the surface water and the water depth is smaller than in July 2022. The temperature profile at the Eendenkooi culvert shows a larger difference. The surface temperature is around 1.0°C colder than the bottom water. In November the outside temperatures were lower than in July and groundwater (and seepage) has a constant temperature during the year. This causes a higher temperature in Winter in comparison to surface water and can explain the temperature profile over the depth at Eendenkooi.

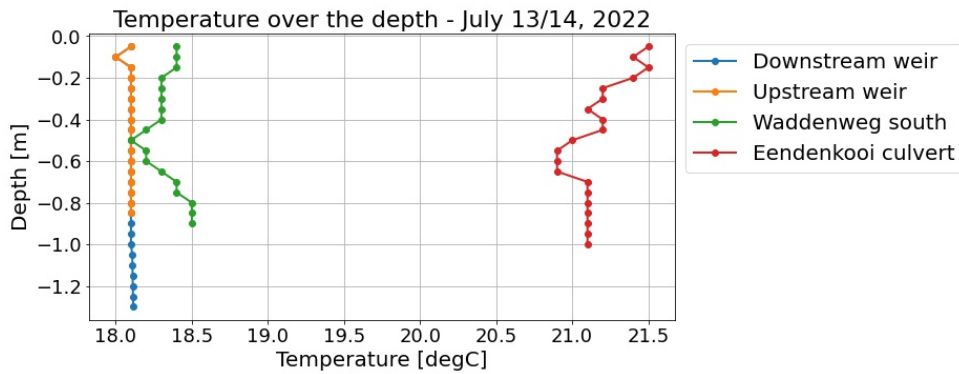


Figure 61: Temperature profiles over the depth – July 2022

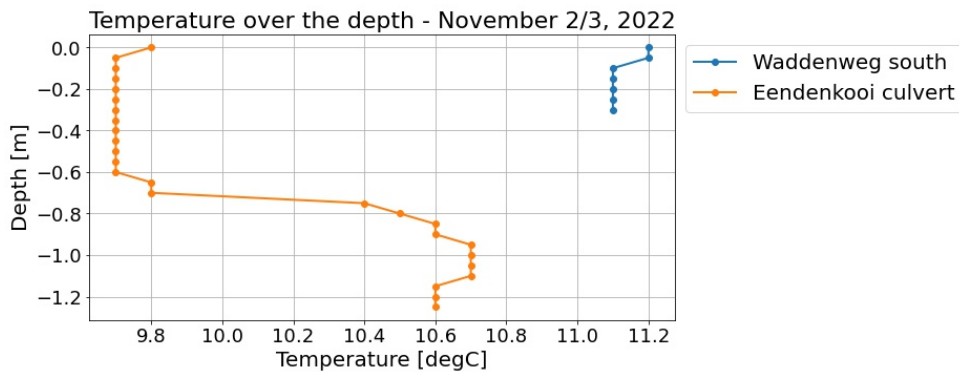


Figure 62: Temperature profiles over the depth – November 2022

## H Temperature measurements at two depths around the weir at Hornhuizerk-lief

In this appendix, measurements of the temperature at three locations around the weir at Hornhuizerk-lief are given. The corresponding conductivity measurements can be found in Chapter 4.1.2.

The results of the temperature measurements around the weir can be seen in Figure 63 for July 2022, and for November 2022 in Figure 64. In November 2022 the difference is minimal, so the surface and bottom water layer can be considered as one. The range in measured values in July is wider than in November. The maximum difference in the surface and bottom values in July 2022 is  $0.6^{\circ}\text{C}$ . Further, in July 2022 bottom water at 4 m upstream of the weir is warmer than at 1 m upstream and 1 m downstream of the weir. The surface water stays around the same value everywhere.

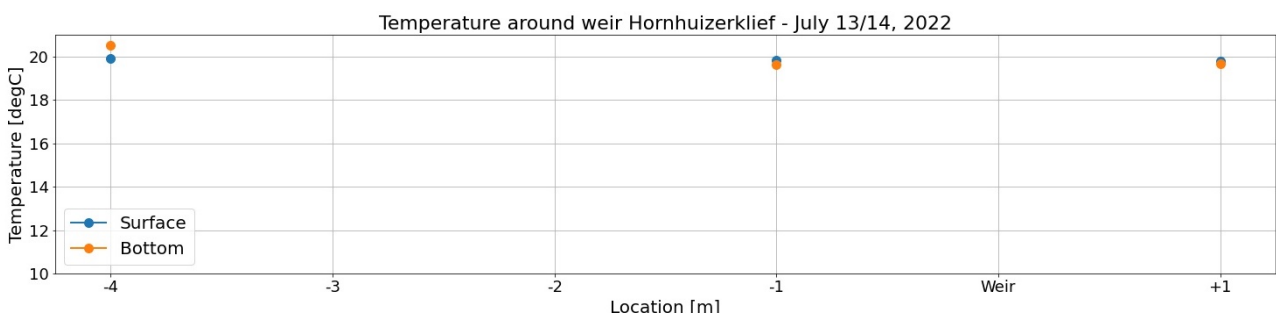


Figure 63: Temperature measurements at two depths around weir at Hornhuizerk-lief – July 2022

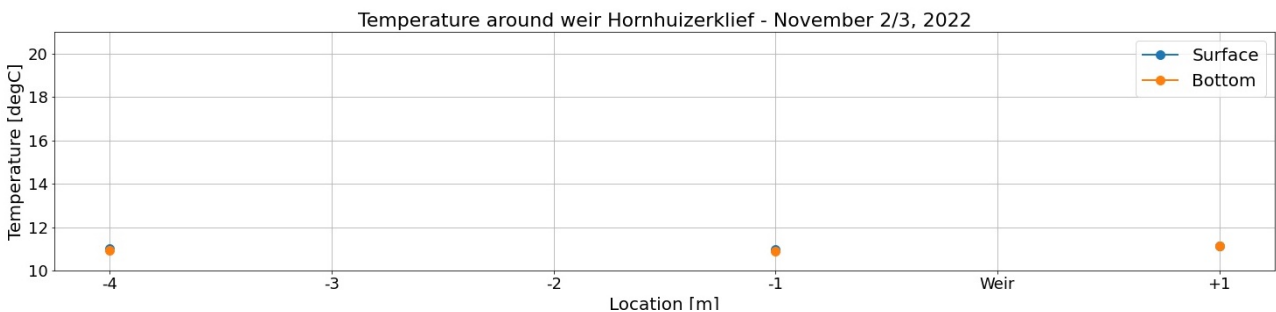


Figure 64: Temperature measurements at two depths around weir at Hornhuizerk-lief – November 2022

## I Temperature measurements at two depths along two transects in the Negenboerenpolder

This appendix contains the results of three transects, along which the temperature at two depths is measured. The corresponding conductivity measurements can be found in the main report (Chapter 4.1.2). Figures 66 (Summer) and 67 (Winter) are results from the same transect (Waddenweg) from south to north. Figure 65 are results along the dead end of the Dijkslot from the west to the east.

Figure 65 shows that the temperature decreases from west to east in the Dijkslot transect. In the total distance of the transect (800 m), the temperature decreases gradually with  $5^{\circ}\text{C}$ . In the transect,

three culverts can be found between 150 and 180 m, at a 500 m distance, and at around 700 m. Water contracts and mixes at the culverts. The best example of this is that the entire water column has the same temperature at 150 m.

Figures 66 and 67 are both results of temperature measurements along the Waddenweg transect, but give entirely different results. Figure 66 shows that the temperature slightly increases towards the dike in the north. On the elevation map of the Negenboerenpolder (Figure 13) an old dike (elevated area) in the landscape can be seen between 300 and 800 m of the transect. The surface water here is slightly warmer than around this area. However, the difference in temperature in July is small. In November, the range in measured values is even smaller. November (Figure 67) does not have the same pattern as July. The measurements vary, but the water temperature at the bottom is almost always higher than at the surface.

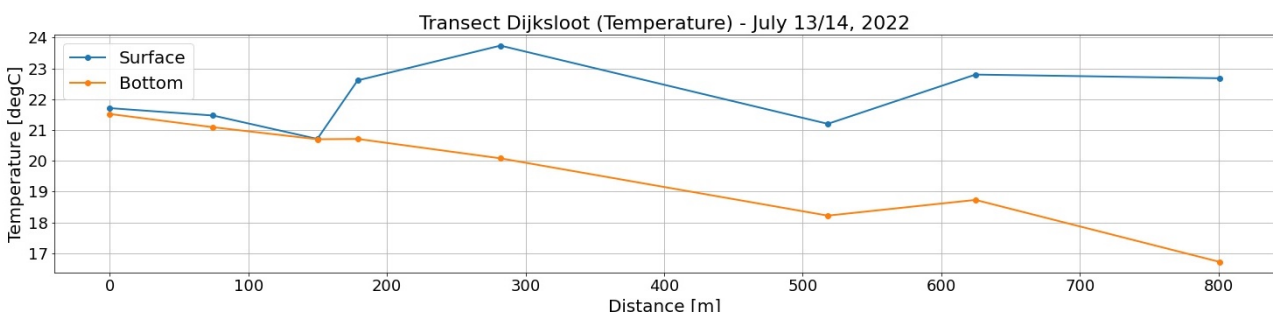


Figure 65: Temperature measurements at two depths along Dijkslot transect – July 2022

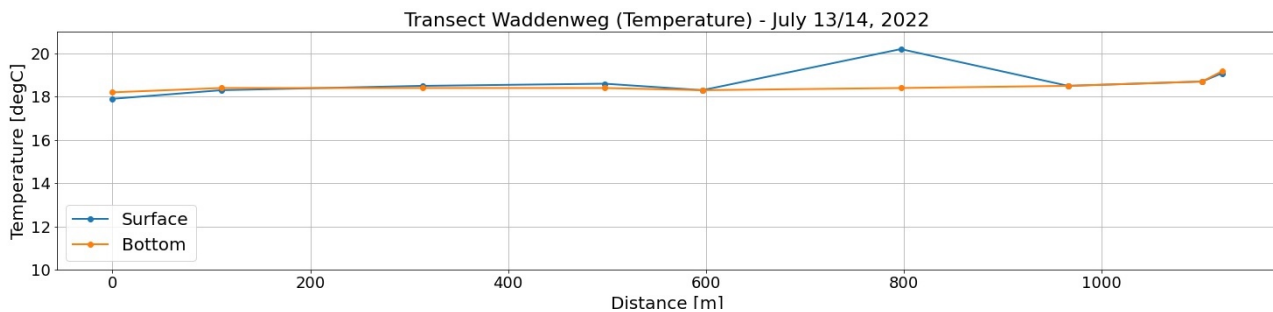


Figure 66: Temperature measurements at two depths along Waddenweg transect – July 2022

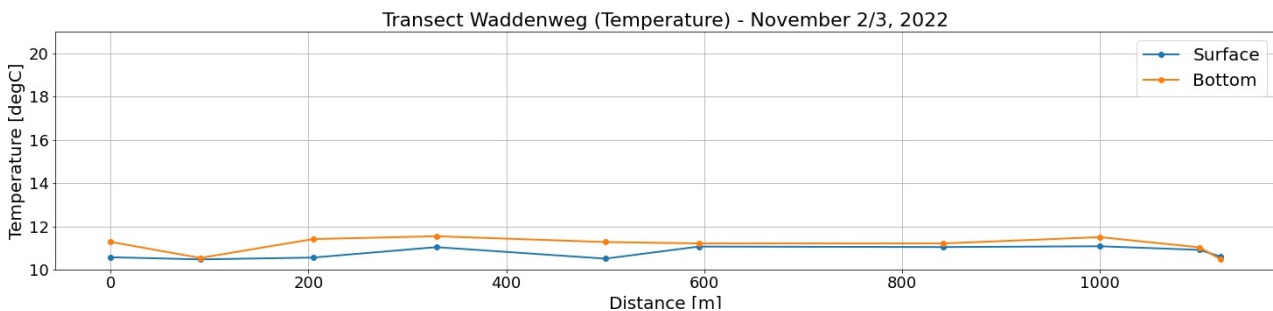


Figure 67: Temperature measurements at two depths along Waddenweg transect – November 2022

## J Possible explanations for the water levels and EC at the measurement locations in the Negenboerenpolder

This appendix contains the figures in which the water levels in the Negenboerenpolder are compared to the precipitation and tides. Detailed results of the analysis are discussed in Chapter 4.1.4.

Figures 68 and 69 show the Wadden Sea tides with the measured continuous water levels in the Negenboerenpolder. During Period 1 (Figure 68) the locations downstream and upstream of the weir show the same pattern. The upstream level is more constant, this is probably due to the weir. All water levels do not directly show a similar pattern with the tides, but the beginning of the time period and the levels at Lutjewat could be interesting to analyse in detail. Period 2 (Figure 69) presents more constant water levels than Period 1. Lutjewat has some periods with fluctuating water levels.

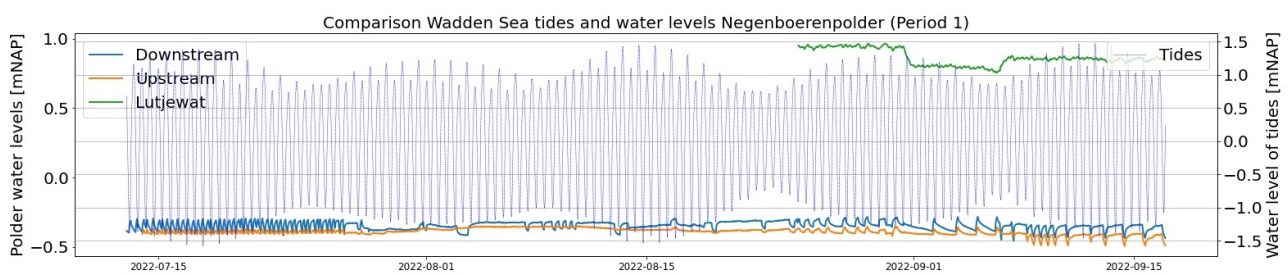


Figure 68: The Wadden Sea tides and the water levels in the Negenboerenpolder (Period 1)

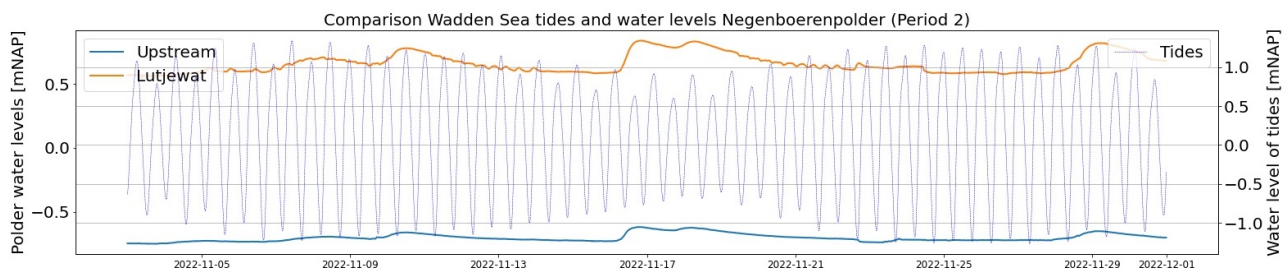


Figure 69: The Comparison of Wadden Sea tides and the water levels in the Negenboerenpolder (Period 2)

Figures 70 and 71 display the Wadden Sea tides with the conductivity levels in the Negenboerenpolder. The conductivity levels measured downstream at the bottom at the beginning of Period 1 are again fluctuating (Figure 70), which can be caused by malfunctioning of the equipment. At first glance, the four peaks in conductivity at the beginning of September cannot be caused by the tides. During Period 2 (Figure 71) the conductivity levels upstream of the weir are more constant than at Lutjewat.

In Figures 72 and 73 the precipitation at Lauwersoog with the conductivity levels in the Negenboerenpolder is compared. During Period 1 (Figure 72) no pattern can be found between the two. However, in Period 2 upstream of the weir, the surface conductivity levels go down during precipitation events in December 2022. Also, the conductivity levels at Lutjewat decrease slightly after some precipitation events.

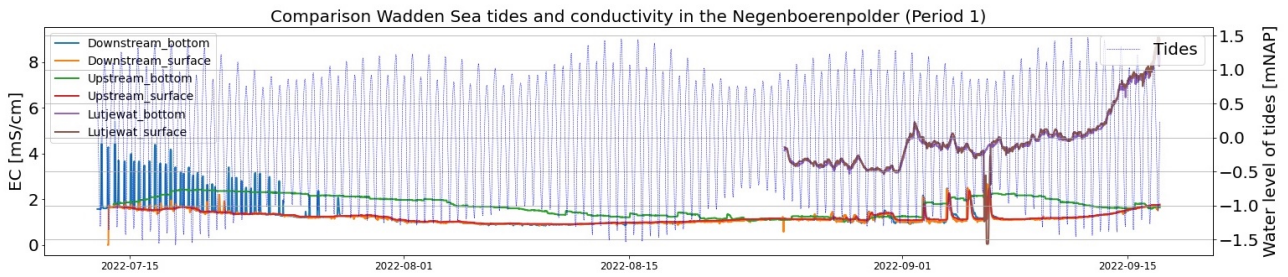


Figure 70: Comparison of Wadden Sea tides and conductivity levels in the Negenboerenpolder (Period 1)

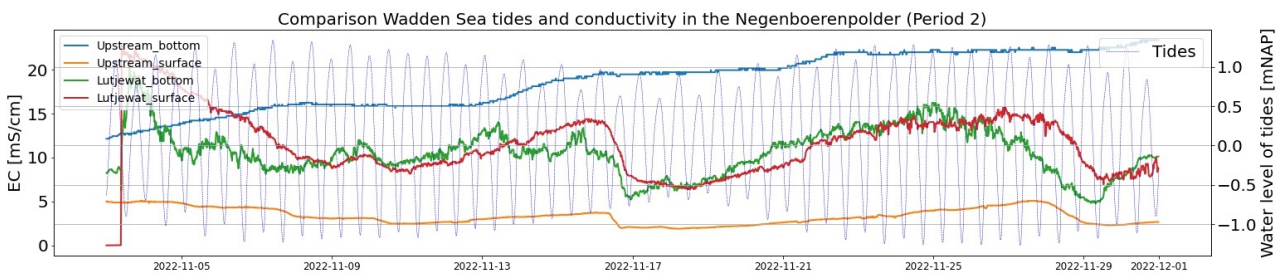


Figure 71: Comparison of Wadden Sea tides and conductivity levels in the Negenboerenpolder (Period 2)

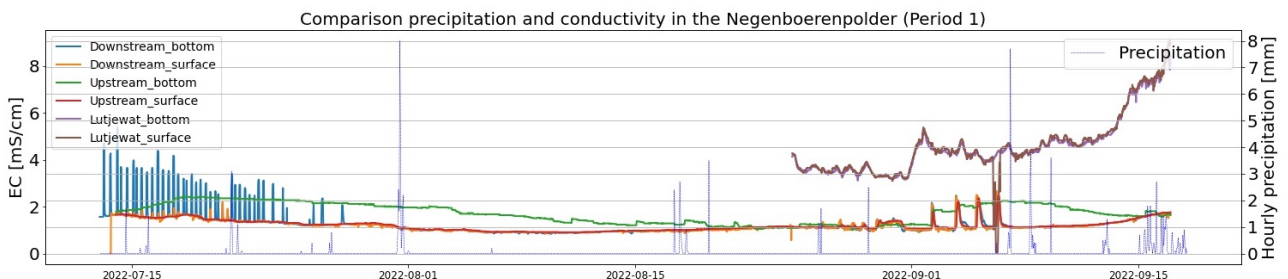


Figure 72: Comparison of precipitation and conductivity levels in the Negenboerenpolder (Period 1)

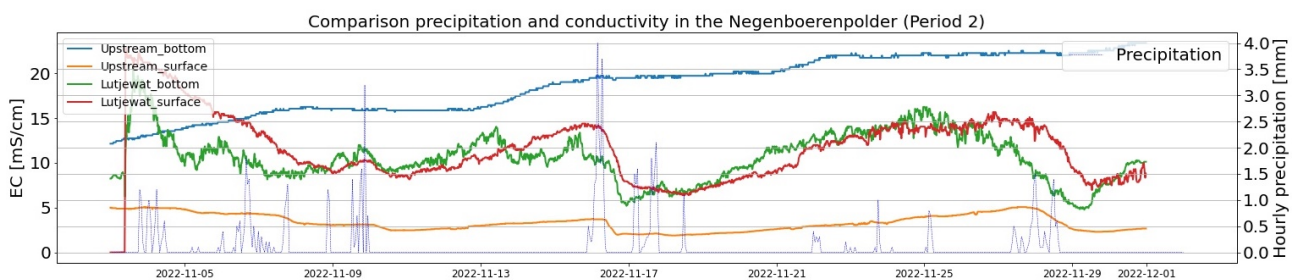


Figure 73: Comparison of precipitation and conductivity levels in the Negenboerenpolder (Period 2)

### K Classification of water canals in the Negenboerenpolder

This appendix contains Figure 74 of the water flow in the Negenboerenpolder, with also a classification of the waterways [van Meijeren et al., 2019]. For every waterway it is indicated if the canal is a primary or a secondary water canal.

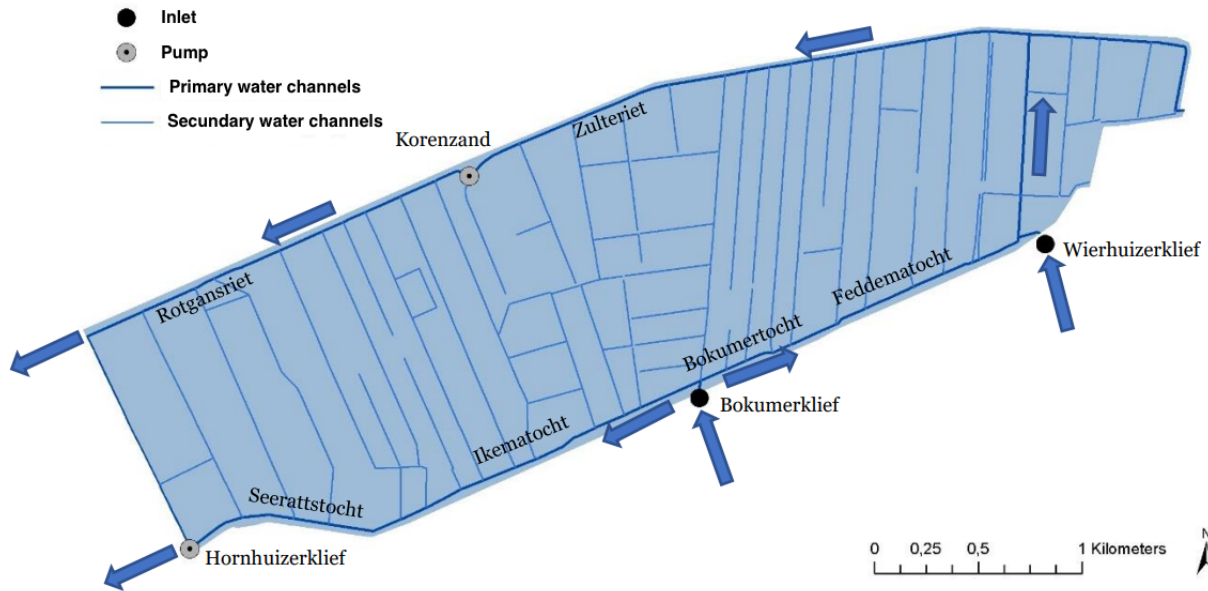


Figure 74: Water flow in the Negenboerenpolder with the classification of the waterways [Translated from van Meijeren et al., 2019]

### L Overview of the four geometries for 2D CFD Model in ANSYS Fluent

This appendix contains the geometries of the four geometries done in ANSYS Fluent, with which three cases are investigated (Table 11). Figures 76, and 77 are used for Case A, about the functioning of a traditional and modified weir. The design in Figures 77 and 78 with two velocities is used for Case B, to compare them with each other. And for the last case, Case C, in which two different designs are compared, Figures 77 and 79 are used. The designs differ in the distance between the underflow gate and the weir. To explain the symbols and colours in said figures, the legend in Figure 75 is included. A list with the settings in ANSYS Fluent can be found in Chapter 3.3.4.

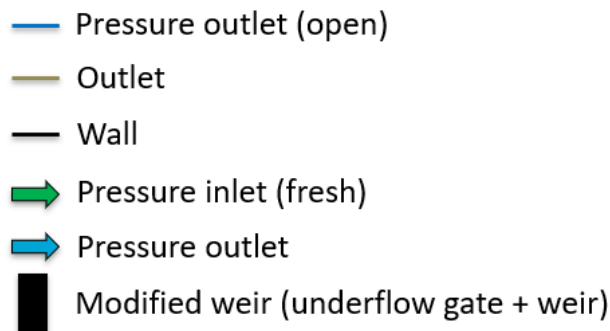


Figure 75: Legend with boundary conditions of the CFD model in ANSYS Fluent





Figure 76: Geometry 1 of the CFD model in ANSYS Fluent

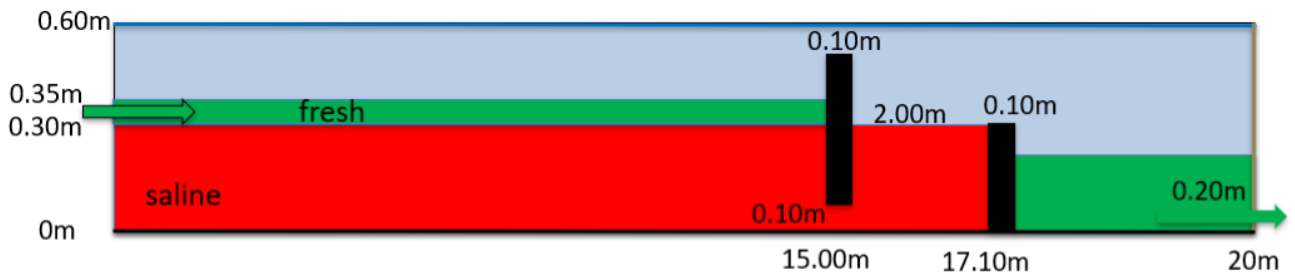


Figure 77: Geometry 2 of the CFD model in ANSYS Fluent

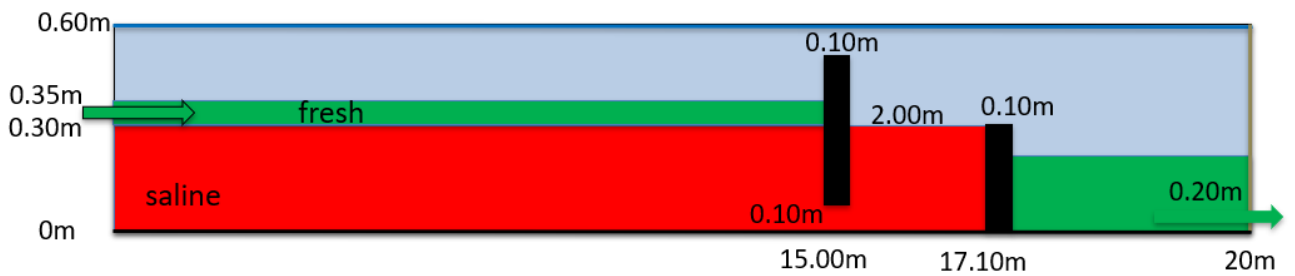


Figure 78: Geometry 3 of the CFD model in ANSYS Fluent

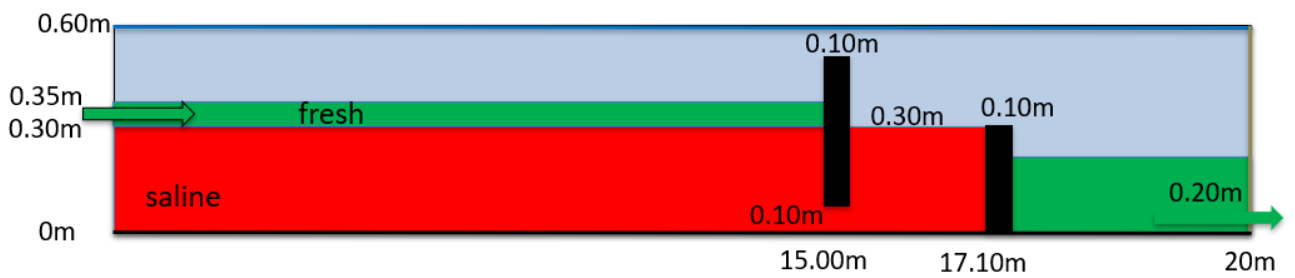


Figure 79: Geometry 4 of the CFD model in ANSYS Fluent

## M Preparation for a 3D model of a modified weir in ANSYS Fluent

A 3D design of a modified weir is made in ANSYS Fluent. The same geometry (geometry 2) as for the 2D design in Figure 23 is used, but now with a water canal width of 1.5 *m*. The exact same settings as for the 2D model are used for the 3D model. The design of the modelled water canal is a rectangle, in contrast to the often trapezoidal-sized water canals in the Netherlands. In such a canal, a 'control notch' (Chapter 2.2.2) is often used at the location of a weir. This design was the base for the 3D model, it is investigated if such a structure can be useful around a modified weir and if it is eventually influencing the weir. The flow with an underflow gate over the total width of the water canal (no 'control notch') is compared with an underflow gate over the same width as the weir ('control notch').

The boundary conditions of a 3D model are mostly the same as those of a 2D model. The bottom and sides will be classified as walls, there is an inlet and an outlet, and a free surface. The inlet and outlet are a pressure inlet and pressure outlet, both with open channel flow. The free surface is open and in contact with air, this will also have a pressure outlet.

There are some discussion points for a 3D model, for example, the design was rectangular instead of trapezoidal. Further, only one dimension (width of 1.5 *m*) was investigated. However, a 3D model limits the accuracy of simulations because the refinement should be in three directions [Hargreaves et al., 2007]. So, a 3D design is not highly reliable, but the total design with the 'control notch' can be investigated with 3D simulations.

## N Animations of the five runs in the 2D CFD model

This appendix contains the five animations of the five runs (Figures 80, 81, 82, 83, and 84) in ANSYS Fluent. The colours indicate the phases: blue is air, yellow is saline water, and red is fresh water. All animations were 2.46 minutes, but they are shortened to be able to include them in this report.

**NOTE:** The animations may not be working properly in all PDF readers.

(Loading animations/geo1-phaseid.mp4)

Figure 80: Animation of the phases in geometry 1

(Loading animations/geo2-phaseid.mp4)

Figure 81: Animation of the phases in geometry 2

(Loading animations/geo2-velocity.mp4)

Figure 82: Animation of the velocity vectors in geometry 2

(Loading animations/geo3-phaseid.mp4)

Figure 83: Animation of the phases in geometry 3

(Loading animations/geo4-velocity.mp4)

Figure 84: Animation of the velocity vectors in geometry 4